

REPORT NO.  
UCB/EERC-87/09  
JULY 1987

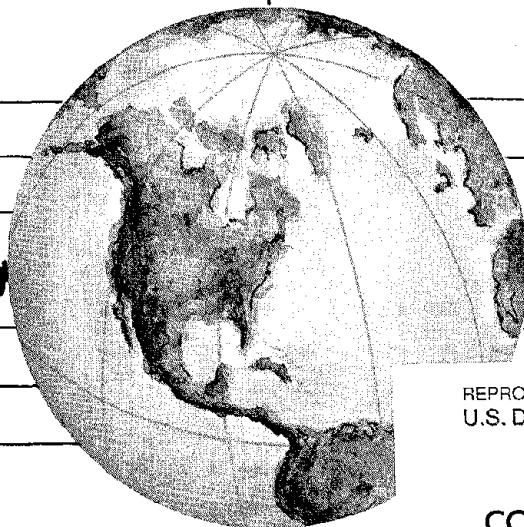
EARTHQUAKE ENGINEERING RESEARCH CENTER

# HYBRID SOLUTION TECHNIQUES FOR GENERALIZED PSEUDODYNAMIC TESTING

by

CHRISTOPHER R. THEWALT  
STEPHEN A. MAHIN

Report to the National Science Foundation



REPRODUCED BY  
U.S. DEPARTMENT OF COMMERCE  
NATIONAL TECHNICAL  
INFORMATION SERVICE  
SPRINGFIELD, VA. 22161

COLLEGE OF ENGINEERING

UNIVERSITY OF CALIFORNIA • Berkeley, California

For sale by the National Technical information Service, U.S. Department of Commerce, Springfield, Virginia 22161.

See back of report for up to date listing of EERC reports.

**DISCLAIMER**

Any opinions, findings, and conclusions or recommendations expressed in this publication are those of the authors and do not necessarily reflect the views of the National Science Foundation or the Earthquake Engineering Research Center, University of California, Berkeley.

PAGE		NSF/ENG-87036	PB88-179007	
4. Title and Subtitle Hybrid Solution Techniques for Generalized Pseudodynamic Testing			5. Report Date July 1987	
7. Author(s) Christopher R. Thewalt and Stephen A. Mahin			6.	
9. Performing Organization Name and Address Earthquake Engineering Research Center University of California 1301 South 46th Street Richmond, California 94804			8. Performing Organization Rept. No. UCB/EERC - 87/09	
12. Sponsoring Organization Name and Address National Science Foundation 1800 G. Street, N.W. Washington, D.C. 20550			10. Project/Task/Work Unit No.	
			11. Contract(C) or Grant(G) No. (C) (G) CEE83-16662	
15. Supplementary Notes			13. Type of Report & Period Covered	
16. Abstract (Limit: 200 words)  Previous work on the pseudodynamic method has primarily considered simple planar structures subjected to a single horizontal component of base excitation. This has been generalized to consider arbitrary structural configurations subjected to a fixed base excitation with up to six components. The extended system of equations of motion was verified using a three degree of freedom steel specimen that was tested on a shaking table as well as using the pseudodynamic method. Practical observations on implementing and operating a pseudodynamic test system are given based on experience gained in using the test system implemented at the University of California at Berkeley. An attempt is also made to specify criteria to be used to determine the reliability of results from a given test. A new formulation of the method that can be used to perform tests at or near real time is presented. This new technique uses force control, and would be useful in testing structures composed of rate sensitive materials where the conventional pseudodynamic method is not applicable. A new method is proposed that allows fully implicit integration methods to be used without requiring iteration or estimation of tangent stiffness properties. Verification tests showed that the method does give unconditional numerical stability as well as accurate results.			14.	
17. Document Analysis a. Descriptors  pseudodynamic testing  b. Identifiers/Open-Ended Terms  c. COSATI Field/Group				
18. Availability Statement:  Release unlimited			19. Security Class (This Report) Unclassified	
			20. Security Class (This Page) Unclassified	
			21. No. of Pages 145	
			22. Price A07	



# **Hybrid Solution Techniques for Generalized Pseudodynamic Testing**

by

Christopher R. Thewalt

and

Stephen A. Mahin

A Report to Sponsor  
National Science Foundation

Report No. UCB/EERC-87/09  
Earthquake Engineering Research Center  
College of Engineering  
University of California  
Berkeley California

July 1987



## ABSTRACT

Reliable prediction of inelastic structural response during severe seismic excitations has proven to be an extremely difficult task. Although analytical models exist for structural elements, the accuracy of response predictions is limited by the assumptions inherent in modeling inelastic behavior. Therefore, experimental testing remains the most reliable means of assessing structural performance under dynamic loading conditions.

The pseudodynamic test method has been suggested as a means for overcoming many of the limitations associated with shaking table testing. This method provides realistic seismic simulation using equipment that is considerably less expensive than that needed to build a shaking table. In the pseudodynamic method, conventional time domain analysis procedures are combined with experimentally measured information in order to simulate seismic response. The equations of motion for a discrete parameter model of the test specimen structural system are solved on-line using a step-by-step numerical integration method. Inertial and damping forces are modeled analytically, while nonlinear structural restoring force characteristics are measured experimentally.

Previous work on the pseudodynamic method has primarily considered simple planar structures subjected to a single horizontal component of base excitation. This has been generalized herein to consider arbitrary structural configurations subjected to a fixed base excitation with up to six components. The extended system of equations of motion was verified using a three degree of freedom steel specimen that was tested on a shaking table as well as using the pseudodynamic method. In performing pseudodynamic tests, it has been found that great care must be taken to avoid introducing experimental errors into the test, since these errors tend to propagate and contaminate response results with spurious higher mode response. Practical observations on implementing and operating a pseudodynamic test system are given based on experience gained in using the test system implemented at the University of California,

Berkeley. An attempt is also made to specify criteria to be used to determine the reliability of results from a given test.

A new formulation of the method that can be used to perform tests at or near real time is also presented. This new technique uses force control, and would be useful in testing structures composed of rate sensitive materials where the conventional pseudodynamic method is not applicable.

Most current implementations of the pseudodynamic method use an explicit integration operator. These methods are only conditionally stable and necessitate the use of very small time steps for systems with widely spaced modes. A new method is proposed herein that allows fully implicit integration methods to be used without requiring iteration or estimation of tangent stiffness properties. The basis of the new method is that the equations of motion are solved using a hybrid approach, where part of the solution is performed digitally and the remainder is solved in analog form. Verification tests showed the method does give unconditional numerical stability as well as accurate results. In addition, using a larger time step would allow tests to be performed more quickly and would also reduce error propagation problems. The form of the new method also suggests a completely new hardware layout for pseudodynamic testing, and this new architecture would make several interesting types of tests possible. It would be possible, for example, to use force control testing, eliminating many problems currently found in testing stiff structures. Also, substructure analysis techniques could be used to physically test only critical portions of a structure.

## ACKNOWLEDGMENT

The financial support of the National Science Foundation in sponsoring this project is gratefully acknowledged. The contribution of Amir Gilani in helping to set up the experimental equipment is appreciated, as is the help from the technical staff at the Structural Engineering Laboratory at the University of California, Berkeley.

Any opinions, conclusions or recommendations in this report are those of the authors, and do not necessarily reflect the views of the National Science Foundation.

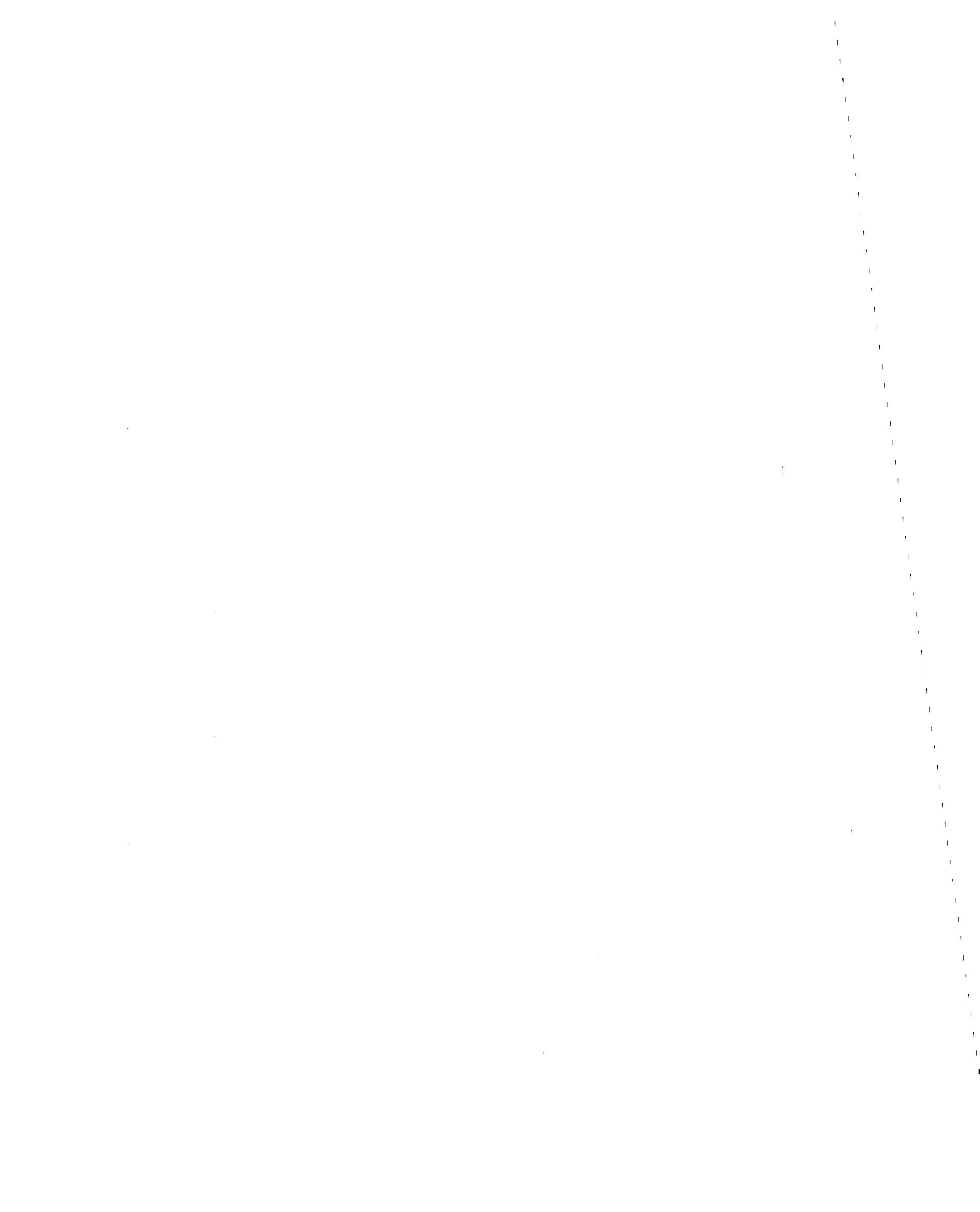
## Table of Contents

ABSTRACT .....	i
ACKNOWLEDGMENT .....	iii
TABLE OF CONTENTS .....	iv
1. INTRODUCTION .....	1
1.0 General .....	1
1.1 Objectives .....	3
1.2 Scope .....	5
2. THE PSEUDODYNAMIC ALGORITHM .....	7
2.0 Introduction .....	7
2.1 Numerical Technique .....	7
2.2 Integration Operators .....	8
2.2.1 The Newmark Method .....	9
2.2.2 The Modified Newmark Method .....	10
2.3 Generalization of the Equations of Motion .....	12
2.3.1 The Forcing Function .....	12
2.3.2 Coordinate Transformations .....	13
2.3.2.1 Geometric Corrections .....	14
2.3.3 Reduction of Degrees of Freedom .....	14
2.3.4 Geometric Stiffness .....	14
2.4 Experimental Error Effects .....	15

2.4.1 Types of Errors .....	15
3. IMPLEMENTATION DETAILS .....	18
3.0 Introduction .....	18
3.1 Sources of Errors .....	18
3.1.1 Digital to Analog (D/A) Converter .....	19
3.1.2 Analog to Digital (A/D) Converter .....	20
3.1.3 Displacement Transducers .....	21
3.1.4 Force Transducers .....	23
3.1.5 Friction .....	23
3.2 Electro-Hydraulic Control Loop .....	23
3.2.1 Description of a Displacement Control Loop .....	24
3.2.1.1 The Servovalve .....	25
3.2.1.2 The Actuator .....	26
3.2.1.3 The Displacement Feedback Signal .....	26
3.2.1.4 The Electro-Hydraulic Controller .....	26
3.2.2 Servo Loop Behavior .....	27
3.3 Software Layout .....	31
3.4 Concluding Remarks .....	34
4. NONPLANAR VERIFICATION TEST .....	35
4.0 Introduction .....	35
4.1 The Test Specimen .....	36
4.2 Experimental Setup .....	38
4.3 Problems Encountered .....	39

4.3.1 Displacement Errors Due to Experimental Geometry .....	39
4.3.2 Inaccurate Displacement Feedback .....	40
4.3.3 Force Oscillation .....	42
4.3.4 Poor Control with Increased Mass .....	42
4.3.5 Force Relaxation During Wait Periods .....	43
4.4 Test Sequence .....	45
4.5 Results .....	45
4.6 Conclusions .....	47
5. RAPID TESTING TECHNIQUE .....	49
5.0 Introduction .....	49
5.1 Procedure .....	49
5.2 Concluding Remarks .....	52
6. AN UNCONDITIONALLY STABLE ALGORITHM .....	53
6.0 Introduction .....	53
6.1 Time Integration Method .....	54
6.2 New Pseudodynamic Algorithm .....	55
6.3 Verification Test .....	58
6.3.1 General Information .....	58
6.3.2 Implementation Details .....	60
6.3.3 Results .....	62
6.4 Extensions of the Implicit Method .....	63
6.5 Conclusions .....	65
7. CONCLUSIONS AND RECOMMENDATIONS .....	67

7.0 Summary .....	67
7.1 Recommended Future Work .....	70
7.2 Concluding Remarks .....	71
REFERENCES .....	73



# 1. INTRODUCTION

## 1.0 General

Reliable prediction of inelastic structural performance during a severe seismic event is an extremely difficult task, due to the complex nonlinear behavior exhibited by members and connectors. Although nonlinear analytical models exist for such structural elements, the accuracy of the resulting response predictions is limited by assumptions in the mathematical description of the model. For this reason, experimental testing remains the most reliable means of assessing seismic performance and devising improved design and analysis methods. Quasi-static testing, in which prescribed displacement or load histories are applied to the specimen, provide valuable information on the performance of various detailing alternatives, but generally it is difficult to relate the energy dissipation capacity of such details with that required for seismic safety.

Shaking table tests can provide realistic response simulation. However, the size and mass of specimens are limited, often making reduced scale models necessary. It is also possible that massive specimens may dynamically interact with the shake table, resulting in ground acceleration histories different from those specified. With current tables available in the U.S., the table excitation is typically limited to one lateral component and possibly an additional vertical component. The acceleration, velocity and displacement of the table excitation are also limited in magnitude and frequency content by the characteristics of the controlling electro-hydraulic system. These restrictions and the cost of performing shaking table tests have limited the usefulness of this method.

The pseudodynamic method is an on-line computer controlled testing technique that overcomes many limitations in shaking table testing, while using the same equipment necessary in quasi-static testing. The pseudodynamic test method was initially implemented in Japan at the Institute of Industrial Science of the University of Tokyo and the Building Research Institute of the Ministry of Construction [1]. The method involves idealizing the test structure as a discrete parameter system, with mass and damping analytically modeled. Conventional time domain dynamic analysis procedures are used to incrementally solve the equations of motion in terms of the specified mass and damping, the measured restoring force, and a predefined ground acceleration record.

The pseudodynamic test method can be visualized as a dual loop system, as shown in Fig. 1.1, where the outer loop represents the computer and associated hardware that solve the equations of motion, and the inner loop is the electro-hydraulic displacement control system responsible for imposing the desired displacements.

The pseudodynamic test method allows large massive structures to be tested and since the test is performed slowly, arbitrarily large ground excitations can be used. Furthermore, since the forcing function is analytically described, excitation can be due to generalized multiple component fixed base movement, given the proper form of the equations of motion. It is even possible to consider hydrodynamic forces exciting the structure, once the analytical model is chosen and the equations of motion are written appropriately in terms of the fluid forces.

The pseudodynamic method has already been used for many actual seismic performance tests [28-35], but difficulties have been reported in some of these tests [20]. In some cases involving stiff multiple degree of freedom systems, force fluctuations have been observed due to the inability of the test system to accurately control displacements. In other cases, the structural response in a pseudodynamic test has been contaminated by spurious higher mode response. The most serious errors have been found to be those resulting from improperly imposing specified displacements. When the displacements are incorrect, the corresponding restoring force is also in error, and the resulting force perturbation propagates throughout the remainder of the test. The displacement errors can be due either to electro-hydraulic control problems, to inadequate instrumentation and setup procedures, or to poor software implementation of the pseudodynamic method.

A study at the University of Michigan, Ann Arbor [6], was performed to investigate improved actuator control techniques. To gain insight into the factors controlling the reliability of pseudodynamic test results, the propagation of experimental errors [8,20,21,22] and the suitability of various integration operators have been studied at the University of California, Berkeley, and elsewhere [2,3,4,11,12]. However, these various studies have yet to be generalized, and the applicability of the pseudodynamic test method to multiple degree of freedom systems remains to be demonstrated by means of well controlled verification tests. In view of the potential benefits of a

reliable and verified pseudodynamic method, the establishment of guidelines for its implementation, and the formulation of methods to increase its accuracy and applicability, a variety of studies have been undertaken as outlined below.

### 1.1 Objectives

The purpose of this investigation is to generalize and extend the capabilities of the pseudodynamic test method and also to study the reliability of test results. The hardware used to perform tests will be reviewed, with an emphasis on identifying sources of experimental error and techniques to mitigate adverse effects of these errors. In particular, the electro-hydraulic control loop will be investigated to see if adequate performance can be achieved. The components of a test system, both hardware and software, will be examined in detail to identify attributes of a system with which successful tests can be performed. In addition, techniques will be presented that would allow faulty components of the system to be identified so that corrective action can be taken. In order to focus attention on important areas in pseudodynamic testing, specific experiences will be highlighted regarding the implementation and operation of the Berkeley pseudodynamic test system.

Verification tests performed to date have considered planar structures subjected to single component base excitations and have been restricted to structures with only a few degrees of freedom. These tests mimic conventional shaking table tests where the ground motion input is limited by shaking table capabilities. The pseudodynamic method can be implemented, using a suitable form of the equations of motion, to consider general structural configuration and fixed base excitation with six degree of freedom. While nonplanar pseudodynamic tests have been performed [28,30], the resulting response was compared with analytical results. In order to verify the pseudodynamic method more fully, a study correlating shaking table and pseudodynamic results is required using a nonplanar multiple degree of freedom specimen.

Several cases where existing pseudodynamic procedures have difficulties have been identified. These relate to specimens that must be tested at speeds approaching real time, and stiff systems with many degrees of freedom. Consequently, studies to solve these problems have also been

initiated.

In some applications, it would be advantageous to perform the pseudodynamic tests at or near real time. However, in the pseudodynamic method tests are performed slowly because dynamic effects are accounted for in the equations of motion. Thus, when near real time tests are desirable, this cannot be achieved by merely using the current algorithm and performing the test more quickly. Actual inertial and damping forces would then be introduced to the specimen. A force control procedure for performing rapid testing is formulated herein. Potential advantages and difficulties are identified.

As experience is gained in pseudodynamic testing, more complex specimens will be considered. The explicit formulation of the numerical integration operator used to date, however, is only conditionally stable. Therefore, it is necessary to limit the time step ( $\Delta t$ ) to be less than  $2/\omega$ , where  $\omega$  is the highest natural frequency of the test specimen. The result may be a very small time step, even if only a few of the lower modes of the structure contribute significantly to the dynamic response. As the number of steps in a test is increased, problems with error propagation also increase. It would be beneficial to select  $\Delta t$  to ensure accuracy in the responding modes, rather than as a stability constraint. In order to achieve unconditional numerical stability, however, an implicit integration operator must be used.

Attempts to use implicit integration schemes have been made, but have shown only limited success. Conventional analytical approaches using iteration cannot be used because the behavior of a real specimen is path dependent. Alternately, implicit schemes could be used if a good estimate of the specimen's tangent stiffness properties could be made on each step. However, the formation of a tangent stiffness matrix using experimental data has proven to be extremely difficult, if not impossible. These problems have lead many researchers to abandon implicit methods. However, a new pseudodynamic algorithm is proposed and tested herein that allows fully implicit integration schemes to be used. The new method is not iterative, and does not require the formulation of a tangent stiffness matrix. Rather than making simplifying assumptions, the new method uses available experimental data and a hybrid approach. Using this hybrid approach, the equations of motion

are solved in part on a digital computer and in part using analog voltage signals and summing amplifiers.

## 1.2 Scope

This thesis is intended to show the applicability of several new areas in pseudodynamic testing and to describe, in general, how a pseudodynamic system should be implemented and how to successfully perform tests. The information will be partially review so that this thesis can be used as a general reference, and where new techniques are proposed, verification tests results and implementation details will be given.

The contents of this thesis are in the following order. In Chapter 2 the governing equations of motion are presented, together with appropriate step-by-step integration methods to implement conventional pseudodynamic tests. Extensions to allow general three dimensional loading are given, together with transformation techniques to allow arbitrary user defined coordinate systems to be used in calculations. The typical effects of error propagation are also described. In Chapter 3 the physical observations collected in performing many tests is presented. Sources of error are identified, together with mitigation techniques, and crucial hardware components are also discussed. The general behavior of electro-hydraulic systems under displacement control is described. The software needed to perform pseudodynamic tests is described in general terms.

The general three dimensional formulation using multiple component base excitation is presented in Chapter 4. Comparisons are made between shaking table and pseudodynamic results to verify this formulation. Problems encountered in performing the pseudodynamic test are described together with remedial actions taken during the test.

In Chapter 5 a new form of the pseudodynamic test method is presented that could be used to perform near real time tests. High speed tests would be useful for structures that are likely to show rate sensitive behavior.

The hybrid form of the pseudodynamic method that allows implicit integration schemes to be used is presented in Chapter 6, together with verification tests using the new method. Different computer architectures that could be used to implement the new method are discussed. Using the

new method with an appropriate hardware layout opens the possibility of performing many different types of tests, such as force control and substructure testing. These possibilities are briefly discussed.

Finally, Chapter 7 summarizes the work, drawing general conclusions and observations. Areas requiring additional research are indicated.

## 2. THE PSEUDODYNAMIC ALGORITHM

### 2.0 Introduction

The pseudodynamic test method combines conventional time domain dynamic analysis procedures with experimentally acquired information to provide realistic dynamic response histories. The test structure is idealized as a discrete parameter system, and the equations of motion for the resulting system can be represented as a system of second-order ordinary differential equations. The inertial and viscous damping properties are analytically described, and the loading function is user specified. In performing a test, the equations of motion are solved by direct step-by-step numerical integration. Hydraulic actuators are used to impose the calculated structural displacements for each of the discrete degrees of freedom, and the resulting restoring forces are measured for use by the integration algorithm on the next step.

The assumption that the structure can be adequately modeled as a discrete spring-mass system and the errors introduced by discretizing time are also present in analytical procedures. However, in the pseudodynamic method the structural stiffness properties need not be idealized because the actual properties are measured during testing. Since the largest errors in dynamic analysis are generally introduced by modeling the structural restoring force characteristics, it is reasonable to expect that the pseudodynamic method will produce very good results, even for structures heavily damaged by earthquakes.

### 2.1 Numerical Technique

Given a discrete parameter model of a structural system, the equations of motion can be stated in matrix form as :

$$\mathbf{M}\ddot{\mathbf{u}} + \mathbf{C}\dot{\mathbf{u}} + \mathbf{r} = \mathbf{f} \quad (2.1)$$

where  $\mathbf{M}$  is the mass matrix

$\mathbf{C}$  is the viscous damping matrix

$\mathbf{r}$  is the structural restoring force

$\dot{\mathbf{u}}$  and  $\ddot{\mathbf{u}}$  are the velocity and acceleration vectors, respectively

$\mathbf{f}$  is a loading function

The restoring force is in general a function of the current displacement state and of the response history. In an elastic system the restoring force can be idealized as  $\mathbf{r} = \mathbf{K}\mathbf{u}$ , where  $\mathbf{K}$  is the stiffness matrix and  $\mathbf{u}$  is the displacement vector. For inelastic systems more complex models are required. The solution of Eq. (2.1) can be approximated using direct step-by-step integration techniques where the time interval  $[0, \tau]$  is divided into  $N$  equal steps of  $\Delta t = \tau/N$ , giving :

$$\mathbf{M}\mathbf{a}_i + \mathbf{C}\mathbf{v}_i + \mathbf{r}_i = \mathbf{f}_i \quad (2.2)$$

where  $\mathbf{a}_i$  and  $\mathbf{v}_i$  approximate  $\ddot{\mathbf{u}}(i\Delta t)$  and  $\dot{\mathbf{u}}(i\Delta t)$ , respectively, and  $\mathbf{f}_i = \mathbf{f}(i\Delta t)$ .

In a pseudodynamic test, the structural restoring force is experimentally measured at each step, whereas  $\mathbf{M}$ ,  $\mathbf{C}$ , and  $\mathbf{r}$  are specified and  $\mathbf{a}$ ,  $\mathbf{v}$  and  $\mathbf{d}$  are computed at each step. The pseudodynamic algorithm can now be described recursively considering the general operations at step  $i$  of a test. The procedure would be :

- calculate the displacements at the next step  $\mathbf{d}_{i+1}$ , using an appropriate numerical integration method
- impose these displacements on the specimen, using computer controlled electro-hydraulic actuators
- wait for actuators to stop and measure the restoring forces  $\mathbf{r}_{i+1}$  associated with the new displacements
- calculate  $\mathbf{a}_{i+1}$ ,  $\mathbf{v}_{i+1}$  and other computed response quantities
- continue

This chapter will study the numerical solution techniques and their behavior when used in pseudodynamic tests. Previous work will be summarized and extended into a more general form, as used in the tests described in Chapter 4. Alternate forms will be presented in subsequent chapters.

## 2.2 Integration Operators

Considerable effort has been made [2,3,8,11,12,15,16] to identify which step-by-step integration algorithms are best suited to pseudodynamic testing. Currently, explicit integration algorithms

are most commonly used. Implicit algorithms that require knowledge of the specimens tangent stiffness on each step have been largely abandoned, for two reasons : a) tangent stiffnesses are only estimates, and have proved difficult or impossible to measure reliably and b) iterative procedures used in analysis to reduce equilibrium errors cannot be used in a pseudodynamic test because specimen restoring forces are in general path dependent. While these two limitations are indeed true, a new method has been developed, as described in Chapter 6, which allows implicit algorithms to be used. However, further discussion in this chapter will be limited to explicit integration procedures.

The two explicit methods most commonly used in pseudodynamic testing are the central difference and the explicit Newmark methods. It was shown by Shing and Mahin [12] that these two methods are in fact numerically equivalent once started, if the computed displacements are used in the calculations. Since the two methods are equivalent, and the Newmark form is a single step method that is self starting, only the Newmark form will be presented here. The properties of the explicit algorithms presented here are adapted from Shing and Mahin [12] and are presented for completeness. The actual development of stability, energy dissipation and period distortion properties will not be presented here in the interest of brevity. Those interested in more detail should refer to the original paper.

### 2.2.1 The Newmark Method

The Newmark method uses Eq. (2.2) along with interpolative functions for displacement and velocity :

$$\mathbf{d}_{i+1} = \mathbf{d}_i + \Delta t \mathbf{v}_i + (\frac{1}{2} - \beta) \Delta t^2 \mathbf{a}_i + \beta \Delta t^2 \mathbf{a}_{i+1} \quad (2.3)$$

$$\mathbf{v}_{i+1} = \mathbf{v}_i + (1 - \gamma) \Delta t \mathbf{a}_i + \gamma \Delta t \mathbf{a}_{i+1} \quad (2.4)$$

Selecting  $\beta=0$  and  $\gamma=\frac{1}{2}$  results in the explicit single step algorithm used in the Berkeley implementation of the pseudodynamic test method. The stability condition for this method in the linear elastic range is :

$$0 \leq \omega \Delta t \leq 2 \quad (2.5)$$

The stability condition must be satisfied for all of a discrete structure's natural frequencies ( $\omega$ ), so

$\Delta t$  must be determined by stability limits related to the highest natural frequency rather than by accuracy considerations in the modes of interest. This is true even if the highest mode does not contribute to the response. A formal stability limit for nonlinear structural systems has not yet been developed, but it has been found [12] that satisfactory results can be obtained by selecting  $\Delta t$  so that the incremental displacements are small enough to accurately trace the response loops. The insight gained from traditional nonlinear analysis shows that this condition is sufficient, if the structure softens with damage as is usually the case.

The explicit form of Newmark's method with  $\gamma=1/2$  is nondissipative. However, the actual response frequencies of the discrete structure are distorted (increased) to  $\bar{\omega}$ , where :

$$\bar{\omega} = \frac{1}{\Delta t} \arctan \left( \frac{\sqrt{4 - (\omega^2 \Delta t^2 - 2)^2}}{2 - \omega^2 \Delta t^2} \right) \quad (2.6)$$

When  $\Delta t$  is selected such that there are 20 or more steps per response cycle (ie.,  $\Delta t/T < 0.05$ , where  $T=2\pi/\omega$ ), the error is less than 1%.

### 2.2.2 The Modified Newmark Method

In dynamically modeling structural systems, it has traditionally been a difficult task to select realistic damping parameters. The usual approach is to select a viscous damping matrix that will give modal damping ratios suitable for the given structure's materials, configuration, and displacement amplitude. Also, in performing pseudodynamic tests, it has been found that certain types of experimental errors lead to the spurious excitation of higher modes, and it is often desirable to damp these modes so that they do not contaminate the dynamic response simulation. Based on elastic analysis procedures, Cauchy damping can be used to obtain prescribed damping ratios at particular frequencies, though usually only mass and stiffness proportional terms are used.

Such viscous damping matrices are convenient analytical tools, but their usefulness in pseudodynamic testing is less clear. It has been shown by Shing and Mahin [16], that using a constant damping matrix based on initial elastic structural properties can lead to unpredictable results. As the structure yields, it was found that the actual modal damping ratios can change substantially. In particular, if the initial damping for the higher modes are set very large to control spurious

oscillations, excessive damping may be introduced in the lower modes when the structure yields.

In an attempt to treat the damping problem more uniformly, Shing and Mahin [12] have proposed a variation of Newmark's method that possesses dissipative properties. Rather than using a viscous damping matrix, the numerical integration scheme can be used to dissipate energy in a controlled fashion. The form proposed in Ref. 11 is particularly attractive in that the damping monotonically increases with  $\omega \Delta t$ , and can be set equal to zero at any specified value of  $\omega \Delta t$ , as shown in Fig. 2.1. The period shrinkage characteristics for this method can be shown in Fig. 2.2. The modified form of the equations of motion is :

$$\mathbf{M} \mathbf{a}_{i+1} + \left[ (1 + \alpha) \mathbf{K} + \frac{\rho}{\Delta t^2} \mathbf{M} \right] \mathbf{d}_{i+1} = \mathbf{f}_{i+1} + (\alpha \mathbf{K} + \frac{\rho}{\Delta t^2} \mathbf{M}) \mathbf{d}_i \quad (2.7)$$

and

$$\mathbf{d}_{i+1} = \mathbf{d}_i + \Delta t \mathbf{v}_i + \frac{1}{2} \Delta t^2 \mathbf{a}_i \quad (2.8)$$

$$\mathbf{v}_{i+1} = \mathbf{v}_i + \frac{1}{2} \Delta t (\mathbf{a}_i + \mathbf{a}_{i+1}) \quad (2.9)$$

The viscous damping matrix is not included in this formulation because it is anticipated that the damping inherent in the integration method will be used for both the modeling of structural damping and also the mitigation of error induced higher mode response.

To obtain numerical damping that increases with frequency (as shown in Fig. 2.1),  $\rho$  should be negative and  $\alpha$  should be positive. Under these assumptions and letting  $\Omega = \omega \Delta t$  and  $\bar{\Omega} = \bar{\omega} \Delta t$ , the stability condition for this algorithm is :

$$\sqrt{-\rho/\alpha} \leq \omega \Delta t \leq \frac{1 + \sqrt{1 - (1 + \alpha)\rho}}{1 + \alpha} \quad (2.10)$$

The effective damping ratio and shifted frequency are given by :

$$\bar{\xi} = -\frac{\ln(1 - \alpha \Omega^2 - \rho)}{2\bar{\Omega}} \quad (2.11)$$

$$\bar{\omega} = \arctan \left( \frac{\{\Omega^2 - \frac{1}{2}[(1 + \alpha)\Omega^2 + \rho]\}^{1/2}}{1 - \frac{1}{2}(1 + \alpha)\Omega^2 - \frac{1}{2}\rho} \right) \quad (2.12)$$

When  $\Omega < \sqrt{-\rho/\alpha}$ , the damping becomes negative and the solution becomes unstable. By selecting appropriate values of  $\rho$  and  $\alpha$  it is possible to have small damping in the lower modes and large damping for the higher modes. This feature is very useful for pseudodynamic testing. Shing

and Mahin [22] have presented an algorithm that will ensure that the damping will always remain positive, even as the structure yields and the natural frequencies decrease.

## 2.3 Generalization of the Equations of Motion

### 2.3.1 The Forcing Function

The pseudodynamic test method is usually formulated in terms of seismic loads, but the loading function is in fact quite arbitrary. Impact, vehicle, aeroelastic and other loads may be considered. Where appropriate, the equations of motion can be modified to include hydrodynamic and other nonlinear effects.

In the simplest case of seismic loading, a planar structure is excited by a single lateral ground acceleration, giving :

$$\mathbf{f}_i = \mathbf{M} \{1\} a_{g_i} \quad (2.13)$$

where  $\mathbf{f}_i$  is the force vector at time  $i \Delta t$

$\{1\}$  is a vector of ones

$a_{g_i}$  is the ground acceleration at time  $i \Delta t$

The above formulation essentially permits tests to be performed as they are performed on shaking tables with a single horizontal component of motion. The pseudodynamic method, however, can easily be extended to non-planar structures subjected to multiple component fixed base excitations. Examples and verification studies of this extension are included in Chapter 4. The forcing function in this case becomes :

$$\mathbf{f}_i = \mathbf{M} \mathbf{B} \mathbf{a}_{g_i} \quad (2.14)$$

where  $\mathbf{B}$  is the ground acceleration transformation matrix

$\mathbf{a}_{g_i}$  is the ground acceleration vector

The component  $\mathbf{B}_{ij}$  is the acceleration at structural degree of freedom  $i$  when the structure acts as rigid body under unit acceleration of ground component  $j$ . The  $\mathbf{B}$  matrix is constant for a

given test, once specimen configuration and ground motion inputs are determined. This form of the forcing function makes it possible to conduct tests that could not be performed on conventional shaking tables, since a completely general fixed base motion may be specified.

### 2.3.2 Coordinate Transformations

The coordinate system determined by the location of the actuators on a structural specimen may not be the most convenient one for analytically describing the inertial and damping properties of the structure. A linear transformation between the actuator degrees of freedom and any other desired set is easy to implement, and can be very useful. The transformation can be described in matrix form as :

$$\mathbf{d} = \mathbf{T} \bar{\mathbf{d}} \quad (2.15)$$

where  $\mathbf{d}$  is the displacement vector in actuator coordinates

$\mathbf{T}$  is a user supplied transformation matrix

$\bar{\mathbf{d}}$  is the displacement vector in a new coordinate system

The equations of motion become :

$$\mathbf{M} \mathbf{T} \bar{\mathbf{a}} + \mathbf{C} \mathbf{T} \bar{\mathbf{v}} + \mathbf{r} = \mathbf{f} \quad (2.16)$$

Premultiplying by the force transformation matrix, which is the transpose of  $\mathbf{T}$ , gives :

$$\mathbf{T}^T \mathbf{M} \mathbf{T} \bar{\mathbf{a}} + \mathbf{T}^T \mathbf{C} \mathbf{T} \bar{\mathbf{v}} + \mathbf{T}^T \mathbf{r} = \mathbf{T}^T \mathbf{f} \quad (2.17)$$

Rewriting in the new coordinate system, we have :

$$\bar{\mathbf{M}} \bar{\mathbf{a}} + \bar{\mathbf{C}} \bar{\mathbf{v}} + \bar{\mathbf{r}} = \bar{\mathbf{f}} \quad (2.18)$$

$$\bar{\mathbf{f}} = \bar{\mathbf{M}} \bar{\mathbf{B}} \mathbf{a}_g \quad (2.19)$$

In this form the user would supply information in the new coordinate system ( $\bar{\mathbf{M}}$ ,  $\bar{\mathbf{C}}$ ,  $\bar{\mathbf{B}}$  and  $\mathbf{T}$ ), and the solution algorithm would be :

- calculate  $\bar{\mathbf{d}}_{i+1}$
- impose  $\mathbf{d}_{i+1} = \mathbf{T} \bar{\mathbf{d}}_{i+1}$
- measure  $\mathbf{r}_{i+1}$
- calculate  $\bar{\mathbf{r}}_{i+1} = \mathbf{T}^T \mathbf{r}_{i+1}$

- calculate  $\bar{\mathbf{a}}_{i+1}$  and  $\bar{\mathbf{v}}_{i+1}$
- continue

### 2.3.2.1 Geometric Corrections

In a nonplanar test, such as the one described in Chapter 4, the finite actuator length may induce geometric displacement errors as shown in Fig. 2.3. The transformation of both actuator force and structural displacement into the internal coordinate system may in this case be nonlinear. The solution algorithm described for linear coordinate transformations would still apply, since the actuator forces would need to be transformed to the internal coordinate system, and the internal displacements would need to be transformed into appropriate actuator displacements, but the transformations would be performed by general subroutines rather than by simple matrix multiplication.

### 2.3.3 Reduction of Degrees of Freedom

In an experiment where there are many actuators, it is possible to perform the test in terms of a reduced set of degrees of freedom by using a set of Ritz shape functions. The implementation would be very similar to the general coordinate transformation described above, except that  $\mathbf{T}$  would not be square, and the number of degrees of freedom in the equations of motion would be less than the number of actuators. This approach would ease the numerical stability constraint on  $\Delta t$  by only including the lower modes of a complex structure. That is, the maximum natural frequency of the system is reduced. The penalty, of course, is that by selecting Ritz shapes the actual response is constrained, and effects like soft story formation may be lost. Since the purpose of the pseudodynamic method is to determine realistic response histories, this method should be used with caution, and in light of the globally stable integration scheme described in Chapter 6, the method may not be necessary.

### 2.3.4 Geometric Stiffness

In some tests a specimen may not have actual masses installed to simulate realistic gravity loads. This is possible in a pseudodynamic test because the inertial forces are modeled analytically.

It may, however, be desirable in these tests to approximate the geometric stiffness effects of the missing mass. A simple linear correction can be achieved by allowing the user to supply a geometric stiffness matrix for the structure and using this matrix to correct the measured force vector in terms of the current displacements, as in :

$$\bar{\mathbf{r}} = \mathbf{r} - \mathbf{K}_g \mathbf{d} \quad (2.20)$$

where  $\bar{\mathbf{r}}$  is the modified force vector

$\mathbf{K}_g$  is the user specified geometric stiffness matrix

The researcher must decide whether this approach is appropriate for a given experiment, since the gravity loads may actually be necessary to ensure the proper stress states exist in structural members, particularly in columns.

## 2.4 Experimental Error Effects

In a pseudodynamic test, any errors occurring while imposing a desired displacement or in measuring restoring forces at a given step tend to propagate throughout the remainder of the test. These errors are the most important indicator of the quality of test results in a pseudodynamic test, and have been extensively studied [8,12,13,20,21,22]. Performing pseudodynamic tests without considering these error effects will almost certainly lead to poor results, but it is now clear that if the significant errors are minimized very good results can be achieved.

### 2.4.1 Types of Errors

Shing and Mahin [8] categorized errors as either systematic or random, where systematic errors were directly related to structural response and random errors were independent of the structural behavior. It was found that small random errors did not significantly effect the structural response, but certain types of systematic errors could dramatically effect the response, even when the individual stepwise errors were very small. Errors introduced by imposing incorrect structural displacements result in an incorrect measured force vector. If each incremental displacement is systematically incorrect (either too large or too small) the errors would actually numerically add or dissipate energy. Such energy effects can have a significant influence on the response of the system.

Other errors that affect the accuracy of the restoring force vector, such as relaxation and rate of loading effects, can also play an important role in the response, even though they are not systematic in the same sense.

When imposed incremental displacements are smaller than (lagging behind) the desired displacement, it has been found that energy is numerically added into the system. This lagging results in spuriously amplified responses, especially in higher modes, and the high frequency response can quickly contaminate the desired structural response. Applying excessive incremental displacements, or 'overshooting', numerically dissipates energy and is characterized by an excessively damped response.

Error propagation effects have been seen in actual tests [20]. Although compensation techniques to mitigate the effects of error contributions have been proposed [8,20,22], the best technique is to avoid introducing errors of the type that affect the test results. The verification tests in Chapter 4 show that significant systematic errors can be almost completely eliminated using existing electro-hydraulic control equipment and a suitable implementation of the pseudodynamic algorithm.

In evaluating the performance of a pseudodynamic experimental setup, some of the most useful information is the error time history for each actuator. This time history gives the difference, at each step of the test, between calculated and actually imposed displacements for each actuator. If a fast Fourier transform (FFT) of these records shows that the error has a significant peak at one or more of the structural natural frequencies, then there is a problem with the setup that must be resolved before performing the actual test. These errors can be detected on low level elastic tests that do not cause damage to the specimen. The FFT of each actuator's error history is such an important measure, that it should probably be monitored during a test by doing a running window FFT to ensure that the test is proceeding without error. In addition to these displacement errors, it may also be necessary to monitor the magnitude of the force relaxation effect in nonlinear tests.

Previous work [8,20,21,22] has shown that inelastic tests can produce good results, even when stepwise errors are present. There are several reasons for this. As the structure yields a displacement

error will generally produce a smaller error in the measured forces. More important, however, the hysteretic energy dissipation of the structure dominates the smaller numerical energy effects of errors. Although this is good, since the pseudodynamic test method is intended primarily for simulating nonlinear dynamic response, it has been found that errors can in fact be reduced to the point where accurate elastic results are possible, making the confidence in the inelastic results even greater. In Chapter 3, sources of error and their likely effects are identified, together with specific recommendations for reducing important types of errors.

### 3. IMPLEMENTATION DETAILS

#### 3.0 Introduction

The pseudodynamic test method can be a powerful tool, but the experience of many tests has shown that it is the attention to experimental implementation that ultimately leads to good results. Successful tests require good hardware that is properly adjusted, proper setup of the physical test apparatus, and a good implementation of the pseudodynamic test method in the controlling software. The hardware concerns will be largely related to the performance of the electro-hydraulic control loop that is responsible for imposing specified displacement patterns on the structure. The software that runs the experiment must be tuned to the capabilities of the hardware, and must sometimes compensate for known hardware inadequacies and quirks. This Chapter will present some of the accumulated knowledge on how to successfully perform tests, and how to design the major software components. Major sources of error will be identified, together with possible compensation techniques. A reasonable software layout will be presented, and general information about the behavior of electro-hydraulic systems under displacement control will be given.

#### 3.1 Sources of Errors

The errors of interest here are those that enter into the solution of the equations of motion from the experimental interface. These errors can come from various components in a pseudodynamic test, which are symbolically shown in Fig 3.1. Provided computed displacements are used in computations, experimental errors enter into the solution of the equations of motion through the measured restoring force vector. Force errors are, however, sensitive to position error, and can be influenced by rate of loading and relaxation effects. Intrinsic errors, such as discrete parameter modeling of the structural system and step-by-step integration of the equations of motion are shared with analytical methods and cannot be removed from the pseudodynamic test method. These errors should be considered, but can be investigated using conventional analytical methods.

Many components in the physical test implementation can introduce errors, and the effect of each of these errors must be understood. In each of the following subsections, a source of error is

identified as well as its effect on a pseudodynamic test.

### 3.1.1 Digital to Analog (D/A) Converter

The D/A converter is the component through which the computer sends out actuator command voltages that represent desired displacements. The value of the displacement variables within the controlling program must be accurately converted into voltages that are used as a command signal by the electro-hydraulic control system. The D/A converter is the first of three electronic devices responsible for imposing displacements correctly. The hydraulic controller must make the feedback signal from the transducer equal to the command from the D/A converter, and the transducer/conditioner must give the same relation between volts and displacement units that the D/A converter has used.

The D/A device is often categorized by the number of bits of control (for example a 12 or 14 bit converter). The number of bits is a measure of the resolution of the converter, in that the full scale range of the device is discretized into  $2^n$  steps, where  $n$  is the number of bits. Thus, a 12 bit converter, whose output is  $\pm 10$  volts, has a resolution of  $20/2^{12} = 0.0049$  volts. There is a calibration constant associated with each D/A converter that gives the number of physical units moved for a one bit change in D/A output.

The D/A calibration factor is the most crucial calibration constant in a pseudodynamic test. Other factors may change apparent specimen stiffness, but miscalibration of the D/A converter results in precisely the systematic type of errors that must be avoided. In generating displacement signals, the pseudodynamic algorithm calculates incremental displacements at each step and then calculates the number of bits to apply to produce the desired incremental change. Thus, if the incremental displacement is erroneously converted to a bit change, either consistent lagging or overshooting behavior will result.

The D/A calibration factor depends on three things : 1) the relation between bits and volts for each D/A board; 2) the relation between volts and displacement units for the associated transducer; 3) the amount of command signal attenuation introduced by the servo-controller. It is implicitly assumed here that the controller is capable of setting the command and feedback signals

to be equal at all times, which has proven to be a reasonable assumption. To minimize the potential for error in calculating the D/A constant, one should take A/D samples of the controller attenuated command signal as if it were the actuator position feedback signal. With the hydraulic system turned off, many readings can be taken over the full range of D/A output, and a least squares fit can be performed to establish the calibration constant. In this fashion, all relevant equipment is included in calibration, resulting in the best possible calibration factor.

### 3.1.2 Analog to Digital (A/D) Converter

The A/D converter is responsible for converting all the analog signals of interest in an experiment to digital values suitable for storage in the computer running the experiment. As with the D/A converter, the resolution is specified by the number of bits, such as a 14 bit converter. There are a variety of errors that have been observed with A/D converters, some of which have very serious implications for a pseudodynamic test.

To take advantage of the resolution of the converter, one must select an appropriate range. Considerable precision is lost if low level tests are performed using a subrange of the available bits. The ranging problem can be overcome with A/D converters that have programmable gains, so that on a low level test the maximum number of bits could be returned for a smaller voltage reading, without redoing the transducer calibration.

The most serious problem is that there are occasional 'glitches' that cause apparently arbitrary readings to be taken. These glitches can be substantially different from the actual data value. In a conventional experiment where data is merely recorded, the bad readings can be ignored. In a pseudodynamic test, the bad readings may occur in one of the restoring force channels, causing the solution of the equations of motion to be incorrect. Even worse, although the measured displacements should not be used in the solution of the equations of motion, they are used in calculating the desired displacement increment for a given step. The displacement increment is given by the difference of the new calculated displacement and the previous measured displacement for each actuator. Clearly, if a measured displacement value is substantially in error, a catastrophic displacement increment command may be sent to the actuators. It is suggested that consecutive data

readings be taken until all data values are repeated to within  $\epsilon$  bits, where  $\epsilon$  is a user specified value. This technique is used in the Berkeley test facility and typical tolerances are 4 or 5 bits on a 14 bit converter (ie. 4 out of 16384 bits).

In addition to the large errors introduced by glitches, the D/A converter also contains low level noise, where a given voltage can be converted to digital numbers that differ in the lower order bits. The slight randomness in conversion could be reduced by averaging a few readings. Using an average would also reduce the contribution of electrical noise on the analog data line. The best approach would be to use a subroutine to get a set of clean data readings, and this routine would both guard against glitches and remove noise through averaging.

The last problem that must be considered for the A/D device is the linearity of the conversions. In the A/D system used at Berkeley, a plot of voltage versus bits over the full range of  $\pm 10$  volts showed that although the positive and negative portions varied linearly and had equal slopes, there was a three bit discontinuity at the origin. The system software was modified to account for this effect, since it was systematic and occurred in all data channels.

### 3.1.3 Displacement Transducers

The only place where digital displacement values are used in the pseudodynamic algorithm is in the calculation of incremental displacements to be applied using the D/A hardware. The analog representation of displacements, however, is of crucial importance to the displacement control loop (electro-hydraulic control loop). Since the computer controls displacements by sending out voltage command signals to each servo-controller, and the controller moves the specimen until command and feedback signals are equal, it is important that the displacement feedback voltages be accurate. Otherwise, a specimen will be in a displacement configuration that is different than the computer "thinks" it should be in. This type of error is undetectable from the controlling software, since it implicitly assumed that the relation between physical displacement and volts is exactly as specified by the calibration constant specified to the program. For example, if a 2 volt signal should indicate a 1 inch (25.4 mm) displacement, the specimen may actually be at 1.1 inches (27.9 mm) due to transducer miscalibration or nonlinearity. The computer cannot detect this, since the correct

voltage has been applied and the computer has no other understanding of physical displacements. These position errors will be reflected in an erroneous force vector, since the restoring force depends on the actual displacements imposed.

It is necessary, therefore, that the transducers and associated conditioning amplifiers have small nonlinearities. Linear potentiometers have been found to be unacceptably nonlinear. The transducers should also be able to resolve small changes in displacement, and should be able to reproduce repeated readings when a physical position is approached from either direction. This requirement ensures that the transducer does not trace a hysteresis loop while cycling. Such a loop would cause energy dissipation errors in a pseudodynamic test. These requirements eliminate many classes of transducers, particularly those that use any form of mechanical contact for their operation, since this tends to induce hysteresis, or those whose design results in stepped output, giving limited resolution.

A new type of displacement transducer, based on an electro-magnetic principle overcomes most of the problems described above, and has successfully been used in the Berkeley system. The device is manufactured by Temposonic, Inc. and the model used at Berkeley is a  $\pm 6$  inch model ( $\pm 152$  mm) that is factory calibrated to give a  $\pm 10$  volt output at the maximum displacements. Tests of the transducer on a calibration bench showed that the worst nonlinearity over the full range was less than 0.002 inches (0.05 mm). The resolution is so fine that it is below the typical noise level in analog lines, and the repeatability is better than 0.002% of full scale.

In addition to using a high quality displacement transducer, one must also select appropriate connection details. This may entail building separate isolated reference frames for the transducers, and also designing the mounting system so the desired global displacements are measured as closely as possible. Using actuator supports as the displacement reference frame is usually a poor idea, since the supports may move as the load is applied, due to flexibility or slippage. Motion of the actuator supports would result in incorrect readings of global displacements through the transducers. Accurate global measurement is often aided by using long transducer connectors, so that local effects like specimen twist do not effect global readings. If long connectors are used, care must be

taken to avoid axial distortion in the connectors. In particular, using long lengths of piano wire under tension has proven to give poor results. Thin walled aluminum tubing has given much better results.

#### **3.1.4 Force Transducers**

The force transducers used in pseudodynamic testing are installed between the actuator and the specimen, often as part of the actuator assembly. The transducers are standard strain gauge based load cells that have been calibrated in a testing machine over a range larger than the expected test range to ensure linearity. One must also consider nonlinearity introduced by the conditioning amplifier. Low quality amplifiers have been found to introduce significant errors. Errors in miscalibration of the force transducer will cause an apparent change in structural stiffness and, therefore, in the natural frequencies of the system. However, the miscalibration errors will not cause numerical energy changes in the system like lagging or overshooting errors would.

#### **3.1.5 Friction**

The connection of the specimen to actuators is a physical constraint, and often additional constraints are added to the system to limit motion. Teflon sliders, for example, are often used to limit out of plane motion. The connectors and actuator clevises induce friction as the specimen is moved, and this friction causes energy dissipation that would not be present in a prototype tested dynamically. This is especially important for small specimens. A well designed experimental setup will attempt to reduce friction effects, but some friction is unavoidable. The inherent damping in the system should be established using a pseudodynamic free vibration test before adding additional damping using a viscous damping matrix or a dissipative integration algorithm.

### **3.2 Electro-Hydraulic Control Loop**

In performing a pseudodynamic test, it is assumed that the displacement history specified by the ramp generator output is accurately imposed on the test specimen by the electro-hydraulic control system. Experience has shown that this assumption is justified, if good transducers are used and the controller is adjusted properly. A series of tests was performed at Berkeley to study the

response of the servo-loop during linear displacement ramps, some of the results are shown in Fig. 3.2. The accuracy and stability of the servocontrol loop is probably the most important parameter in pseudodynamic testing, due to its influence on error propagation. Consequently, the behavior of the displacement control loop must be predictable and well understood.

Considerable information is available describing basic servo-loop operation. For example, overall loop behavior is described by Merrit [36] as well as in various technical bulletins [37,39], and in equipment descriptions supplied by manufacturers, such as Moog [38] and MTS [39]. Theoretical studies of control loops are underway at the University of Michigan, Ann Arbor [6] in an effort to guaranty the accuracy and stability necessary in the pseudodynamic test method. However, much of the available information on loop behavior is conceptual or theoretical in nature. Where quantitative data are provided, they are usually related to manufacturer's minimum performance specifications rather than real system behavior. In this section, some practical and theoretical information on performance of conventional closed loop displacement control systems is reviewed.

Although very accurate displacement control is achievable, there are additional problems associated with testing stiff multiple degree of freedom structural systems. In such systems, even minute displacement errors can cause significant errors in the restoring force vector. It has been found during pseudodynamic tests that systems responding in lower mode displacement patterns had force vectors that contained significant higher mode contributions due to small displacement errors and large stiffness coupling. Such errors could be overcome by running the test under force control, and a recommendation for such a system will be made in Chapter 6.

### 3.2.1 Description of a Displacement Control Loop

There are four basic components in a displacement control loop: a servo controller, a servo-valve, an actuator and a displacement transducer, as shown in Fig. 3.3. As discussed subsequently, the test specimen and support apparatus will also affect dynamic loop behavior, but first the operation of the four primary components will be described individually.

### 3.2.1.1 The Servovalve

The servovalve is an electromechanical device that directs oil flow to either end of a double acting actuator in response to an input current of varying magnitude and direction. The fluid flow increases with increasing current, up to the rated flow that is specified at the peak rated current of the valve. This rated flow is typically specified by the manufacturer in terms of the flow [in gallons per minute (gpm)] at the rated valve current with 1000 psi (6.89 MPa) system supply pressure. Typical system supply pressures are on the order of 3000 psi (20.7 MPa). When no external loads are applied to the actuator the pressure drop across the valve can exceed 1000 psi (20.7 MPa). Thus, flows larger than the rated capacity are possible. Conversely, as external loads increase, the available pressure drop across the valve decreases, resulting in decreased flow capacity. When the external load becomes equal to the static load capacity of the actuator, no further forward movement of the actuator is possible.

This flow relationship is graphically described in a typical servovalve flow curve, given in Fig. 3.4. Note that when a load is applied, even at zero current there is oil flow due to leakage across both the valve spool and the actuator piston seals.

The natural frequency of a servovalve is the main characteristic used to describe its dynamic behavior. This frequency is defined as the point where its response signal lags behind the command signal by  $90^\circ$  for a sinusoidal input motion. For a particular valve size, the natural frequency will increase with both increasing supply pressure and decreasing amplitude motion. Valves that have higher flow capacity will have lower natural frequencies in general, although for a given valve size, higher quality valves have higher natural frequencies. This frequency is specified by the manufacturer. As an example, a good 10 gpm (0.63 liter/sec) valve at its full rated current in a 3000 psi (20.7 MPa) hydraulic system might be expected to have a natural frequency of about 120 Hz. The frequency is important for both the ability to accurately trace desired signals, and also in stability considerations. In both cases, higher natural frequencies are better than lower ones, all other things being equal.

### 3.2.1.2 The Actuator

The parameters used to describe an actuator are its total stroke and its static force capacity, given by the product of the system supply pressure and the piston area. The oil column acts as a spring and its stiffness is approximately given by [37]:

$$K'_A = \frac{4A\beta}{L} \quad (3.1)$$

where  $K'_A$  = oil column stiffness (lb/in)

$A$  = actuator piston area (in<sup>2</sup>)

$\beta$  = bulk modulus of hydraulic fluid (psi)

$L$  = actuator total stroke (in)

Total actuator stiffness also includes the stiffness of the drive linkage, such as load cells and clevises, but the drive linkage is usually much stiffer than the oil column and is therefore often assumed inextensible. In addition, the apparent actuator stiffness varies with leakage across the piston, compliance of the hydraulic supply lines and the presence of entrained air in the hydraulic fluid (which directly affects the fluid's bulk modulus). The stiffness of the actuator support is not included in the actuator stiffness, but plays an important part in the servo loop behavior and will be discussed separately.

### 3.2.1.3 The Displacement Feedback Signal

The displacement transducer and its signal conditioner convert a measured displacement into an electrical signal (typically full scale displacements giving a  $\pm 10$  volt output). The characteristics of displacement transducers were discussed in Section 3.1.2.

### 3.2.1.4 The Electro-Hydraulic Controller

The last loop component is the servo-controller. It has considerable influence on overall loop behavior, primarily through the setting of controller gain. In the controller the command signal ( $E_C$ ) is compared with the displacement transducer output signal ( $E_T$ ). Any position error ( $E_C - E_T$ ) is amplified, producing a current used to drive the servovalve. This in turn causes oil

flow to correct the error. It is important to note that only voltages are compared. The relation between voltage and displacement is given only by the transducer calibration, so it is essential to have the transducer accurately calibrated or erroneous displacements will be imposed. The controller gain setting, in milliamps of valve current per volt of displacement error, determines the amount of valve current resulting from a given position error. In a proportional controller, the gain effectively controls the displacement error necessary to move the actuator at a specified velocity. Thus, the gain setting controls how closely the loop follows the command signal and is a very important parameter in predicting loop accuracy and stability. It is possible to use velocity, acceleration or force instead of (or in addition to) displacement feedback, but controllers using these inputs are not commonly used for structural testing. Although there may be cases where these controllers may be desirable, they will not be discussed here.

### 3.2.2 Servo Loop Behavior

A block diagram of a proportional displacement control loop is shown in Fig. 3.4. As the command signal changes, the actuator moves in order to reduce the error. A constant velocity command signal (a linear ramp) will cause the errors to initially increase as the response lags. When the two velocities become equal, the displacement error remains constant and the overall response is characterized by the lag time between the two signals. This lag time is primarily a function of the controller gain setting. Proper gain settings result in an accurate reproduction of the command signal with a small lag time. When the command signal is constantly changing the controller will not be able to remove the error but a proper gain setting will ensure that the response is very close to that specified. When gains are low, errors become large and response is sluggish. However, excessive gain will cause the system to become unstable, resulting in uncontrolled oscillation.

An external force ( $F_D$ ) applied to the actuator can cause movement without a change in the displacement command signal. The actuator must then move in the direction opposite to the force input in order to correct this displacement offset, but this requires an error signal of finite magnitude to be developed. The magnitude of the displacement error is minimized by having a high

controller gain. The overall loop stiffness against such force inputs is given by [37] :

$$\frac{F_D}{x} = 20K_L \left( \frac{A^2 P_S}{Q_R} \right) \quad (3.2)$$

where  $F_D$  = force disturbance (lbs)  
 $x$  = resulting displacement error (in)  
 $A$  = actuator piston area (in<sup>2</sup>)  
 $P_S$  = system supply pressure (psi)  
 $Q_R$  = rated valve flow capacity (in<sup>3</sup>/sec)

The term  $K_L$  is the overall loop gain, an important parameter given by [37] :

$$K_L = \frac{K_C K_V K_T}{A} \quad (3.3)$$

where  $K_L$  = loop gain (sec<sup>-1</sup>)  
 $K_C$  = controller gain (ma/volt)  
 $K_V$  = servovalve flow gain (in<sup>3</sup>/ma)  
 $K_T$  = transducer gain (volt/in)

A typical system with a large actuator and a system supply pressure of 3000 psi, is extremely stiff against such external force inputs. In Eq. (3.2) it is assumed that the structural displacements are measured relative to ground, so the actuator support compliance is included within the loop. Support movement will result in increased flow demands in order to position the specimen accurately. If the displacement feedback is measured relative to the support (directly across the actuator), actuator and support stiffnesses act in series and the overall system cannot be stiffer than the support. Thus, transducer location plays an important role in overall system stiffness.

The accuracy attainable can be estimated considering servovalve anomalies such as hysteresis, threshold and null shifts, as well as friction and lost motion in the drive linkage. Valve threshold is the increment of input current required to produce a change of flow, and hysteresis is the maximum difference in input currents required to produce the same flow after a complete cycle through the flow range. The null shift is the change of input current required to maintain a specified flow

as operating conditions, such as temperature or supply pressure, change. In a tight system with no lost motion (tight clevises), up to 5% of the rated current is used to overcome valve threshold and an additional 5% could be used to overcome actuator friction. This 10% signal with no movement can be represented as a position uncertainty error given by [37]:

$$X_U = \frac{Q_R}{10 A K_L} \quad (3.4)$$

where  $X_U$  = position uncertainty error (in)

$Q_R$  = rated flow (in<sup>3</sup>/sec)

In addition, there is a position error due to the lag time between command and response signals (see Fig. 3.2) given by [37]:

$$X_L = \frac{V}{K_L} \quad (3.5)$$

where  $X_L$  = position error due to response lag (in)

$V$  = actuator velocity (in/sec)

This lag error is not particularly important during a conventional pseudodynamic test, since no data sampling occurs during the ramp, but it is necessary to wait somewhat after ramp completion to allow the response to get to the command level. These errors are both minimized by high loop gains, but again overall accuracy is also limited by that of the transducer.

The actuator velocity capabilities are given in terms of the system supply pressure, the actuator area and the valve flow equations. The no load flow is given as :

$$Q_{NL} = Q_R \sqrt{P_S / 1000} \quad (3.6)$$

where  $Q_{NL}$  = flow with no external load (in<sup>3</sup>/sec)

$Q_R$  = rated flow capacity (in<sup>3</sup>/sec)

$P_S$  = system supply pressure (psi)

Now, the loaded flow capacity is :

$$Q_L = Q_{NL} \sqrt{(P_S - P_L) / P_S} \quad (3.7a)$$

or

$$Q_L = Q_R \sqrt{(P_S - P_L)/1000} \quad (3.7b)$$

where  $P_L$  = external force over piston area (psi)

The maximum actuator velocity under load is then given by flow divided by piston area :

$$V_{\max} = \frac{Q_R}{A} \sqrt{(P_S - F/A)/1000} \quad (3.8)$$

where  $V_{\max}$  = maximum loaded actuator velocity (in/sec)

$F$  = external force (lbs)

Based on this, a common rule of thumb for systems operating at 3000 psi is that the rated flow can be achieved for loads up to about 2/3 of the static actuator capacity. It is, however, desirable to use Eq. (3.8) with a suitable safety factor to determine ramp velocities. By doing this, one can take full advantage of available flow capacity at all load levels to allow an experiment to run quickly.

The loop behavior described above has been quasi-static in nature, but it must be recognized that the actual servo-loop is a dynamic system as indicated in Fig. 3.5. It has been found that optimal gain depends on specimen mass and stiffness as well as electro-hydraulic components. The most common procedure for adjusting system gains is to test a prototype and increase gains until adequate response is achieved. The controllers in use at Berkeley (MTS model 406) were modified to allow a much higher servo-controller gain to be used, and with the modified gain circuit it was, in fact, possible to make the loop unstable. When performing an actual test, the gains should be nowhere near the stability limit, since instability will not only halt the test, but may also destroy the specimen.

Increasing specimen stiffness does not lead to instability, but increasing the mass may cause the system to become unstable. Conceptually, as the natural frequency of the complete system decreases, it may be necessary to decrease the system gain. Although unfortunate, no more formal means are available for setting system gain, and the servo-controller manufacturer's guidelines should be followed.

A simple one degree of freedom test specimen was used to investigate the response characteristics described above. Some of the results of this test are shown in Fig. 3.2. The response graphs show that there is a larger lag time when gains are low, but that excessive gains can cause instability. Also, as the force level on the actuator increases, flow limiting can be seen.

### 3.3 Software Layout

In this section major components of the basic software needed to implement the pseudodynamic method will be described. The purpose of the section is not to provide actual code or to discuss what the user interface should look like. Rather, it will describe in general terms how the pseudodynamic algorithm should be implemented. It will be assumed that software exists to perform auxiliary tasks such as calibration, data storage, analysis and plotting. These operations are fundamental to a laboratory computer and are not unique needs of a pseudodynamic system. Also, special purpose routines may be desirable, but they will not be described here. These would include routines to measure specimen stiffness or flexibility properties, unloading utilities to bring actuator forces to zero and general purpose positioning utilities that would allow the specimen to be moved into arbitrary specified positions. The information presented will primarily relate to the main loop of the controlling program, in which the pseudodynamic algorithm is coded.

Some initialization must occur before entering the main loop of the program. User specified mass and damping matrices must be input, as well as control parameters for the numerical integration procedure. Also, routines to perform coordinate transformations must be supplied. The initial displacement, velocity and acceleration of the specimen must be set, and an initial data reading of all channels must be taken to establish offsets for zero readings. Also, the initial ground motion component(s) must be read so that the force vector can be calculated. It is also possible to stop and subsequently restart a test. If this is done, the initialization code must then establish appropriate displacement, velocity and acceleration values and skip to the correct step of the ground motion record. The specimen must be moved into the correct position before the main loop is entered.

The main loop of the program would contain the following operations on each step of a test. For convenience of notation it is assumed here that the actuators have just completed the ramps for

step  $i$ .

- Read all data channels. One must ensure that the data reading is accurate. A clean data reading can be achieved by requiring that two consecutive data readings be the same to within some specified tolerance. Also, averaging several readings could be used to reduce the amount of low level noise in the signal. After a good reading is established, all data should be checked to make sure it is within bounds. If a full scale reading is detected, the user should have the opportunity to take appropriate action, possibly aborting the test.

- Extract the restoring forces  $r_i$  from the data vector and apply user specified transformations if the computations are to be performed in a coordinate system other than that given by the actuator locations. This transformation may be nonlinear, so a simple matrix multiply cannot generally be used. There are several ways in which a general transformation could be implemented. One could provide an interpreter that would allow the user to symbolically describe the desired transformations, using a simple language. If speed is a major factor, it may be better to dynamically link object code modules. A simple call interface could be specified to allow information to be passed in and out of the generic routine.

- Solve the equations of motion. The solution would involve solving for  $a_i$  and  $v_i$ , using the measured current restoring force vector and the previously calculated displacement vector  $d_i$ . After the state at step  $i$  is completely established, the displacements on the next step  $d_{i+1}$  are calculated and checked to make sure they are within acceptable limits. It would probably be best to provide a generic implementation where the modified form of the Newmark method is used and all parameters could be user specified. In addition, dynamic loading of an alternate object module would allow special case applications like substructuring to be performed without the need to relink the executable program.

- The calculated displacements are transformed to those that should be applied to the actuators, if a different internal coordinate system is used. The transformation should be implemented like the force transformation described above. Once the new actuator displacements are known, desired incremental displacements can be calculated by subtracting the last measured displacement

from the new desired displacement. Using the measured displacements in this way ensures that the specimen does not wander away from the desired position when errors occur.

- Using the incremental displacements and known information about each actuator, calculate the duration of the ramp for the next step. The duration should be the minimum value that ensures that specified actuator velocities are not exceeded. The velocity/load relationship given in Eq. (3.8) should be used in the calculation as well the specified no-load velocity limit. Minimizing the ramp duration allows the test to proceed more quickly and has also been useful in mitigating the force relaxation effect described in Chapter 4.

- Send the desired displacement increments to the D/A hardware. In the Berkeley system, the D/A boards are given a the desired increment and a duration, and control returns immediately to the hosts computer.

- While the new displacements are being applied, perform the following tasks. Write the data for the current step to the disk. Read in the next ground motion step and calculate the force vector using Eq. (2.14). Selected data can be reduced and plotted.

- Wait until the D/A boards have completed. This is achieved by polling the hardware, so the program 'busy waits' at this point. When the ramps complete, take an immediate reading of all channels. As usual, the data reading should be inspected to ensure that it is glitch free. This immediate data can be used to minimize the force relaxation problem, as described in Section 4.3.5. If the the force levels increased in magnitude on the current step, and the immediate reading is larger in magnitude than the delayed reading, the immediate value should be used, otherwise the delayed value should be used.

- Wait a user specified interval for the displacements to converge to the command values. the duration of this wait is a function of the servo-control loop gain. In inelastic tests, the wait period should be reduced to minimize the force relaxation effects.

### 3.4. Concluding Remarks

The algorithm described here, together with good hardware has given excellent results in the

verification tests performed at Berkeley. The system as described here was used for the nonplanar verification test as described in Chapter 4. A change in the algorithm was implemented, together with some additional hardware to perform the implicit tests described in Chapter 6, but the overall layout was very similar and performed well. The new algorithm proposed in Chapter 6 may, however, be better implemented using a completely new hardware configuration. This possibility is addressed at the end of that Chapter 6.

## 4. NONPLANAR VERIFICATION TESTS

### 4.0 Introduction

Properly formulated equations of motion as presented in Eqs. (2.18) and (2.14) permit pseudodynamic tests of complex three dimensional structures subject to multiple ground acceleration components. Although some simple nonplanar pseudodynamic tests [28,30] have been performed, the resulting responses were only compared to analytical results, making verification of the pseudodynamic method difficult. Verification tests based on shaking table data have, to date, been restricted to low rise planar structures subjected to a single horizontal component of ground motion. A large part of the attractiveness of the pseudodynamic method is in performing tests that could not be performed on conventional shaking tables. Thus, verification studies for three dimensional response simulation under multiple components of excitation would be desirable.

In order to verify the pseudodynamic method for both general structural configuration and multiple component base excitation, a series of matched tests were performed on a shaking table and using the pseudodynamic test method. The shaking table test used only one lateral component of base motion due to limitations of the shaking table. However, the specimen was placed on the table skewed  $45^\circ$  from the direction of excitation. Thus, the input was effectively two correlated components along the structure's major axes. In addition, the structure was designed to be stiffness eccentric, so that torsional as well as translational response components would result. Since shaking tables are unable to perfectly apply specified signals, the measured acceleration of the table was used as input in the pseudodynamic tests. These accelerations included accidental rotational accelerations that occurred during testing. Thus, the input to the pseudodynamic tests consisted of five components of acceleration : two lateral acceleration component and the three rotational acceleration components (pitch, roll and twist). The magnitude of twist and roll components were small, but it was found that the equivalent lateral component due to table pitch was up to 10% of the applied lateral acceleration magnitude. Vertical components of motion were not believed to be important for this test and were disregarded in the formulation.

This chapter will review the design of the specimen and experimental configuration. Problems encountered in performing the pseudodynamic portion of the test will be described, together with the solutions used. The sequence of earthquakes used will be described and the response data will be presented. General hardware and software details were presented in Chapter 3, and only details relevant to the verification test will be presented here.

#### 4.1 The Test Specimen

The specimen was not designed to represent a realistic building, rather it was designed to satisfy several experimental constraints. It was anticipated that many tests would need to be performed, so a simple one story specimen was selected. The structure consisted of a rigid diaphragm supported on four replaceable columns at its corners. This configuration, shown in Fig. 4.1, allowed three degrees of freedom to completely describe the deck motion. The internal degrees of freedom, used in the solution of the equations of motion, and the external or actuator degrees of freedom are shown in Fig. 4.2. All the results presented later in this chapter are based on the internal degrees of freedom.

At the time of this test only the explicit form of the integration operator was available, so it was necessary to select members with properties such that the highest natural frequency of the structure was low enough to allow a reasonable time step to be used. Reducing the maximum natural frequency was achieved by making the structure flexible with a large mass. Also, it was desirable to make the elastic displacement range as large as possible, so that the behavior of the pseudodynamic method could be compared with simple analytical models. The elastic displacement range is largely a function of the depth and length of the members, which suggested using long slender elements. The top and bottom platforms were extremely rigid compared to the four corner columns so the displacement response is due entirely to deformation in the columns. The columns selected were S3x7.5 sections and had a clear height of 48 inches (1.22 m) between base plates. The yield displacement for structure, assuming the columns to be fixed at both ends, is approximately 0.25 inch (6.4 mm), which is sufficiently large to allow a variety elastic tests to be performed. Finally, since the test was intended to examine nonplanar behavior, the specimen was

designed to have a large stiffness eccentricity to excite torsional behavior even under a single lateral component of base excitation. Figure 4.1 shows that the stiffness eccentricity was introduced by rotating one of the four columns 90°, thereby switching the strong and weak axes of bending.

Two different masses were used in the tests, in the first sequence of tests a 10 kip (44.5 kN) weight was used and for the second series a 14 kip (62.3 kN) weight was used. Table 3.1 shows the mass matrix elements for the internal coordinate system shown in Fig. 4.2. The natural frequencies for the specimen are shown in Table 3.2. The highest natural frequency (in the low mass case) was 7.2 Hz, which results in  $\Delta t < 0.044$  seconds, to satisfy the stability condition given by Eq. (2.6).

The actual pseudodynamic tests and the shaking table tests were performed using columns cut from the same piece of stock. In order to ensure that the pseudodynamic test setup was performing well, extra column stock was purchased so that several sets of test columns could be used while adjusting the system. Such practice of setting up and evaluating a test system is highly recommended, since it allows the system to be fine tuned, removing errors and replacing inadequate equipment without endangering the actual specimen. Many problems were identified in these preliminary tests. These problems are examined in Section 3.3, together with the solutions identified. Once the problems were remedied, the real columns were installed and the exact test sequence performed on the shaking table was reproduced pseudodynamically.

---

Deck Weight	DOF 1 (kip sec <sup>2</sup> /inch)	DOF 2 (kip sec <sup>2</sup> /inch)	DOF 3 (kip sec <sup>2</sup> )
10 kips	0.02591	0.02592	29.2
14 kips	0.03627	0.03627	40.2

**Table 3.1 - Mass Matrix Values (1 kip = 4.448 kN)**

---

The natural frequencies are given in Table 3.2 for all three modes, but preliminary analysis indicated that only the first two modes contributed to the response under earthquake loading. The first mode damping was found to be slightly less than one percent of critical from the free vibration

tests on the shaking table. When tested pseudodynamically, it was found that friction in the clevises dissipated energy equivalent to roughly 1% viscous damping. Therefore, the pseudodynamic tests were performed with a zero viscous damping matrix and with no numerical damping in the time integration algorithm.

---

Deck Weight	Mode 1 (Hz)	Mode 2 (Hz)	Mode 3 (Hz)
10 kips	3.0	4.4	7.2
14 kips	2.5	3.7	6.1

Table 3.2 - Natural Frequencies (1 kip = 4.448 kN)

---

#### 4.2 Experimental Setup

The shaking table setup was simple, it consisted of rigidly attaching the lower deck to the table, with the structure skewed at 45° to the direction of motion, as shown in Fig. 4.3. The instrumentation consisted of displacement potentiometers connected by wire to stationary reference frames, and accelerometers attached to the specimen's upper deck and to the table.

Figure 4.4 shows a detailed layout of the pseudodynamic test implementation. The lower rigid platform was fixed to the test floor and the location of the upper platform was controlled by three actuators. The actuators each had a bore diameter of 8 inches (203 mm), and a static load capacity of 150 kips (445 kN). The actuators for degrees of freedom 1 and 2 used MTS 10 gallon per minute (gpm) servovalves (0.63 liter/sec), and the third actuator used a Dynamic Valve 5 gpm (0.32 liter/sec) servovalve. Three MTS model 406 controllers were used, but the gain circuits were modified, since the default gains were found to be insufficient for accurate control with the actuator/servovalve/transducer combination used. The hydraulic interlock circuits on the three controllers were daisy chained so that excessive error from any controller would cause the entire hydraulic system to depressurize. Each actuator used a Temposonic ±6 inch (±152 mm), ±10 volt transducer, with analog output, for positional feedback. The transducers were connected to an

isolated instrumentation frame rather than to the actuator support frame so that true global specimen motion could be measured. The connection between specimen and reference frame used thin walled aluminum tubes to avoid the distortion inherent in using wire connections. The tubes were also made long, approximately 12 feet (3.66 m), to minimize errors associated with transverse movement. Low friction swivel joints were used to allow lateral motion as well as the transducer extension.

The computer controlling the experiment was a Data General 840 and custom built hardware was used for digital to analog (D/A) conversion of the actuator command signals. The D/A boards used coprocessors to generate linear ramps, where the voltage increment and duration of the ramp were under software control. A NEFF high speed data acquisition was used to convert all analog transducer signals to digital form for storage in disk files. This A/D system could read up to 128 channels and sample at 20 KHz.

During the test, it was found that while running under displacement control, the actuator forces oscillated at a high frequency while the system was moving, as shown in Fig. 4.5. The force oscillations were small, but were present even when the displacement response followed the command signal very closely. These were due to the dynamics of the electro-hydraulic control system. In order to ensure that recorded force signals were reliable, an analog filter was used on each force channel, and the filtered signal was recorded by the data acquisition system. Low pass were used filters that attenuated sharply above 2 Hz. This had no effect on the actual data, since the experiment was run very slowly.

### **4.3 Problems Encountered**

#### **4.3.1 Displacement Errors Due to Experimental Geometry**

The finite length of the actuators and displacement transducers create a global position error, relative to the internal degrees of freedom, as shown in Fig. 4.6. As discussed in Chapter 2, two general transformations can be used to compensate for this. In addition to correcting geometry errors, the transformations described below are used to convert between the internal and external

coordinate systems shown in Fig. 4.2. The actuator forces must be transformed to forces in the internal coordinate system, taking into consideration the actuator angles, and the desired internal displacements must be converted in to an actuator displacement vector that will give the correct global displacements. Both of these transformations will depend on the specimen's current position. The actual numbers in the following equations are a results of the lengths of the actuators and displacement transducers used in the pseudodynamic test, as well as the size of the rigid platform forming the upper deck of the specimen, as shown in Fig. 4.4. Following the notation of Chapter 2, the transformations used between the internal and external coordinate system, including geometric error correction, were (for inch and kip units) :

$$d_1 = \bar{d}_1 - 54 \bar{d}_3 + |\bar{d}_2|/120 \quad (4.1)$$

$$d_2 = \bar{d}_1 + 54 \bar{d}_3 + |\bar{d}_2|/120 \quad (4.2)$$

$$d_3 = \bar{d}_2 + |\bar{d}_1|/76 + 27/38 |\bar{d}_3| \quad (4.3)$$

$$\bar{f}_1 = f_1 + f_2 + \left( \frac{d_2}{76} + \frac{d_3}{8640} \right) \quad (4.4)$$

$$\bar{f}_2 = f_3 + (f_1 + f_2) \left( -\frac{d_1}{306} + \frac{d_2}{340} - \frac{d_3}{102} \right) \quad (4.5)$$

$$\begin{aligned} \bar{f}_3 = 54(f_2 - f_1) + (f_1 + f_2) \left( \frac{23 d_1}{51} - \frac{69 d_2}{170} + \frac{23 d_3}{17} \right) \\ + f_3 \left( \frac{d_1}{2} - \frac{23 d_2}{19} - \frac{d_3}{224} \right) \end{aligned} \quad (4.6)$$

#### 4.3.2 Inaccurate Displacement Feedback

The quality of the displacement feedback signal is important for the physical control of the specimen in the electro-hydraulic control loop. It is also important for the acquisition of accurate restoring force vectors, since the force vector will be in error if the specimen is positioned incorrectly. There were numerous modifications of the instrumentation during the pilot tests to upgrade the quality of the displacement signal. In many cases, removing one problem often revealed inaccuracies elsewhere in the system.

The response of the shaking table specimen dictated using displacement transducers with a range of at least  $\pm 3$  inches ( $\pm 76$  mm). The initial transducers employed were linear potentiometers. These pots had a  $\pm 3$  inch ( $\pm 76$  mm) range, but were quite nonlinear, having real errors on

the order of hundredths of an inch. They also exhibited small hysteresis loops on cycling due to the actual physical contact friction of the internal slider. Additionally, the pots were connected from the actuator mounting frame to the specimen using piano wire. Tension was induced in the wire by stretched rubber bands that kept the transducer retracted. In using this setup, it was found that the apparent system stiffness was different depending on whether the actuator was moving outwards or inwards. This effect was eventually traced to the wire stretching in proportion to the force exerted by the rubber bands. A quick calculation showed that a one ounce change in pull-back force on the wire caused about 0.003 inch stretch over the length of the wire.

The potentiometers were replaced by Temposonic  $\pm 6$  inch ( $\pm 152$  mm) transducers that were found to have nonlinearity errors less than 0.002 inch along the full range, specified to be better than 0.05% of full scale. The transducers work by an electromagnetic principle rather than by mechanical means, therefore, the resolution is excellent and the repeatability is better than 0.002% of full scale. While a variety of methods for inducing constant tension in the wire connectors were investigated, these were eventually abandoned in favor of thin walled aluminum tubing. These tubes were essentially inextensible and had low friction swivel joints at each end to allow lateral motion.

With accurate transducers and inextensible connectors it was still found that the global specimen displacements were incorrect when compared with dial gages. The problem was found to be that the specimen motion was measured relative to the actuator supports. As the actuators applied loads to move the specimen, both the specimen and the actuator supports moved. Although the supports were intended to be rigid, elastic distortion, prying and slippage resulted in small displacements. Thus, the global specimen motion was only 95% of the imposed displacement. Rather than solving the actuator support motion problem by stiffening the reaction frame, displacements were measured relative to a separate, isolated reference frame. Since the errors were linear in nature, this proved to be the simplest solution.

The performance of the system with the Temposonic transducers, rigid connectors and separate reference frame was very good. The displacement signal was used directly as feedback in

the electro-hydraulic control loop, and it was found that any desired displacement could be very accurately imposed by giving the appropriate command voltage to the controller. The finite length of the actuators and displacement transducers made it necessary to correct for geometric errors in software, as described previously, but the electro-hydraulic control loop performed its task of keeping the feedback signal equal to the command signal well.

#### 4.3.3 Force Oscillation

When using displacement control in the electro-hydraulic control loop, it was found that the actuator forces oscillate when the actuators are moving, as shown in Fig. 4.5. This oscillation occurs even when the displacement signal follows the command signal very accurately. The oscillation is due to the controller's changing signals to the servovalve. The peaks are not large, but it would be undesirable to perform the A/D conversion capturing an arbitrary point on the oscillating signal. A more reliable reading can be achieved by low pass filtering the force signal and using the filtered signal as input to the A/D converter. In the nonplanar test each force channel was low-pass filtered removing content above 2 Hz. The filtering process did not remove any of the desired signal because the test was performed slowly. As Fig. 4.5 shows, the filter also induces a slight phase shift in the signal, so that the time lag between ramp completion and A/D sampling should be adjusted to account for this effect.

#### 4.3.4 Poor Control with Increased Mass

The pseudodynamic experimental configuration included a 2 kip (8.9 kN) rigid upper deck and an additional 12 kip (53.4 kN) concrete block. The concrete block was necessary to reproduce the stress state in the columns and also so that the geometric stiffness effect would be the same as on the specimen tested on the shaking table. The hydraulic system was initially tested without the block using a set of test columns, and the controller gain was adjusted to give good control. It was found that when the block was added the gain was excessive and instability developed in the control loop. Adjusting the gains again to give stable response resulted in very sluggish actuator response. The actual displacement took almost a second to converge to the command signal.

The necessity to reduce gain as the system mass increases is a well known property of electro-hydraulic control loops under displacement control [36,37]. For these tests better displacement tracking was desired. Because the gravity load was necessary for the reasons mentioned above, attempts were made to isolate the vertical and horizontal effects of the deck mass. This was done by hanging the mass from the upper deck by long steel cables. Dampers were used to prevent the mass from swinging excessively. Using this configuration, the gravity effects are still reproduced, but each actuator only 'sees' the mass of the upper deck, the inertial mass of the block is essentially hidden from the electro-hydraulic control loop. Suspending the block in this way allowed the gains to be increased again, and the control became much more responsive. While this technique may not be useful in other experimental configurations, it is always necessary to optimize the performance of the displacement control loop as much as possible.

#### 4.3.5 Force Relaxation During Wait Periods

The typical sequence in a pseudodynamic test is : 1) to impose the displacements using linear ramps, 2) to wait a short period, on the order of 1 second after ramp completion, for the displacements to converge to the command signals, 3) to read all the data, 4) to solve the equations of motion, and to repeat the sequence for the next step. The behavior of the test system during these steps was examined in detail by performing a series of experiments in which the displacement and force signals were sampled continuously at a high rate (500 samples per second per channel). The results of this investigation are shown in Figs 4.7 through 4.9.

For elastic level tests, as shown in Fig. 4.7, it was found that as the displacements followed the command signal, the force signals were well behaved and remained essentially proportional to the displacements at all times (ignoring the force oscillations already mentioned). However, when the specimen yielded, and displacement continues in the same direction as shown in Fig. 4.8, the force levels drop rapidly as the actuators slow and stop (during the wait periods). The drop, in the steel specimens tested, was as large as 10% in 1.5 seconds. When a yielded system is unloaded, as in Fig. 4.9, the forces become stable again and the relaxation effect disappears.

This relaxation effect presents a systematic error to the pseudodynamic tests. The energy dissipated during each hysteretic cycle is decreased, since the apparent force levels are reduced, and it was found that the peak response increased slightly. The effects of these errors were non-oscillatory, but were reflected in significant permanent offsets introduced into the displacement response. Earlier tests on hydraulic control showed that smoothly varying ramps, such as haversine functions, were better behaved for elastic specimens. However, the low velocity portion at the end of these smoothly varying ramps would clearly compound the relaxation problem, so for inelastic tests linear ramps seem preferable.

Several changes were made in the pseudodynamic algorithm to attempt to compensate for this relaxation effect. Linear displacement ramps were retained, but the original pseudodynamic formulation used constant duration ramps for all steps of the tests. The specimen is most likely to be yielding as it approaches its maximum displacement. At this point the specimen also is moving at low velocity, and in a pseudodynamic test the actual velocity may be so slow as to introduce relaxation effects. It is desirable to keep the wait states as short as possible and to keep the specimen moving as quickly as possible in such cases. The controlling program was, therefore, modified so that the user could specify a maximum velocity for each actuator. The program would then examine the desired displacement increments for each actuator, and calculate the minimum ramp duration so that no actuator would exceed the specified velocity. Using this technique, the specimen was kept moving quickly, since on each step at least one actuator would be moving at the maximum specified velocity. Also, the test duration decreased dramatically, since the ramp duration on the many small increments during low level elastic response became much smaller. In computing the maximum velocity for each actuator, the dependence of servovalve flow capacity on applied loads must also be considered. These velocity-load relationships were discussed in Chapter 3.

In addition to keeping the specimen moving, the data sampling strategy was also changed to attempt to capture the forces before relaxation occurred. Based on observations of behavior during the ramps, the new strategy was to take a reading of all channels immediately after ramp completion, and a second sample after the usual wait period. If the force magnitude increases across the

step, and the immediate reading has a larger magnitude than the reading after the wait, then the immediate reading is used for the dynamic calculations, otherwise the later reading is used. For nonlinear tests the duration of the wait period was also reduced to 0.8 seconds, from 1.5 seconds used in the elastic tests. More refined methods requiring several data readings during ramp motion, and curve fitting could be used but were not necessary in these tests. Special purpose response procedures to compensate for strain rate and relaxation effects may be appropriate in some tests.

The changes made to the algorithm improved the response in the nonlinear runs dramatically. The response envelope improved and the permanent offsets were closer to the offsets measured in the shaking table tests.

#### 4.4 Test Sequence

Once the reliability of the test procedure and setup were verified in the pilot tests, a series of eight earthquakes were run on the specimen using columns cut from the same stock as those used in the shaking table tests. The exact sequence that was run on the shaking table was repeated using the pseudodynamic method, using the measured table lateral accelerations, as well as the accidental rotational table accelerations. Two records were used, the NS component of the 1940 El Centro record and the S74W component of the 1971 Pacoima Dam record. The peak accelerations varied from 0.13 g to 1.6 g. The complete test series is summarized in Table 3.3. As discussed previously, the friction due the pseudodynamic setup, primarily due to the actuator clevises, gave approximately one percent damping in the first mode, so a non-dissipative form of Newmark's method was used for time integration ( $\alpha = \rho = 0$ ).

#### 4.5 Results

The results are presented in Figs 4.10 through 4.41. In order to compare the results more easily, the displacement response is broken into two graphs, the first from 0 to 10 seconds, and the second from 10 to 20 seconds. The displacement values refer to the internal coordinate system. Since the validity of the pseudodynamic results are a function of the magnitude and type of experi-

---

Test Number	Deck Weight (kips)	Earthquake Record	Peak Acceleration (g's)
1	10	1940 El Centro NS	0.13
2	10	1940 El Centro NS	0.26
3	10	1940 El Centro NS	0.96
4	10	1940 El Centro NS	1.56
5	10	1971 Pacoima Dam S74W	0.74
6	14	1940 El Centro NS	0.13
7	14	1940 El Centro NS	1.6
8	14	1971 Pacoima Dam S74W	0.84

Table 3.3 - Test Sequence (1 kip = 4.448 kN)

---

mental errors introduced during the test, the displacement error histories are presented for each actuator, together with a Fast Fourier Transform (FFT) of each signal. That gives an indication of the randomness of the displacement errors. The error results show that the control loop performed well through all tests, since the errors were very small and random in all cases.

The errors were reduced to such a small level in these tests that even Test 1, the elastic level test shown in Figs. 4.10 through 4.13, gave very good correlation between the shaking table and pseudodynamic response. In Tests 2 and 6, shown in Figs. 4.14 to 4.17 and 4.30 to 4.33 respectively, the structural response was just beyond the yield level and again the correlation was excellent. The significant response portions of Tests 1, 2 and 6 are faithfully reproduced, but some of the low level response is not captured perfectly. In elastic tests with such low damping, however, even the slightest shift in natural frequencies can cause significant response changes, so the deviation in the response values may well be due to entering an approximate mass matrix in the pseudodynamic test. Also, the damping characteristics were different, the pseudodynamic tests had a friction damping effect associated with clevises rather than the viscous damping and friction occurring in dynamic tests. This alternate damping form could also account for some of the discrepancies in the low level tests.

The inelastic tests, increasing in magnitude between Tests 3 to 5 and 7 to 8, the overall correlation was again excellent. The envelope magnitudes were very good and individual cycle shapes

were reproduced well. In Tests 3 and 4 there are considerable permanent offsets in the pseudodynamic results. This drift was due to force relaxation effect described in Section 4.3.5. The program changes described in that section were implemented after Test 4. The results of Tests 5, 7 and 8 show that the changes effectively eliminated the drift problem and the results are again very good. As in the elastic tests, there were some errors in the low level response portions of these tests, and again these errors are probably due to the sensitivity of the response to natural frequencies for structures with low damping.

There was no attempt made to 'optimize' the mass matrix to get the best correlation between pseudodynamic and shaking table results, the calculated mass matrix was used in all pseudodynamic tests. The primary performance criterion used to judge the success or failure of the pseudodynamic tests was the FFT's of each actuator's error history, and no parameter adjustments were done other than to remove experimental errors. For comparison, results from an initial test without corrections are shown in Fig 4.42 and can be compared to those shown in Fig. 4.10. It can be seen that the errors introduced in the early test caused a frequency shift in the first mode, leading to incorrect response.

#### 4.6 Conclusions

The results of this nonplanar test show that the pseudodynamic can reliably generate dynamic response results, both elastic and inelastic, for complex structures subjected to multiple components of base excitation. In this test the single lateral component of excitation was decomposed into two equal components along the specimens major axes, so the overall base excitation was two lateral components and three rotational components. The coupling induced by the stiffness eccentricity resulted in nonplanar response even though there was only one effective ground motion component. Since the response to the lateral component was nonplanar, it is reasonable to expect that the method could be equally well used with two independent lateral ground motion components, an application that has very interesting possibilities for structural testing.

The algorithm used for pseudodynamic testing, with the modification described in Section 4.3.5 provided very reliable results. Applying displacements by setting command signals and letting

the electro-hydraulic controller balance command and feedback signals worked very well here. If the feedback signals are reliable, and the controller gain is adjusted properly, the controller is very capable of properly positioning the specimen to any desired location. Of course the computer must generate the correct voltage, using the D/A hardware, for the desired displacement, but it seems that the pseudodynamic algorithm need not be complicated by additional strategies intended to make sure the specimen gets to the desired location. Failure to get to the desired location is an indication of electro-hydraulic control loop problems, not of a pseudodynamic implementation problem. However, for stiff or massive systems it may be necessary to use better controllers to achieve the required level of accuracy.

## 5. RAPID TESTING TECHNIQUE

### 5.0 Introduction

The conventional pseudodynamic test method is not appropriate for structures composed of materials with significant rate sensitivity. Methods in which the present form of the pseudodynamic method is executed at faster rates have been proposed [9]. However, as the test rates approach real time one must account for the fact that real inertial and damping forces are being introduced into the experiment. Error propagation problems may also become more severe due to poorer positional control at higher test rates. A new testing technique, based on force control, has been developed that allows specimens to be tested at speeds approaching real time. These higher speed tests are more demanding on the electro-hydraulic system, requiring high quality controllers and servovalves. However, since each actuator only moves a portion of the structure, the hydraulic control problem is much simpler than that encountered on a shaking table, where both the structure and the table must be moved.

### 5.1 Procedure

The test model must be constructed so as to satisfy standard similitude relationships, as a shake table specimen would be, with mass added so that the modal frequencies change by a factor of the square root of the physical model scale. Real time will refer to the time scale appropriate for the model, which may actually be a compressed time scale relative to the prototype, depending on the scale of the specimen. Experimental time will be numerically equal to the real time, in that both can be used to measure the elapsed time of response. However, an experimental second will take a longer time to physically apply as the rate of testing is reduced.

The specimen is connected to actuators as in a conventional pseudodynamic test, but in addition to force and displacement feedback, acceleration and velocity will also be measured for each degree of freedom. Using analytically modeled mass and damping matrices, the equations of motion are :

$$\mathbf{M} \mathbf{a} + \mathbf{C} \mathbf{v} + \mathbf{r} = \mathbf{f} \quad (5.1)$$

The forcing function  $\mathbf{f}$  can be completely determined as a function of time once the experimental configuration and the mass matrix are established and the rigid base acceleration histories are specified. Using calibration constants in force units per volt for each actuator degree of freedom, analog histories are created for each force component and stored on a multi-track analog tape recorder, or could be generated on the fly with suitable digital to analog hardware. Performing an experiment in real time can be achieved by running the experiment in force control and using the loading function  $\mathbf{f}$  as the command signal to the actuators  $\hat{\mathbf{f}}$ .

$$\hat{\mathbf{f}}(t) = \mathbf{f}(t) \quad (5.2)$$

The actuator forces will be composed of the sum of inertial, viscous and structural restoring forces since the experiment is performed in real time and Eq. 5.1 will be solved continuously. A data acquisition system could then measure and record all desired response quantities as it would on a shaking table. Although conceptually simple, this places great demands on the electrohydraulic control loop, in that it must dynamically impose the desired force vector in real time, a difficult task. Assuming that the servo-control loop is able to perform this task, the inability of the controller to impose  $\mathbf{f}$  on the specimen would be an indication of impending failure. Actuators could then be turned off and the test terminated. Also, maximum displacements could be specified for each degree of freedom and the controllers could shut the hydraulic pressure off, if the specified limits were exceeded. It should be noted that using this technique may impose a very high oil flow demand, and a sophisticated hydraulic supply would probably be necessary.

A more useful method of testing would allow the experiment to be slowed down by a factor of  $\mu$ . In this way, demands on the hydraulic system and servovalves could be reduced so that commonly used control systems could be used. The measured restoring force  $\mathbf{r}$  would now be in error since the actual acceleration and velocity would now be reduced. Representing the desired response values as  $\mathbf{a}(t)$ ,  $\mathbf{v}(t)$ , and  $\mathbf{d}(t)$ , the measured acceleration, velocity and displacement histories in experimental time would be given by :

$$\hat{\mathbf{a}}(\hat{t}) = \frac{1}{\mu^2} \mathbf{a}(t) \quad (5.3)$$

$$\hat{\mathbf{v}}(\hat{t}) = \frac{1}{\mu} \mathbf{v}(t) \quad (5.4)$$

$$\hat{\mathbf{d}}(\hat{t}) = \mathbf{d}(t) \quad (5.5)$$

$$\hat{t} = t / \mu \quad (5.6)$$

When the test is performed slowly, the actuator force would be given by :

$$\hat{\mathbf{f}} = \mathbf{M} \hat{\mathbf{a}} + \mathbf{C} \hat{\mathbf{v}} + \mathbf{r} \quad (5.7a)$$

or

$$\hat{\mathbf{f}} = \frac{1}{\mu^2} \mathbf{M} \mathbf{a} + \frac{1}{\mu} \mathbf{C} \mathbf{v} + \mathbf{r} \quad (5.7b)$$

The solution of Eq. 5.1 can no longer be obtained by using Eq. 5.2. Instead, corrective terms must be added to dynamically alter the commanded force vector. The corrective terms are necessary because the inertial and damping contributions in the force vector decrease as the rate of testing decreases. The equations of motion including these corrections is :

$$\hat{\mathbf{f}} + (\mu^2 - 1) \mathbf{M} \hat{\mathbf{a}} + (\mu - 1) \mathbf{C} \hat{\mathbf{v}} = \mathbf{f} \quad (5.8)$$

Rewriting this in terms of the force that must be imposed on the specimen gives :

$$\hat{\mathbf{f}} = \mathbf{f} - (\mu^2 - 1) \mathbf{M} \hat{\mathbf{a}} - (\mu - 1) \mathbf{C} \hat{\mathbf{v}} \quad (5.9)$$

The command forcing function can no longer be explicitly determined before a test, but analog signals representing  $\hat{\mathbf{a}}$  and  $\hat{\mathbf{v}}$  are available from transducers at each degree of freedom. By amplifying or attenuating these signals so that the force quantities  $M_{ij} \hat{a}_j$  and  $C_{ij} \hat{v}_j$  correspond to the calibration constant for degree of freedom  $i$  (in force units per volt), analog corrections can be made to the dynamic force vector. Applying the corrected force as the command to the actuator controllers should then result in the correct specimen response, with appropriate scaling of acceleration and velocity due to the rate of testing.

Unlike a conventional pseudodynamic test, it is beneficial in this force method to perform the experiment as rapidly as the hydraulic system will allow. The quality of measured acceleration and velocity will likely decay as the test rate is slowed down, and the multipliers for these signals will increase. This combination introduces the possibility of large errors. It may also be necessary to provide analog low pass filtering on the feedback values to remove spurious signals introduced by random noise and actuator dynamics.

The errors associated with discrete integration operators in a pseudodynamic test would be removed with this new method. However, the preparation of the continuous function  $\mathbf{f}$  must be

done carefully. The nature of error propagation problems using this method will have to be evaluated, since this is a different problem than the propagation of experimental errors through the step-by-step integration operator that occurs in a conventional pseudodynamic test.

## **5.2 Concluding Remarks**

The new method proposed here will be useful in certain cases, such as impact loading tests or tests with rate sensitive materials. However, the method will require verification tests, and also a study of the error propagation effects from any errors in the feedback signals.

## 6. AN UNCONDITIONALLY STABLE ALGORITHM

### 6.0 Introduction

The general Newmark time integration method presented in Chapter 2 can give unconditional stability when suitable values of  $\beta$  and  $\gamma$  are selected. Since this class of stable algorithms is implicit, their use in pseudodynamic testing has been limited. The problem in using an implicit integration scheme is that no iteration can be used in a pseudodynamic test, since a real specimen is being moved and its behavior is in general path dependent. Consequently, proposed schemes for implementing implicit integration in a pseudodynamic test have all relied on being able to formulate an accurate estimate of the tangent stiffness matrix at each step. If a good estimate of tangent stiffness was achievable, this method could be used to calculate incremental displacements. However, computed incremental displacements have been found to be sensitive to errors in the tangent stiffness matrix. Furthermore, experimental evidence to date indicates that it is difficult to measure even the initial elastic stiffness matrix of a structure. The estimation of accurate tangent stiffness values at each step of a test would be a formidable task.

The formation of a tangent stiffness estimate on some steps may in fact be impossible, due to the nature of the displacement increment vector on the given step. Even with a suitable displacement vector, it may be difficult to estimate tangent stiffness in a yielded structure due to ill conditioned measured property matrices. Also, the incremental displacements calculated for the next step may be quite sensitive to errors in the tangent stiffness matrix as the structure yields and becomes softer. On steps where an estimate of tangent stiffness cannot be formed, compensation techniques will need to be used, such as reusing the last calculated tangent stiffness matrix.

The difficulties in measuring tangent stiffness and the inappropriateness of iterative techniques have forced pseudodynamic implementations to use explicit integration schemes. However, there is a great motivation to successfully implement an unconditionally stable scheme. As more complex experiments with many degrees of freedom are tested, the explicit form limits the size of  $\Delta t$  on the basis of the highest natural frequency of the system. This is true even though the seismic response of the structure may be dominated by a few lower frequency modes. This limit on

step size is undesirable because it physically increases the duration of a test, but more importantly, because the number of steps to completion increases and error propagation problems increase with the number of steps in a test. In addition, incremental displacements within each step become smaller, introducing the potential for problems associated with stress relaxation. An unconditionally stable algorithm would allow  $\Delta t$  to be selected to give accurate response in the modes of interest without regard for higher mode characteristics. Thus, the number of steps could be minimized.

Using the current form of the pseudodynamic test method, it would seem that implicit integration methods are not feasible and therefore that unconditional stability cannot be achieved. This conclusion is based largely on a purely analytical perspective, and ignores the fact that during a pseudodynamic test there is much more structural information available, in the form of physically measured quantities, than in an analytical simulation. A new method has been devised that allows an unconditionally stable integration algorithm to be used, without requiring either iteration or the estimation of tangent stiffness properties. The new method relies on conceptual changes in the way pseudodynamic tests are performed, but does not require any additional simplifying analytical assumptions.

### 6.1 Time Integration Method

In order to describe and use the new pseudodynamic algorithm, it is necessary to select an appropriate integration method. A variation of Newmark's method by Hilber, Hughes and Taylor [24] has many properties that are desirable in pseudodynamic testing. In particular, its numerical dissipation properties are ideal, with small numerical damping in the lower modes, and increasing damping in higher modes. The level of damping is variable using an independent parameter, so that dissipation at a given frequency can be adjusted for any selection of  $\Delta t$ . This algorithm is very similar in form to that proposed by Shing and Mahin [12], but the  $\rho$  terms in the latter method do not have physical significance, and cannot be used in the implicit implementation proposed in the next section. The final form of the Hilber, Taylor and Hughes algorithm will be presented here for completeness, interested readers are directed to the original paper for the actual development. The

formulation presented here will exclude viscous damping, since it is anticipated that numerical dissipation would be used to model viscous damping in the lower modes and to prevent error propagation effects from introducing spurious higher mode response. The viscous damping terms can be easily added, but it has been shown by Shing and Mahin [22] that the constant viscous damping matrix may produce unexpected results in nonlinear tests. Following the notation of Chapter 2, the method is :

$$\mathbf{M}\mathbf{a}_{i+1} + \mathbf{C}\mathbf{v}_{i+1} + (1+\alpha)\mathbf{r}_{i+1} - \alpha\mathbf{r}_i = \mathbf{f}_{i+1} \quad (6.1)$$

$$\mathbf{d}_{i+1} = \mathbf{d}_i + \Delta t \mathbf{v}_i + (\frac{1}{2} - \beta) \Delta t^2 \mathbf{a}_i + \beta \Delta t^2 \mathbf{a}_{i+1} \quad (6.2)$$

$$\mathbf{v}_{i+1} = \mathbf{v}_i + (1 - \gamma) \Delta t \mathbf{a}_i + \gamma \Delta t \mathbf{a}_{i+1} \quad (6.3)$$

The parameters  $\gamma$  and  $\beta$  are the same as in Newmark's method. When  $\gamma > \frac{1}{2}$  numerical dissipation is present, and with  $\beta \geq \frac{1}{4}(\gamma + \frac{1}{2})^2$  the algorithm is unconditionally stable for linear systems. The additional parameter  $\alpha$  controls damping characteristics. Unconditional stability and desirable damping characteristics were achieved in Ref. 24 by selecting :

$$\beta = (1 - \alpha)^2/4 \quad (6.4)$$

$$\gamma = \frac{1}{2} - \alpha \quad (6.5)$$

where the useful range of  $\alpha$  was found to be  $-1/3 < \alpha < 0$ . When  $\alpha = 0$  these equations reduce to the trapezoidal rule. The dissipative and period distortion properties are presented in Ref. 24 and are shown in Figs 6.1 and 6.2.

It is important to note that the new form of the pseudodynamic method presented here is not dependent on a particular form of step-by-step integration scheme, but the Hilber, Taylor and Hughes method will be used here because it has desirable stability and dissipative properties.

## 6.2 New Pseudodynamic Algorithm

The significant difference between the new form presented here and conventional pseudodynamic tests is that in the old form the equations of motion were solved entirely digitally. In other words, the solution was numerical, but based on measured quantities that were converted to digital form. In the new method, a true hybrid approach is used. A portion of the solution is performed digitally, and the remainder is done in analog form using feedback voltages from the specimen.

The development of the new form was driven by the observation that as the specimen is moved by the actuators, the voltages representing restoring forces also continuously change. Considering the system behavior on a typical step, as the commanded D/A ramp voltage ( $V_d$ ) changes to impose the desired displacement, the actual restoring force voltages  $V_r$  change also. Thus, letting  $\delta$  describe the portion of each step completed, where  $0 \leq \delta \leq 1$ , at any displacement  $\mathbf{d}_{i+\delta}$ , the corresponding restoring force is completely described by  $V_r$ . As the step completes ( $\delta = 1$ ), the restoring force  $\mathbf{r}_{i+1}$  is available in analog form. These voltages representing forces are not available digitally to the computer until an A/D read occurs, but can still be used to implement an implicit integration scheme.

Recognizing that analog force signals are available that represent the restoring forces for the actual structural displacements, the equations of motion can be rearranged as follows. From Eq. (6.1) we can solve for the accelerations at step  $i+1$ .

$$\mathbf{a}_{i+1} = \mathbf{M}^{-1} \left[ \mathbf{f}_{i+1} - (1 + \alpha)\mathbf{r}_{i+1} + \alpha\mathbf{r}_i \right] \quad (6.6)$$

Viscous damping terms have been disregarded in this formulation as explained previously, but can be easily added if one wishes to use a constant viscous damping matrix. Now we can rewrite Eq. (6.2) using Eq. (6.6) giving :

$$\mathbf{d}_{i+1} = \mathbf{d}_i + \Delta t \mathbf{v}_i + (\frac{1}{2} - \beta) \Delta t^2 \mathbf{a}_i + \beta \Delta t^2 \mathbf{M}^{-1} \left[ \mathbf{f}_{i+1} - (1 + \alpha)\mathbf{r}_{i+1} + \alpha\mathbf{r}_i \right] \quad (6.7)$$

Collecting terms and using Eq. (2.14) ( $\mathbf{f} = -\mathbf{M}\mathbf{B}\mathbf{a}_g$ ) gives :

$$\begin{aligned} \mathbf{d}_{i+1} = \mathbf{d}_i + \Delta t \mathbf{v}_i + (\frac{1}{2} - \beta) \Delta t^2 \mathbf{a}_i - \beta \Delta t^2 \mathbf{B} \mathbf{a}_g + \beta \alpha \Delta t^2 \mathbf{M}^{-1} \mathbf{r}_i \\ - \beta (1 + \alpha) \Delta t^2 \mathbf{M}^{-1} \mathbf{r}_{i+1} \end{aligned} \quad (6.8)$$

Eq. (6.8) gives the implicit form for the displacements, and it can be seen that all terms except the last one on the right hand side can be calculated with available information (and thus are explicit). In an analysis based procedure the last term is estimated using an approximated tangent stiffness. In an experiment, good estimates of tangent stiffness are difficult or impossible to achieve, and the last term will not be known to the computer until the specified displacement is reached.

This apparent dilemma can be solved by changing the way the command signal is generated. In conventional pseudodynamic tests, the command signal to the servo-controller is precisely the output signal from the D/A ramp generator. It is proposed here that this be modified so that the command signal to the actuator is the analog sum of the ramp outputs, representing the explicit terms of Eq. (6.8) and some analog function of the restoring force voltages representing the last term of Eq. (6.8). It should be noted that analog addition or subtraction of voltages is a simple task that can be accurately performed. Furthermore, the coefficient of  $\mathbf{r}_{i+1}$  in the last term of Eq. (6.8) is a constant matrix that can be entirely calculated before the test begins.

There is a defined relationship between digital and analog representations of the displacement and force signals which is given by :

$$\mathbf{d} = \mathbf{G}_d \mathbf{V}_d \quad (6.9)$$

$$\mathbf{r} = \mathbf{G}_r \mathbf{V}_r \quad (6.10)$$

where the  $\mathbf{G}$  matrices are diagonal matrices of calibration constants in physical units per volt.

The explicit terms of Eq. (6.8) are :

$$\hat{\mathbf{d}}_{i+1} = \mathbf{d}_i + \Delta t \mathbf{v}_i + (\frac{1}{2} - \beta) \Delta t^2 \mathbf{a}_i - \beta \Delta t^2 \mathbf{B} \mathbf{a}_g + \beta \alpha \Delta t^2 \mathbf{M}^{-1} \mathbf{r}_i \quad (6.11)$$

Now, in analog form, we can generate the command signal for the implicit displacements at step  $i+1$  as :

$$\mathbf{V}_{COMMAND} = \mathbf{G}_d^{-1} \hat{\mathbf{d}}_{i+1} - \beta (1 + \alpha) \Delta t^2 \mathbf{M}^{-1} \mathbf{G}_d^{-1} \mathbf{G}_r \mathbf{V}_r \quad (6.12)$$

where the the  $\mathbf{G}$  matrices and their inverses are diagonal.

The command signal described above is used as the desired displacement signal to the servo-controllers. By creating the command signal using analog feedback it can be seen that at ramp completion, Eq. (6.8) will indeed be satisfied. Both the explicit terms and the term depending on  $\mathbf{r}_{i+1}$  have been applied, although the latter term is never known to the host digital computer. The displacement arrived at after ramp completion depends on the forces generated by the new position, and is unknown to the computer. Thus, the computer must read both  $\mathbf{d}_{i+1}$  and  $\mathbf{r}_{i+1}$  for use in subsequent calculations.

It should be noted that the implicit scheme is implemented here without any simplifying

analytical assumptions. However, there are some important differences between this method and conventional pseudodynamic tests. In this test, the command signal depends on the force signal. As mentioned previously, the force signal tends to oscillate due to servocontrol system dynamics. This oscillation can be easily removed from the analog signal using a low pass filter, while the underlying changes in restoring forces can be retained. The summation is easily and accurately obtained using a summing amplifier (actually a differencing amplifier). Finally, the host digital computer never knows the next displacement and must measure it after step completion. This means that there can be no checking of errors by the host computer, since there is no way to check if the final position is correct. The lack of ability to track errors is not believed to be a serious drawback, however, since initial elastic tests can be performed using an explicit formulation, to ensure that the experimental setup is working correctly. These elastic level tests are used in any case to assess system performance, and once the system is verified, the implicit tests can proceed assuming the actuators are imposing the correct displacements. Also, the method of imposing displacements must be a one step process. Schemes that use multiple substeps to converge to a desired displacement cannot be used with this implicit form, since the final displacement is unknown.

Hardware and software modifications necessary to implement the method for a specific application will be presented in the next section. These are representative of the general implementation strategy. However, alternate implementation methods will be described in subsequent sections.

### **6.3 Verification Test**

#### **6.3.1 General Information**

A simple two degree of freedom specimen, shown in Fig. 6.3, was designed to verify the new implicit form of the pseudodynamic method. The purpose of the test was to show that the method worked, and that  $\Delta t$  could be selected to give accurate response in the modes of interest without regard for the highest natural frequency of the system. The specimen selected was a simple two degree of freedom cantilever, with the analytical masses chosen to give widely separated natural frequencies. The two natural frequencies were separated to model a multiple degree of freedom struc-

ture where a group of the lower modes are responsible for the seismic response, and the upper modes might contribute very little. In this simple two degree of freedom model, the masses used were 0.001 and 0.01 *kip sec<sup>2</sup>/inch* (175 and 1750 kg) for degrees of freedom one and two, respectively. The resulting natural frequencies for the system were 3.9 and 19.9 Hz. The seismic response of the system with these natural frequencies consisted entirely of first mode. The stability bound on  $\Delta t$  given these frequencies was  $\Delta t < 0.016$  sec. for the conventional explicit method.

The displacement at each degree of freedom was imposed by a 150 kip (667 kN) hydraulic actuator. The actuators each had a 10 gpm (0.63 liter/sec) MTS servovalves, and used  $\pm 6$  inch ( $\pm 152$  mm) Temposonic displacement transducers for positional feedback. Two MTS model 406 controllers were used, and these units had modified gain circuits, so that the controller gain could be raised to give more accurate control. Two Validyne summing amplifiers were used to add the voltages required to create the implicit command signal, as described later.

The tests used the NS component of the 1940 El Centro ground motion record, scaled to have a 0.18 g peak acceleration. This record caused the structure to respond elastically, so that changes in structural behavior due to loading history could be ignored. As mentioned previously, elastic pseudodynamic tests are the most difficult to perform correctly, so showing that the method works in the elastic range is a sufficient validation, although it may be necessary to compensate for force relaxation effects in nonlinear tests. Given the 0.016 sec. bound on  $\Delta t$  for the explicit method, it was decided to use time steps of 0.01 and 0.02 sec to test the method. In this case, the time step values are not based on accuracy consideration in the lower modes, since the value of 0.02 sec. gives only 12 points per response cycle in first mode. This value of  $\Delta t$  will introduce period elongation of about 3% in the first mode response and will introduce some errors due to the large step size, but the purpose of the test is to show that lower mode response can be tracked without regard to higher mode frequencies. In a real multiple degree of freedom test,  $\Delta t$  would typically be selected to give at least 20 points per cycle in the highest mode of interest.

Three experimental runs were performed, together with two analytical simulations. The properties of the runs are summarized in Table 6.1. An explicit test using a time step of 0.02 sec. was

not performed because it would have damaged the specimen, so the analytical run was used to demonstrate the effects of numerical instability. Preliminary experimental tests showed that friction in the experimental setup resulted in roughly 1% effective viscous damping in the first mode, so nondissipative forms of the integration method were used. In the explicit analytical simulations, the modified Newmark method [12] was used, with  $\alpha = 0.05$  and  $\rho = 0$  to give roughly equivalent damping characteristics. It should be noted that in the explicit form  $\alpha$  was positive and  $\rho$  was negative or zero, whereas in the implicit form of Ref. 24,  $\alpha$  is a negative constant.

---

Test	$\Delta t$	$\gamma$	$\beta$	$\alpha$	Description
1	0.01	0.5	0.0	0.05	Explicit analytical simulation
2	0.02	0.5	0.0	0.05	Explicit analytical simulation
3	0.01	0.5	0.0	0.0	Explicit experimental test
4	0.01	0.5	0.25	0.0	Implicit experimental test
5	0.02	0.5	0.25	0.0	Implicit experimental test

**Table 6.1 - Implicit Verification Test Sequence**

---

### 6.3.2 Implementation Details

In performing a test using the new method, there are both new hardware and software considerations. In hardware, one must sum the ramp outputs and the scaled restoring force outputs to give a displacement command signal. The restoring force component is given by (from Eq. 6.12) :

$$-\beta(1+\alpha)\Delta t^2\mathbf{M}^{-1}\mathbf{G}_d^{-1}\mathbf{G}_r\mathbf{V}_r \quad (6.13)$$

For the given test specimen,  $\mathbf{M}^{-1}$  and the  $\mathbf{G}$  matrices are diagonal. Therefore, each displacement command voltage will only depend on the ramp voltage and the actuator's associated restoring force voltage. If  $\mathbf{M}$  were not diagonal or if viscous damping terms were included, each command signal would in general depend on all restoring force voltages. However, for the set of parameters described above, the coefficient matrix is diagonal and all its elements are less than one in magnitude. Multiplying by the coefficient matrix can, therefore, be achieved by physically attenuating the restoring force voltage before summing to create the displacement command signal. High precision ten turn potentiometers were used to attenuate the voltage according to the diagonal elements

of the resulting coefficient matrix. The final command signals for each of the two degrees of freedom was then created by adding the D/A ramp output to the attenuated force signal. This setup required two summing amplifiers and two potentiometers to implement the implicit summation. It should be noted that since the implicit portion of the displacement has a negative sign, the attenuated signal is actually subtracted from the ramp output. In analog form this can be achieved by inverting the signal before adding.

The software performing the pseudodynamic algorithm also requires changes to account for the new way in which displacement commands are formed. The flow of the algorithm is basically similar to a conventional test, but the details are quite different. The algorithm is best described by considering the operations performed during an arbitrary step. If we have completed the motion necessary to move the specimen to the beginning of step  $i$ , the algorithm would be :

- Read the current displacement and restoring force vectors, as well as other data. Unlike conventional tests, the measured displacements must be used in subsequent calculations. The reason for this requirement is that on the previous step, the computer only calculated a portion of the displacement increment, the rest was contributed in analog form. Therefore, the previous computed displacement is not expected to equal the current physical displacement.

- Calculate the acceleration and velocity terms for step  $i$  using the force and displacement vectors measured in the first step.

- Calculate the explicit component of the displacement ( $\hat{d}_{i+1}$ ) for the next step. The incremental displacement is given by the difference between the calculated explicit component and the current measured displacements. The incremental displacement is sent to the D/A boards and forms the explicit portion of the command signal.

- Continue

The major changes, with respect to a conventional test are that measured displacements are used, a different equation is used to calculate the explicit component of the displacement, and the computer is no longer able to assess how well the servo control system is operating. The importance of the last point cannot be underestimated. If the system is not verified by performing glow level

explicit tests, there is no way to determine if the results are valid while performing an implicit test. Experience with the servo-control loop in these tests have shown that it is capable of the desired level of accuracy. However, blindly running implicit tests without verifying hydraulic performance invites disaster.

### 6.3.3 Results

In comparing the results of the tests, the base case used is the explicit pseudodynamic test using  $\Delta t = 0.01$ . This base case is compared to analytical results and to experimental results obtained using the implicit method. The selection of a pseudodynamic test as the reference test is justified because the experimental equipment and algorithm used were identical to those used in Chapter 4, and that system was shown to provide accurate results.

In Fig. 6.4, the explicit analytical results and explicit experimental results are compared. Numerical instability results within 18 steps when a time step of  $\Delta t = 0.02$  was used in the analytical case. This behavior is expected since the stability limit for the system was  $\Delta t = 0.016$ . The stiffness matrix used for the analytical simulations was experimentally measured. It was quite difficult to get a good estimate of the stiffness for this system, confirming the view that forming a tangent stiffness on each step is infeasible. The slight period difference between the analytical and experimental runs with  $\Delta t = 0.01$  sec. was due to errors in the measured stiffness matrix. The results are quite good, however, and for subsequent comparisons it is assumed that the experimental results reflect the a better estimate of the true response.

Fig. 6.5 shows the explicit and implicit test results with  $\Delta t = 0.01$  and the results are very good. Again there is a very slight period difference, but this time both tests are experimental so the real stiffness properties are measured. The period change is due to distortion induced by the step-by-step integration procedure, where the implicit method causes period elongation and the explicit method causes period contraction [12,24]. This distortion is in agreement with the observed results, and since there are about 25 points per response cycle, it is seen that the amount of period distortion is very small.

The comparison between the stable explicit test and the implicit method with  $\Delta t = 0.02$  is shown in Fig. 6.6. The responses are quite similar, but there is a fairly large period elongation in the implicit test, roughly 3% as Ref. 24 predicts. This period shift is not important here in the sense that the purpose of the test was to show that unconditional stability can be achieved, not that excessively large time steps could be used to give accurate results. In other words, one must still select a value of  $\Delta t$  that gives accurate results for the responding modes, but it is no longer necessary to consider the highest frequency of the system. In the implicit test presented here there are only about 12 points per response cycle and this is not recommended. As stated before, at least 20 points would be more desirable. However, the time step here was chosen to demonstrate stability of the new method.

The magnitude of the explicit and implicit parts of the final displacement can be seen in Fig. 6.7. The implicit portion, contributed in analog form, is quite small, and some higher frequency content is visible. This high frequency content is often present in the restoring force vector even when the displacement vector contains only lower modes and is due to small displacement errors and the stiffness coupling inherent in the specimen.

Finally, to show how well the electro-hydraulic system was performing, a graph of an actuator's error history for an explicit run is given in Fig. 6.8 together with an FFT of the errors. These error levels are extremely small, and show that the assumption perfect servo-control loop behavior is justified when adjusted properly.

#### 6.4 Extensions of the Implicit Method

For systems with diagonal mass matrices, the implicit method is very easy to implement, as described in this chapter, but in other systems the analog summation becomes more complex. In the general case, a displacement command signal for a specific actuator will depend on the restoring acting in all actuators. Also, there is no guaranty that the elements of the coefficient matrix will be less than one. Thus, the simple attenuators used in the verification test described herein may not be useful in a more general case. These observations would seem to indicate that a new computer architecture will be desirable for a pseudodynamic test system.

A much more versatile computer/hardware combination would completely do away with the concept of imposing a linear ramp during each time step. Although the concept of time step for discrete integration of the equations of motion would be retained, it seems desirable to change the way a step is imposed. Ideally, it would be best to be able to continuously update state data and the command signal as a step is being imposed. Given a system capable of performing read/update cycles many times per second (on the order of hundreds or thousands of times per second), the controlling software would be able during a given step to update the desired command signal on the basis of measured quantities. Each step would still be performed slowly as before, but in the many sub-steps measured data would be available that would allow the software to numerically update the desired command signal dynamically. By using a high speed sample and update strategy the computer could digitally simulate what the implicit method proposed here performs in an analog fashion. Such hardware is already available, and achieving the necessary speeds would not be difficult. A powerful host computer would probably not be necessary, custom high speed coprocessor controllers could be used to perform the needed tasks.

At first glance, such a new computer configuration may seem to excessively complicate a simple idea, but the advantages are enormous. If a system is created that can update command dynamically during a step, it no longer matters whether the mass matrix is diagonal, since the summation of force related terms would take place digitally, so analog summing amplifiers would not be required, the computer could generate the implicit command signal. Also, it would no longer matter if the terms of the coefficient matrix that is multiplied by the analog force vector are larger than unity, because analog attenuation would not be performed. Instead a digital matrix multiply could be used to calculate the implicit components. Additionally, problems associated with analog calibration of attenuators would be eliminated, since the various factors could be numerically specified.

In addition to handling a general implicit test without difficulty, the new hardware would also open up a variety of tests not currently possible. Rearranging Eq. (6.8) so that we solve for  $\mathbf{r}_{i+1}$  in terms of known quantities and  $\mathbf{d}_{i+1}$ , gives :

$$\mathbf{r}_{i+1} = \frac{\mathbf{M}}{\beta(1+\alpha)\Delta t^2} \left[ \mathbf{d}_i + \Delta t \mathbf{v}_i + (\frac{1}{2} - \beta) \Delta t^2 \mathbf{a}_i - \beta \Delta t^2 \mathbf{B} \mathbf{a}_g + \beta \alpha \Delta t^2 \mathbf{M}^{-1} \mathbf{r}_i - \mathbf{d}_{i+1} \right] \quad (6.14)$$

Now, using the new hardware configuration it would be possible to perform tests under force control. The ability to perform force control tests would eliminate the problems currently encountered with stiff specimens. The force vectors were often contaminated in such systems by small displacement errors. Under force control, the electro-hydraulic system is very well behaved, so accurate forces could be imposed and the resulting displacements could be measured. It should be noted that the inverse problem of having displacement contamination due to errors in imposing forces is not likely to occur in stiff systems. Such a system should be investigated. It may turn out to be best to run in a mixed hybrid mode where some actuators are under force control and some are under displacement control. This may be useful in extremely flexible systems or systems where stiffness may actually go negative (due to buckling), since there would be problems in such systems under force control.

Another very attractive application of the new method and hardware would be in performing substructuring tests, where only a portion of the structure is physically tested and the rest is analytically modeled on the host's computer. The proposed system would allow the equations of motion for the combined system to be solved using an implicit scheme, rather than the mixed explicit/implicit schemes proposed to date. Also, since sampling and update occurs during a step, it would be possible to continuously update the entire system, ensuring compatibility between the physical and analytical portions. In previously proposed schemes, it was always necessary to move the physical portion, take readings and then update the modeled portions, so response and calculation were always out of step. The new method would allow physical motion to be updated dynamically as the analytical portion requires.

## 6.5 Conclusions

The results of the simple tests performed here show that the new form of the pseudodynamic method proposed here works well and has the desirable unconditional stability property. This method has substantial advantages for testing systems with many degrees of freedom, where only a few modes contribute to the response. The method can also dramatically reduce the time required

to perform tests by reducing the number of steps that are considered. Reducing the number of steps will also mitigate error propagation problems. By increasing the average step size, actuator control and force relaxation problems may also be reduced, especially if combined with the methods described in Chapter 4.

The implicit method can no longer check for displacement errors while a test is running, but hardware performance can be easily verified with preliminary low level explicit tests. Once adjusted, the hardware can be expected to perform well. In addition to the advantages of using an implicit integration scheme, the proposed new hardware configuration and pseudodynamic algorithm would make many exciting new types of tests feasible.

## 7. CONCLUSIONS AND RECOMMENDATIONS

### 7.0 Summary

A generalized form of the pseudodynamic test method has been presented. An attempt has been made to identify the important factors that must be considered by those performing pseudodynamic tests. In particular, a unified formulation of the equations of motion was presented, together with appropriate numerical methods for solving these equations. Also, equipment and techniques for imposing displacements on the test specimen were evaluated, and experimental errors and their effects on the test were discussed. Verification tests were performed to assess the performance of hardware components and to determine the accuracy of pseudodynamic test results. When properly implemented in software and hardware, the pseudodynamic tests were found to give results comparable to those obtained by shaking table testing.

Since the pseudodynamic method is based on well known analytical techniques, one must determine the appropriateness of the discrete parameter model for the given structure, and also recognize the errors (period shifts and energy modification) introduced by step-by-step integration. In particular, the lumped mass idealization used in the discrete parameter model may be inappropriate for structures with significant distributed mass [16,21].

In addition to these purely analytical concerns, one must also consider many physical factors that apply to pseudodynamic tests only. The most important physical factor in a test is the performance of the electro-hydraulic control loop. It has been repeatedly shown that good quality servo-control hardware, electronics and instrumentation is essential. In particular, the quality of the displacement transducer and its signal conditioning amplifier are crucial, as is the overall loop gain. Similarly, a good software implementation and experimental procedures must be used. In addition to mitigating error effects, the program must ensure that specified displacements are imposed correctly. This seems best achieved by sending the entire displacement increment as the command signal for each step. Iterative approaches that attempt to converge onto a desired displacement have been shown to introduce the type of systematic displacement errors that must be avoided in pseudodynamic tests. If the electro-hydraulic control loop is incapable of imposing specified

displacements accurately, it would seem that the loop components and their adjustments should be examined to see where control improvements could be made. Special problems may be expected in yielding systems due to stress relaxation. Software procedures to mitigate these problems were developed and found to be effective. With high quality equipment and proper implementation, the pseudodynamic method can give very good results. This is true even for low level elastic tests, which have proven to be difficult to perform in the past. However, if rate sensitive materials are used, then the conventional form of the pseudodynamic method may not be appropriate.

An effort has been made to unify the approach to pseudodynamic testing. It seems that in most cases it would be best to model damping characteristics through a dissipative numerical algorithm. As shown in Ref. 16, a constant viscous damping matrix for nonlinear tests is not recommended. Since pseudodynamic tests will automatically incorporate many of the sources contributing to effective viscous damping (friction, localized yielding, etc.), and the test setup may add other sources of energy dissipation (clevis friction), a numerical method that can add small or negligible amounts of energy dissipation in the frequency range of interest would be desirable. However, significant energy dissipation may be required in the high frequency response ranges to control error propagation effects. The integration scheme best suited to pseudodynamic testing appears to be one like the modified Newmark form proposed by Shing and Mahin [12] or that proposed by Hilber, Taylor and Hughes [24]. In performing implicit tests, the first form is not applicable, since the additional  $p$  terms do not have physical significance and cannot, therefore, be used in analog summation. Since the two methods are similar in form, both could be implemented simultaneously in software, and the user could select appropriate parameters to obtain the desired method.

In addition to the general observations on pseudodynamic testing described above, several new techniques have been presented, together with verification studies, and the work can be summarized as follows :

- (1) A generalization of the equations of motion to allow testing of nonplanar structures subject to multiple components of base excitation has been implemented. The new form allows a general six degree of freedom fixed base excitation to be used. A series of verification tests were per-

formed using a stiffness eccentric three degree of freedom structure. Tests were performed on a shaking table and using the pseudodynamic test method. Ground acceleration records of various magnitudes were used. These tests showed that very good results can be achieved. Past experience has shown that elastic tests are the most difficult to perform correctly, due to error propagation effects. Reliable inelastic results can often be achieved even when elastic results are not very good. The verification tests described in Chapter 4 showed that the systematic errors can be reduced to a magnitude where even elastic level runs can be performed accurately.

- (2) A formulation has been developed that would allow pseudodynamic test to be performed at or near real time. This method would run under force control, and would be applicable for structures composed of rate sensitive materials. In this formulation, the errors associated with step-by-step time integration are eliminated, but the effects of experimental errors should be investigated.
- (3) A new algorithm and hardware layout has been implemented that allows implicit integration operators to be used. Using implicit integration operators makes it possible to ensure unconditional numerical stability for elastic systems, and to give reasonable assurances of stability for softening inelastic systems. Stability concerns will become increasingly important as more complex structures with many degrees of freedom are tested using the pseudodynamic method. Using conventional explicit algorithms, such tests would require extremely small time steps to be used to ensure stability. Error propagation and other problems would increase with the increased number of steps. The implicit algorithm would require significantly fewer steps. In addition to reducing error propagation problems, this would dramatically reduce the time required to perform a pseudodynamic test. A verification test was performed using a two degree of freedom specimen with widely spaced model frequencies. The results showed that the new method does eliminate the stability bounds on  $\Delta t$  associated with explicit methods, and also provided accurate results. The Hilber, Taylor and Hughes integration method was used and performed well.

- (4) A proposal for extending the implicit method, using a completely new hardware configuration has been presented. Such a system would use high speed electronic read and update capabilities to allow very general schemes to be implemented. New capabilities made possible by this configuration would include force control testing (especially useful for stiff multiple degree of freedom systems), a completely implicit implementation of substructure testing, and a general treatment of multiple support base excitations.

Based on these observations, it appears that the pseudodynamic method, as described herein, can currently be used to accurately test complex structures under general fixed base excitation. It is, therefore, possible to simulate many dynamic tests that could not be performed on available shaking tables. The size and weight limitations in shaking table tests, as well as the limits on the nature and magnitude of the applied excitation, are not present when testing a structure using the pseudodynamic method. New tests must be carefully performed, however. Good results cannot be achieved unless the system is working well. Preliminary elastic tests should always be used to ensure that the electro-hydraulic control loop is performing adequately.

### **7.1 Recommended Future Work**

The pseudodynamic method, as described in Chapters 2 and 3, can be used to perform tests on many structural systems. Additional research is necessary to examine electro-hydraulic behavior for stiff systems under displacement control. Attachment details for connecting actuators to more realistic building frames must be designed, and methods to account for diaphragm flexibility should be investigated. Additional work is needed to extend and evaluate current capabilities for performing tests on structural components using analytical substructuring techniques. Also, software should be developed to automatically perform system evaluation, to be used prior to and during actual tests.

For more complex systems the implicit method can be used to ensure unconditional stability. An exciting prospect is the combination of the implicit methods with a new hardware configuration. The new system would no longer use the linear ramps that are used to impose each step of current pseudodynamic tests. The discrete time interval of a step would still be retained, but high

speed D/A and A/D hardware could be used to implement essentially continuous read and update capabilities. The test would still be performed slowly, but all information about state changes during a step would be available for use while the step is being applied.

The development of such a hardware system would make many new testing areas possible. The implicit method could be implemented digitally, rather than using the partial analog form given in Chapter 6. It would also be possible to perform tests on stiff systems, by running the pseudodynamic method under force control. The availability of structural state data during a step would also make it easy to perform substructuring tests, where only a portion of the structure is physically tested and the rest is modeled analytically. Tests with independent support motion on large structures would also be possible, since the stiffness coupling could be accounted for while the displacements were being imposed on each step.

Investigation of error propagation in the implicit method should be performed. Physical stability of the electro-hydraulic control loop should also be investigated for the analog feedback loop used in the implicit method. Using the new hardware configuration would eliminate the analog feedback loop, but instability could still result if the update frequency was high enough to allow system dynamics to affect the command signal.

Although not addressed in this report, user interface issues will become increasingly important as the pseudodynamic method is used as a production test tool, rather than as the focus of research efforts. In developing system software, one should allow as much flexibility as possible. Many data items should be graphically presented while testing, including error status and user requested information. The user should also be able to actively change test parameters during testing, it is not sufficient to only have the choice of continuing or aborting a test. Such a project must be planned extensively before beginning. The software needed to actually run a test is minimal compared to that required to create a truly useful laboratory tool.

## **7.2 Concluding Remarks**

The results of the verification tests described herein show that the pseudodynamic method can provide seismic response simulations that are as reliable as shaking table tests. In addition, it

has been shown that complex nonplanar structures subjected to multiple components of ground excitation can be tested using a generalization of the equations of motion. The importance of physical setup aspects and of the software implementation of the pseudodynamic test method has been highlighted, but it has been demonstrated that readily available laboratory equipment can be used to perform very accurate tests.

A new hybrid form of the pseudodynamic method, using an implicit integration scheme, has been presented and verified. The test results showed that the method was as accurate as conventional pseudodynamic tests, and in addition provided unconditional numerical stability. The new method will allow complex structures with many degrees of freedom to be tested without stability restrictions. The form of the implicit method suggests a new hardware architecture for pseudodynamic testing systems. The basic layout for such a new system have been presented, and it has been shown that such a system would be capable of performing many tests that would not currently be feasible.

In view of the rapid development of the method and potential difficulties in implementing the system and interpreting the results, a cooperative effort between laboratories would be desirable. This would include the development of benchmark tests to evaluate pseudodynamic facilities, establishing procedures for specifying confidence levels on test results, presenting information (such as error spectra) in standard formats and assessment dissemination of changes in pseudodynamic test formulation.

## REFERENCES

1. Takanashi, K., et al., "Nonlinear Earthquake Response Analysis of Structures by a Computer-Actuator On-Line System", *Bull. of Earthquake Resistant Structure Research Center*, Institute of Industrial Science, University of Tokyo, No. 8, 1975.
2. Okada, T., "Computer-Actuator On-Line System at Institute of Industrial Science, University of Tokyo, with Emphasis on Numerical Integration Methods", *A Brief Note Submitted to Session 2, First Planning Group Meeting, U.S.-Japan Cooperative Research Program Utilizing Large Scale Testing*, Sept. 1977.
3. Powers, W.F., "Preliminary Analysis of the Computer Actuator On-Line System Difference Equation", University of Michigan, Ann Arbor, June 1979.
4. Mahin, S.A. and Williams, M.E., "Computer Controlled Seismic Performance Testing", *Second ASCE-EMD Specialty Conference on Dynamic Response of Structures*, Atlanta, Ga., Jan. 1981.
5. Watabe, M., et al, "Feasibility of Pseudo-Dynamic Testing System", *Progress Report on U.S.-Japan Large Scale Aseismic Experiments for Building Structures*, Building Research Institute, Ministry of Construction, Thirteenth Joint Meeting, U.S.-Japan Panel on Wind and Seismic Effects, Tsukuba, 1981.
6. McClamroch, N.H., Serakos, J., and Hanson, R.D., "Design and Analysis of the Pseudo-Dynamic Test Method", UMEE 81R3, University of Michigan, Ann Arbor, 1981.
7. Okamoto S., et al, "System Check of New BRI Computer On-Line Testing", Third JTCC, *U.S.-Japan Cooperative Research Program, Building Research Institute*, Ministry of Construction, Japan, July 1982.
8. Shing, P.B. and Mahin, S.A., "Experimental Error Propagation in Pseudodynamic Testing", *UCB/EERC-83/12*, Earthquake Engineering Research Center, University of California, Berkeley, June 1983.
9. Takanashi, K., and Ohi, K., "Earthquake Response Analysis of Steel Structures by Rapid Computer-Actuator On-Line System, (1) A Progress Report, Trial System and Dynamic Response of Steel Beams", *News Letter, Bulletin of Earthquake Resistant Structure Research Center (ERS)*, Institute of Industrial Science, Tokyo University, No. 16, 1983, pp. 103-109.
10. Okamoto, S., et al, "Actuator Control Procedure of BRI Pseudo-Dynamic Testing System", *The 4th JTCC Meeting*, Tsukuba, Japan, June 1983.
11. Nakashima, M., "Stability and Accuracy of Integration Techniques in Pseudo-Dynamic Testing", *Research Paper No. 105*, Building Research Institute, Ministry of Construction, Japan, Dec. 1983.
12. Shing P.B. and Mahin S.A., "Pseudodynamic Test Method for Seismic Performance Evaluation: Theory and Implementation", *UCB/EERC-84/01*, Earthquake Engineering Research Center, University of California, Berkeley, 1984.

13. Shing, P.B., Mahin, S.A., and Dermitzakis, S.N., "Evaluation of On-Line Computer Control Methods for Seismic Performance Testing", *Proceedings, Eighth World Conference on Earthquake Engineering*, San Francisco, July 1984.
14. Hanson, R.D., and McClamroch, N.H., "Pseudodynamic Test Method for Inelastic Building Response", *Proceedings, Eighth World Conference on Earthquake Engineering*, San Francisco, July 1984.
15. Dermitzakis S.N. and Mahin S.A., "Development of Substructuring Techniques for On-Line Computer Controlled Seismic Performance testing", *UCB/EERC-85/04*, Earthquake Engineering Research Center, University of California, Berkeley, February, 1985.
16. Shing, P.B., and Mahin, S.A., "Computational Aspects of a Seismic Performance Test Method Using On-Line Computer Control", *Earthquake Engineering and Structural Dynamics*, Vol. 13, 1985, pp. 507-526.
17. Okamoto, S. et al, "Test Control in BRI Pseudo Dynamic Test System", Building Research Institute, Ministry of Construction, Japan, March 1986.
18. Takanashi, K, and Nakashima, M., "A State of the Art: Japanese Activities on On-Line Computer Test Control Method", *Report of the Institute of Industrial Science*, University of Tokyo, Vol. 32, No. 3, June 1986.
19. Thewalt, C.R., Mahin, S.A., and Dermitzakis, S.N., "Advanced On-Line Computer Control Methods fo Seismic Performance Testing", *Third U.S. National Conference on Earthquake Engineering*, Charleston, SC, August 1986.
20. Nakashima, M., and Kato, H., "Experimental Error Growth Behavior and Error Growth Control in On-Line Computer Test Control Method", Building Research Institute, Ministry of Construction, Japan, March 1987.
21. Shing, P.B., and Mahin, S.A., "Cumulative Experimental Errors in Pseudodynamic Tests", accepted for publication in the *Journal of Earthquake Engineering and Structural Dynamics*.
22. Shing, P.B., and Mahin, S.A., "Elimination of Spurious Higher-Mode Response in Pseudodynamic Tests", accepted for publication in the *Journal of Earthquake Engineering and Structural Dynamics*.
23. Newmark, N.M., "A Method of Computation for Structural Dynamics", *Journal of the Engineering Mechanics Division, ASCE*, No. EM3, Vol. 85, July 1959.
24. Hilber, H.M., Hughes, T.J.R., and Taylor, R.L., "Improved Numerical Dissipation for Time Integration Algorithms in Strucural Dynamics", *Earthquake Engineering and Structural Dynamics*, Vol. 5, 1977, pp. 283-292.
25. Clough, R.W. and Penzien, J., "Dynamics of Structures", McGraw Hill, 1975.
26. Manjoine, M.J., "Influence of Strain Rate and Temperature on Yield Stresses of Mild Steel, *Transactions, ASME*, Vol. 66, 1944, pp. A211-A218.

27. Hanson, R.D., "Comparison of Static and Dynamic Hysteresis Curves", *Journal of the Engineering Mechanics Division*, ASCE, No. EM5, Vol. 92, 1966, pp. 87-113.
28. Okada, T., et al, "A Simulation of Earthquake Response of Reinforced Concrete Building Frames to Bi-Directional Ground Motion by IIS Computer-Actuator On-Line System", *Proceedings, 7th World Conference on Earthquake Engineering*, Istanbul, Turkey, 1980.
29. Okada, T., et al, "Nonlinear Earthquake Response of Equipment System Anchored on R/C Building Floor", *Bull. of Earthquake Resistant Structure Research Center*, Institute of Industrial Science, University of Tokyo, No. 13, 1980.
30. Takanashi, K., et al, "Inelastic Response of H Shaped Columns to Two Dimensional Earthquake Motions", *Bull. of Earthquake Resistant Structure Research Center*, Institute of Industrial Science, University of Tokyo, No. 13, 1980.
31. Okamoto, S., et al, "A Progress Report on the Full-Scale Seismic Experiment of a Seven Story Reinforced Concrete Building", Building Research Institute, Ministry of Construction, Tsukuba, Japan, 1982.
32. Yamanouchi, H., et al, "Test Results of Full Scale Six Story Building", Building Research Institute, Ministry of Construction, 4th Joint Technical Coordinating Committee Meeting, U.S.-Japan Cooperative Research Program, Tsukuba, Japan, 1983.
33. Shing, P.B., Javadian-Gilani, A.S., and Mahin, S.A., "Evaluation of Seismic Behavior of a Braced Tubular Steel Structure by Pseudodynamic Testing", *J. Energy Resources Tech. ASME Trans.* **106**, 319-328 (1984).
34. Thewalt, C.R., Mahin, S.A., "Bidirectional Seismic Response of Simple Structures", *Structures Congress*, ASCE, New Orleans, September 1986.
35. Balendra, T., et al, "Behavior of Eccentrically Braced Frame by Pseudo-Dynamic Test", *Journal of Structural Engineering*, , ACSE, Vol. 113, No. 4, April 1987.
36. Merrit, H. E., "Hydraulic Control Systems", John Wiley, 1967.
37. Neal, T. P., "Performance Estimation for Electrohydraulic Control Systems", Technical Bulletin 126, Moog Inc., N.Y., 1974.
38. General Catalog and Technical Bulletins, Moog Inc., East Aurora, N.Y.
39. Product Specifications and Technical Reports, MTS Systems Corporation, Minneapolis, Minnesota.

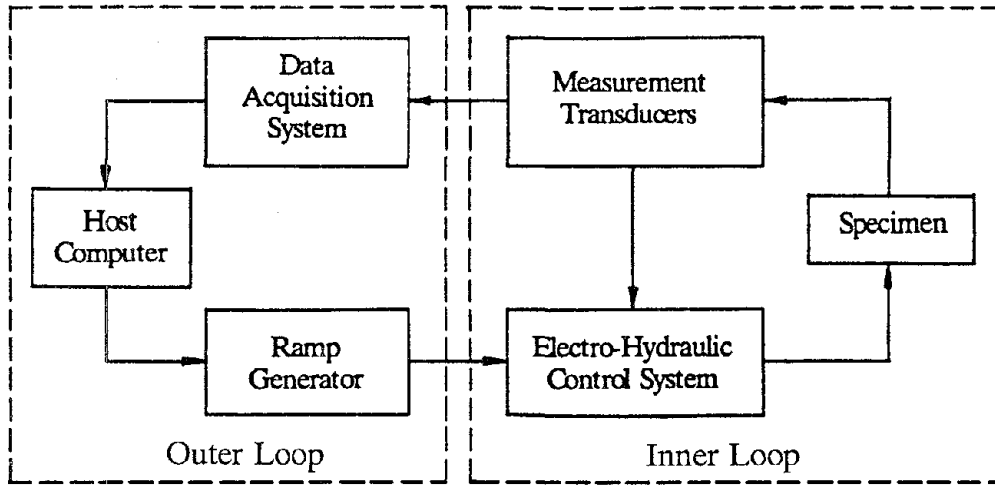


Figure 1.1 - Block Diagram of Pseudodynamic Test Method

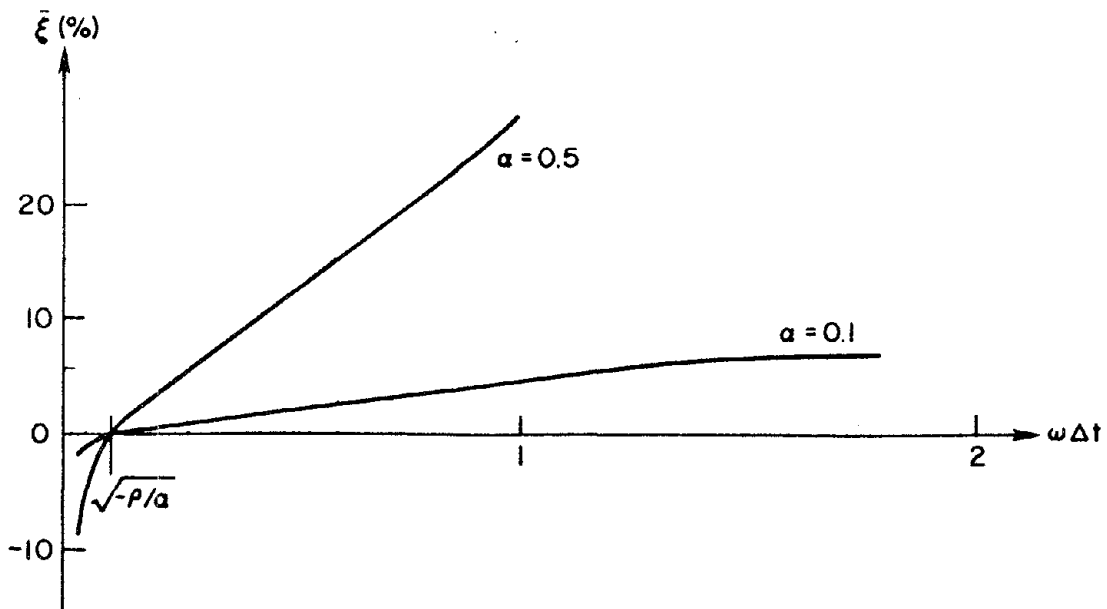


Figure 2.1 - Damping Characteristics of Modified Newmark Method  
(after Shing and Mahin [12])

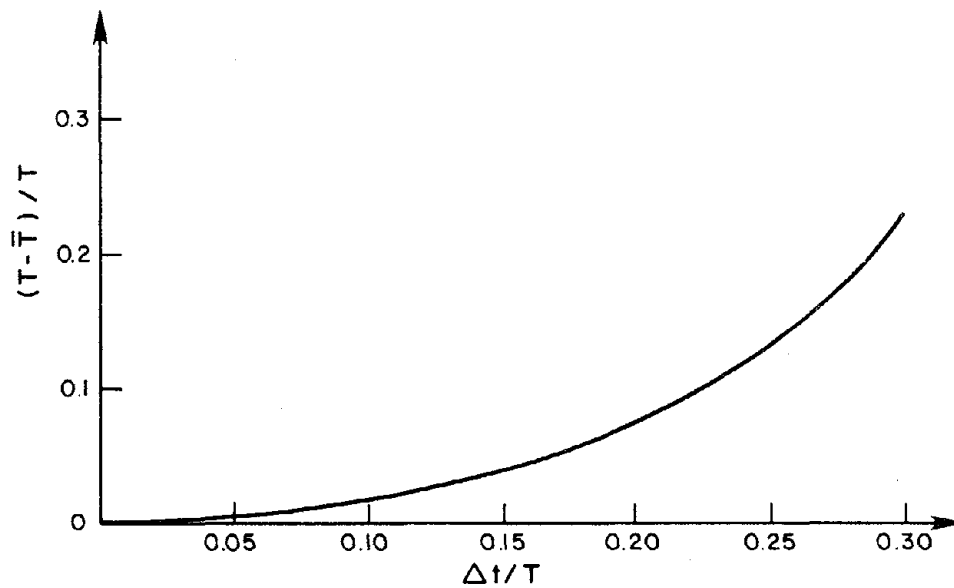


Figure 2.2 - Period Distortion Characteristics of Modified Newmark Method  
(after Shing and Mahin [12])

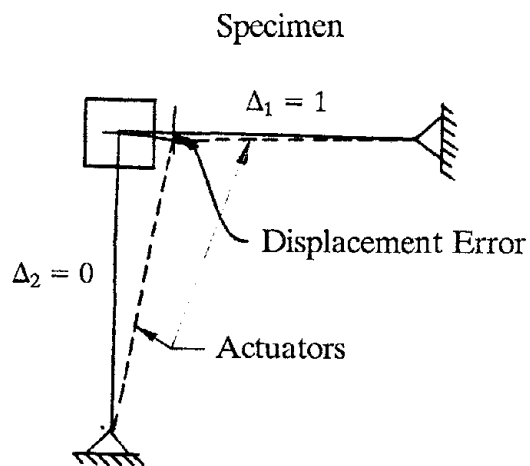


Figure 2.3 - Geometry Errors Due to Finite Actuator Lengths

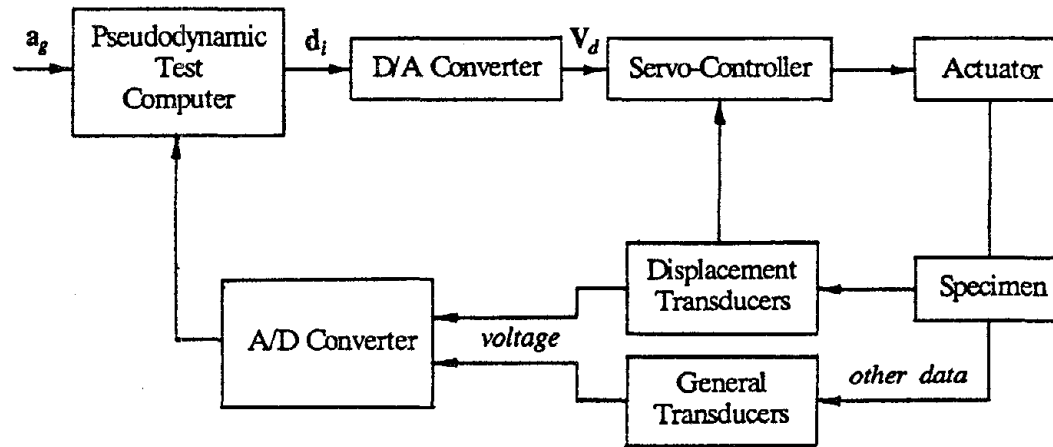


Figure 3.1 - Component Equipment for Pseudodynamic Test Method

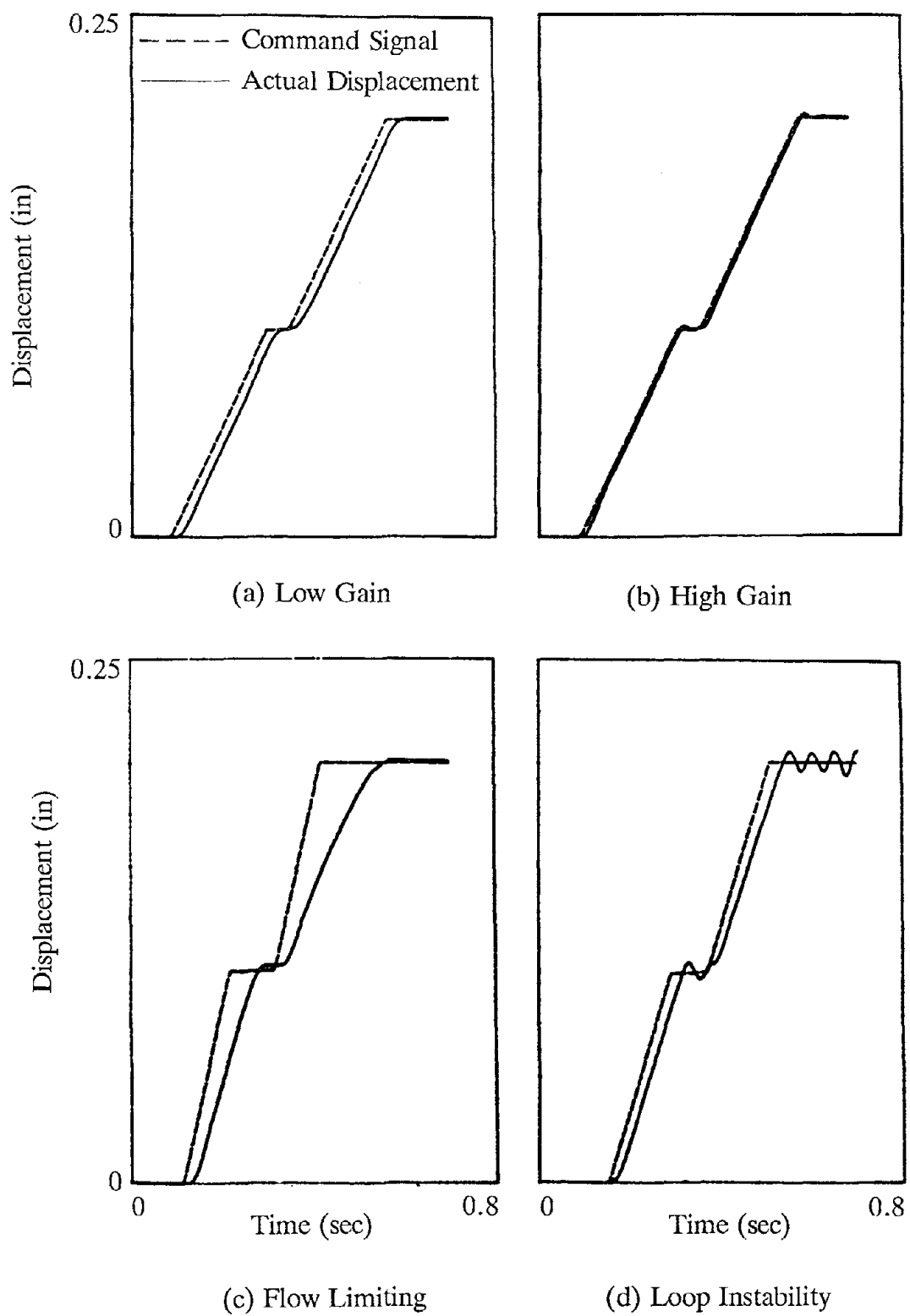


Figure 3.2 - Displacement Control Loop Behavior

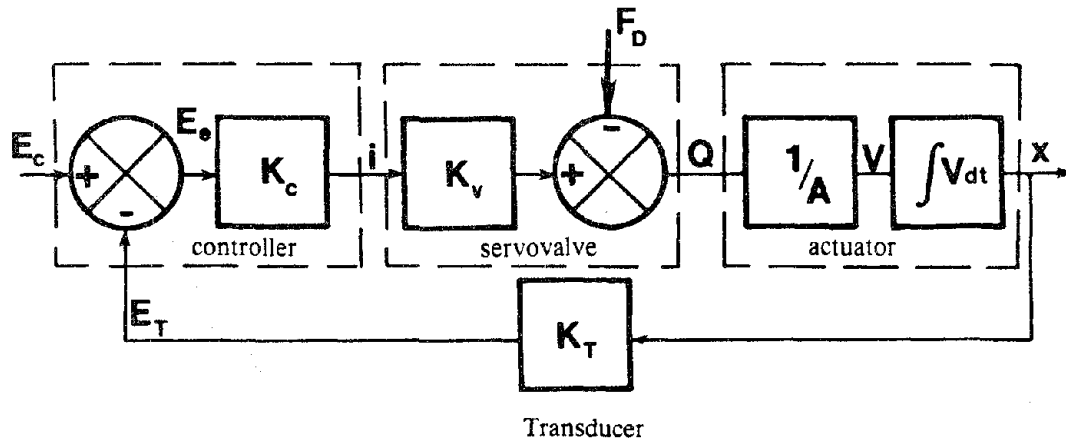


Figure 3.3 - Components of Electro-Hydraulic Control System (after [37])

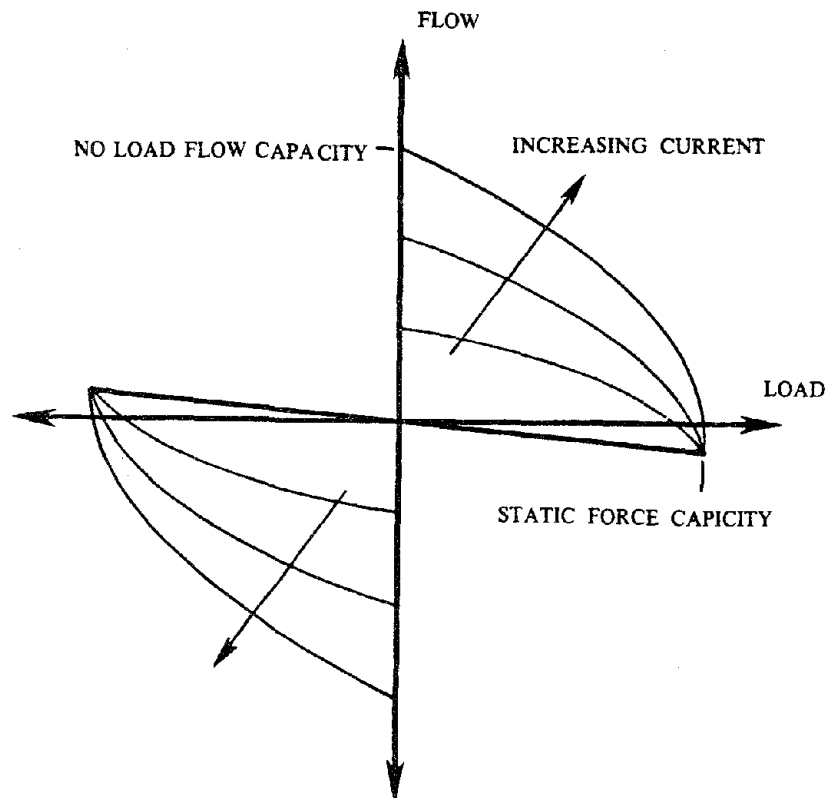


Figure 3.4 - Typical Servovalve Flow Curve

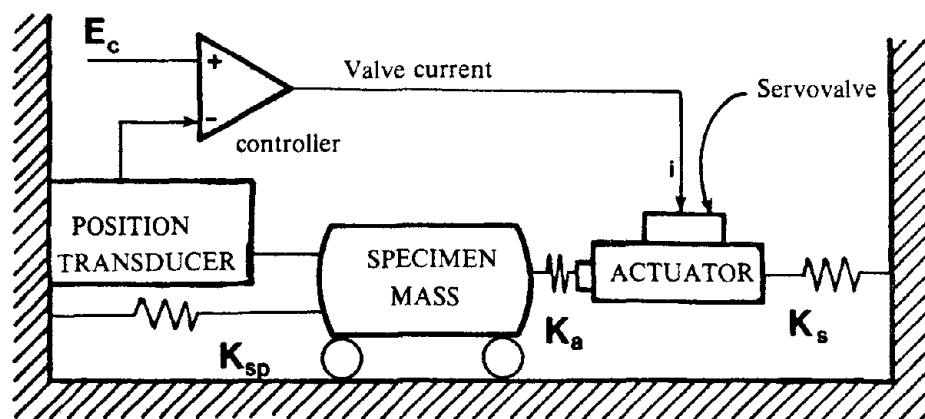


Figure 3.5 - An Electro-Hydraulic Control Loop as a Dynamic System (after [37])

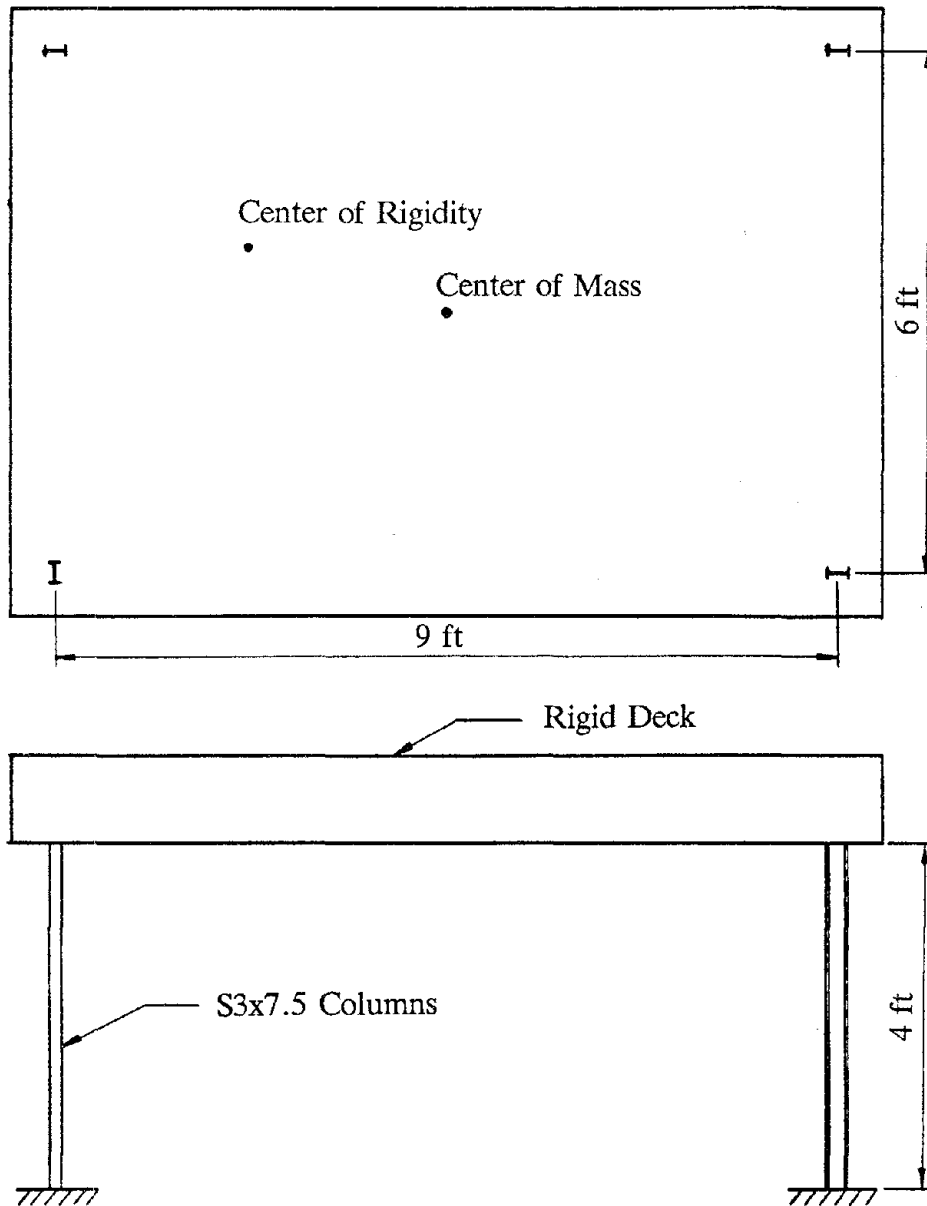


Figure 4.1 - Three Degree of Freedom Test Specimen

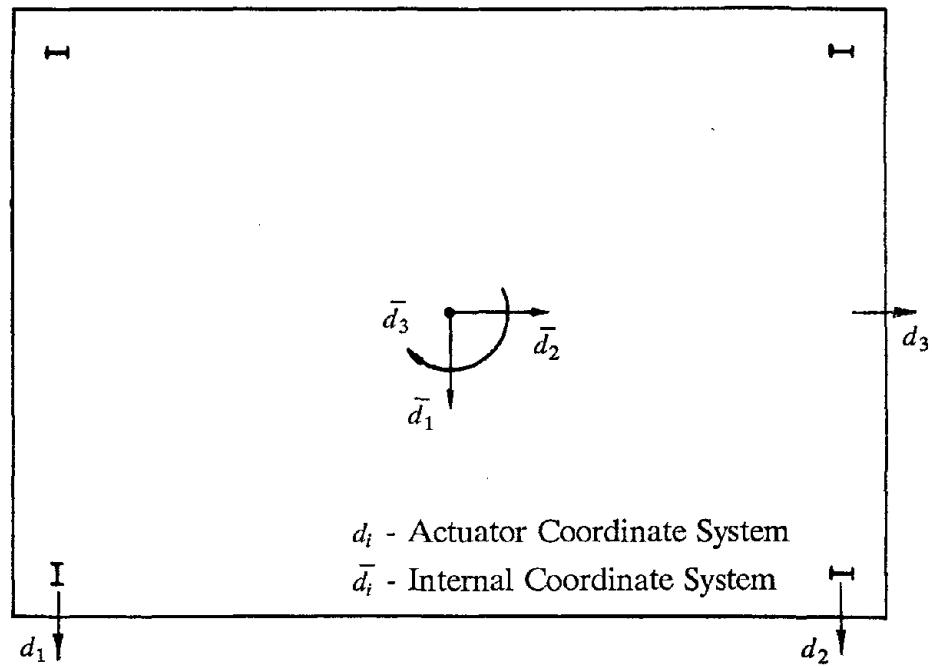


Figure 4.2 - Internal and External Degrees of Freedom

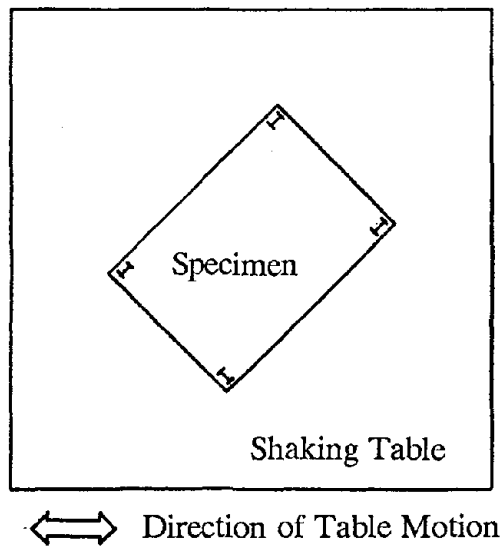


Figure 4.3 - Shaking Table Test Setup

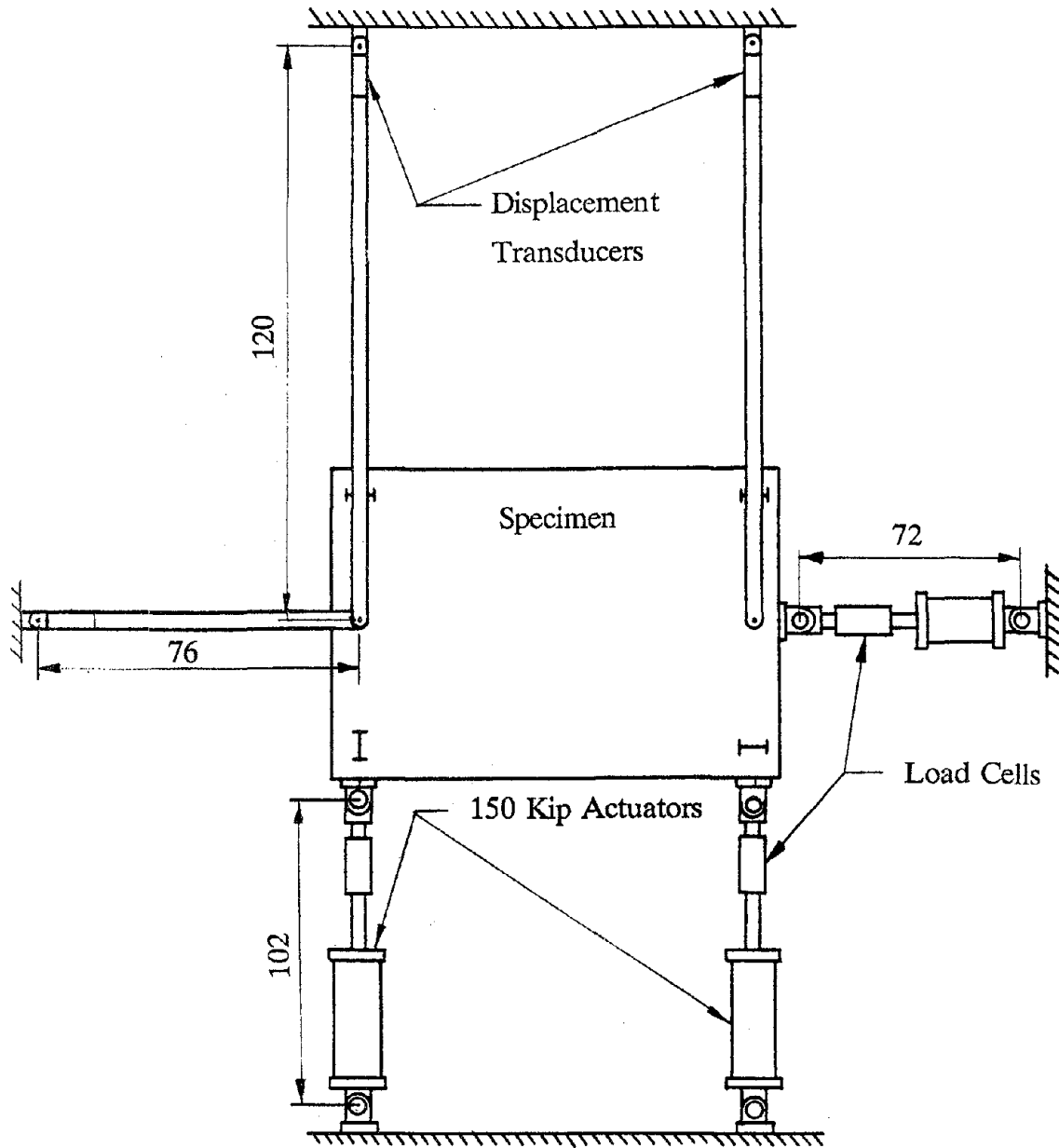


Figure 4.4 - Pseudodynamic Test Setup

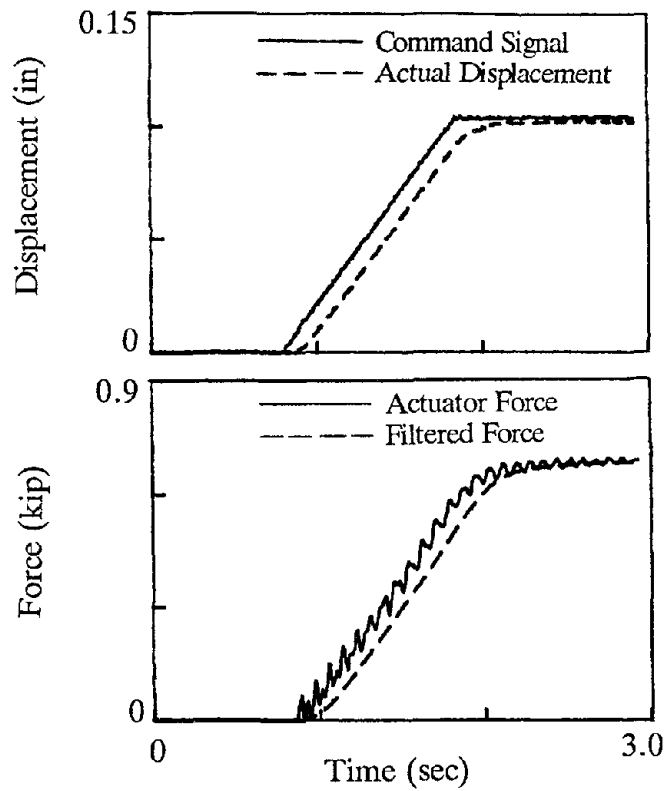
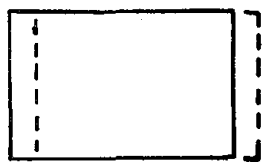


Figure 4.5 - Force Oscillation Under Displacement Control



DESIRED DISPLACEMENT

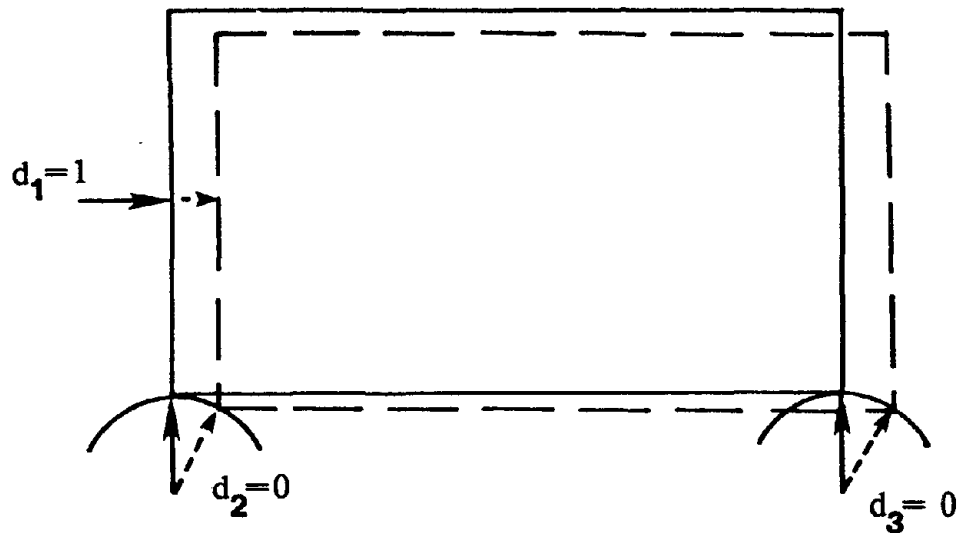


Figure 4.6 - Geometry Errors Due to Finite Actuator Length

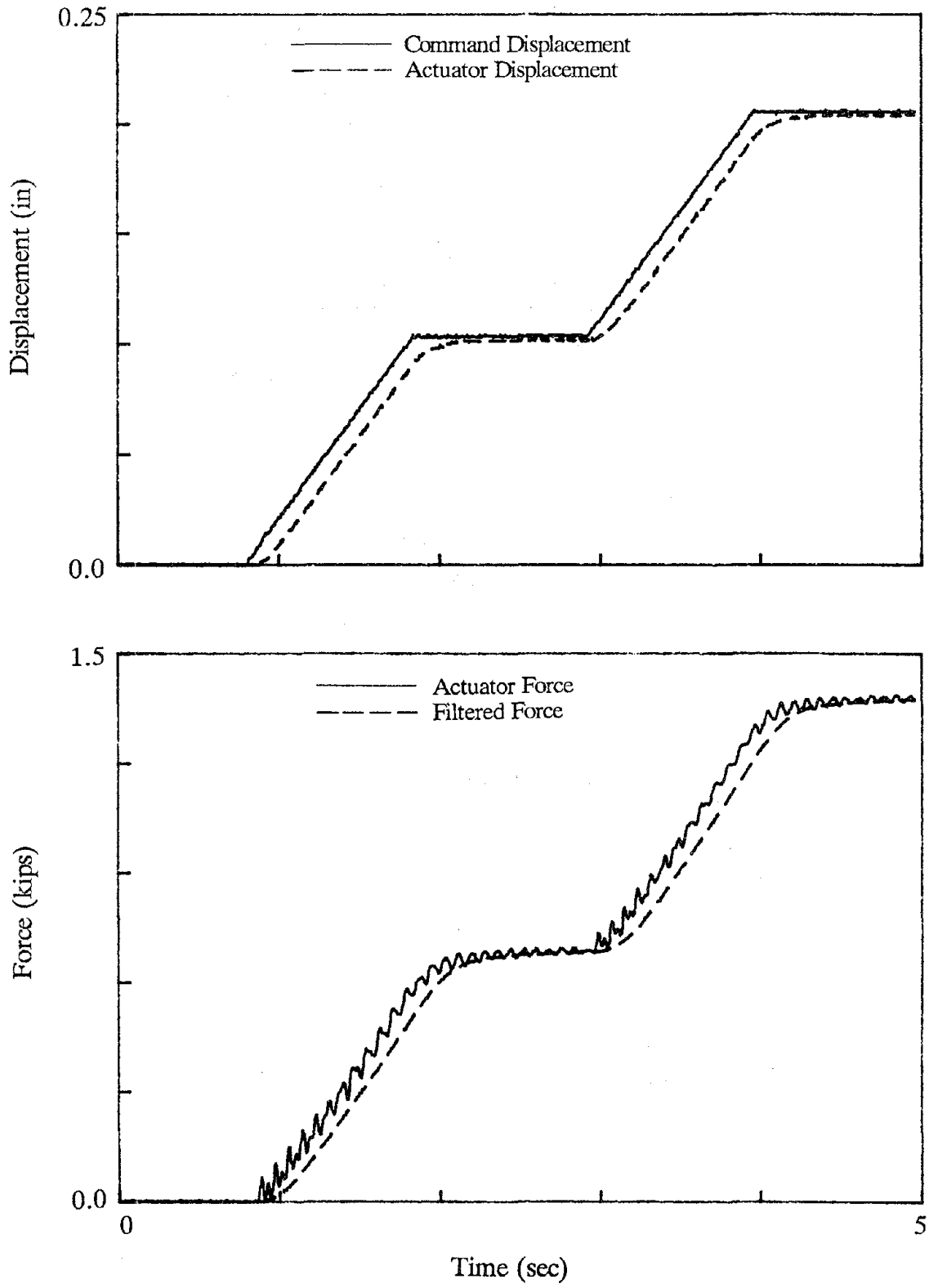


Figure 4.7 - Force Relaxation at Elastic Level

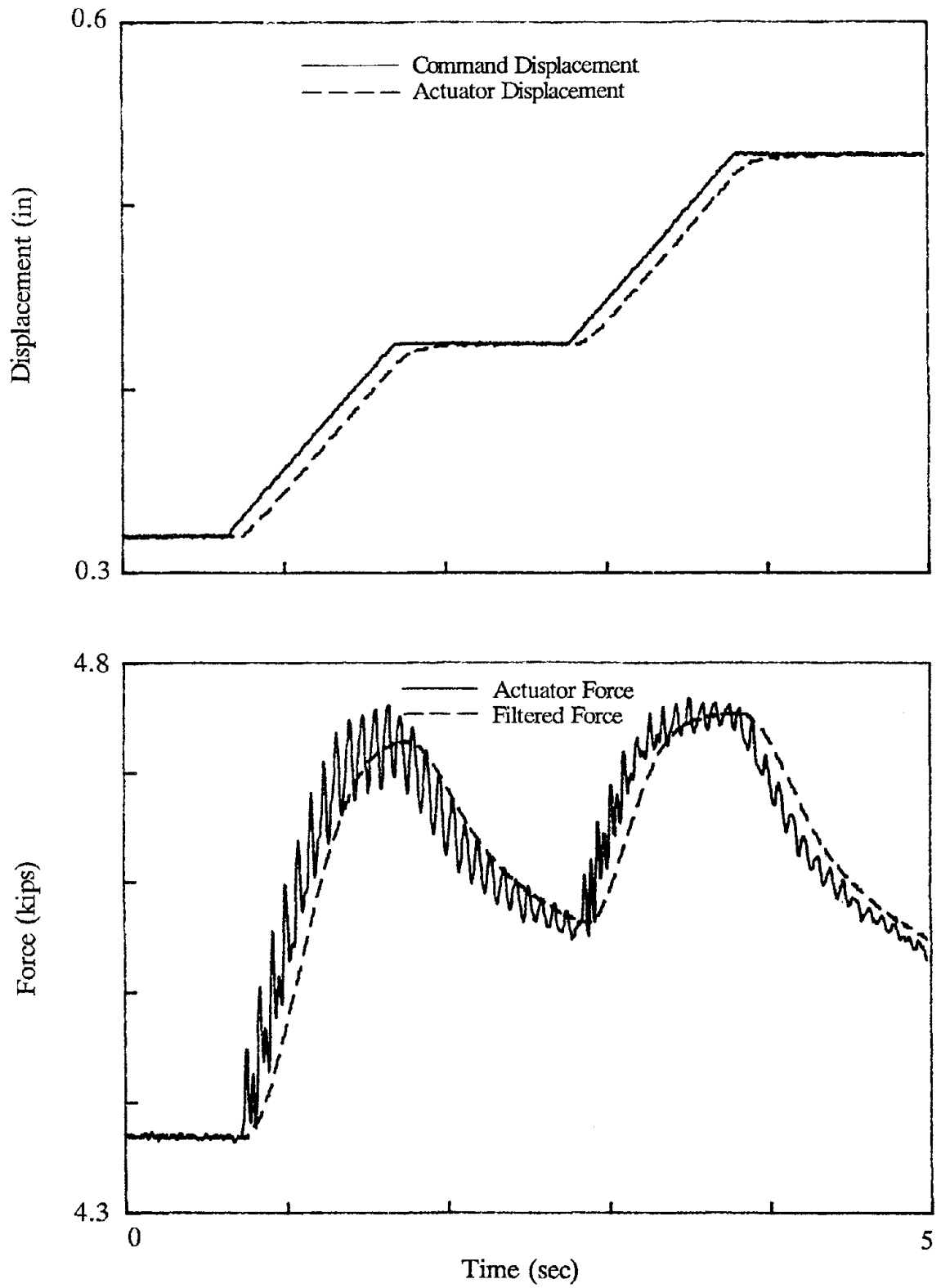


Figure 4.8 - Force Relaxation at Inelastic Level

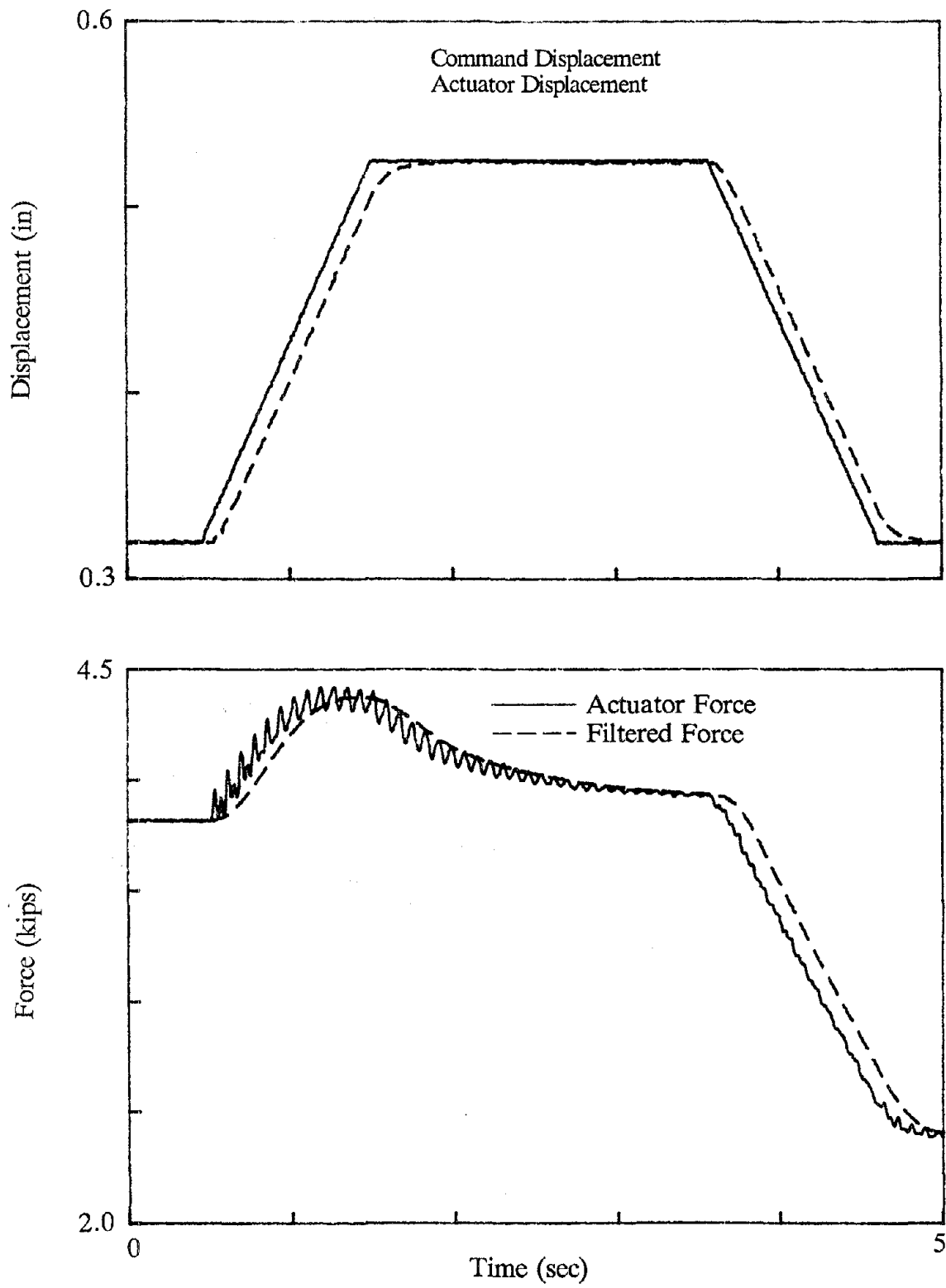


Figure 4.9 - Force Relaxation During Unloading

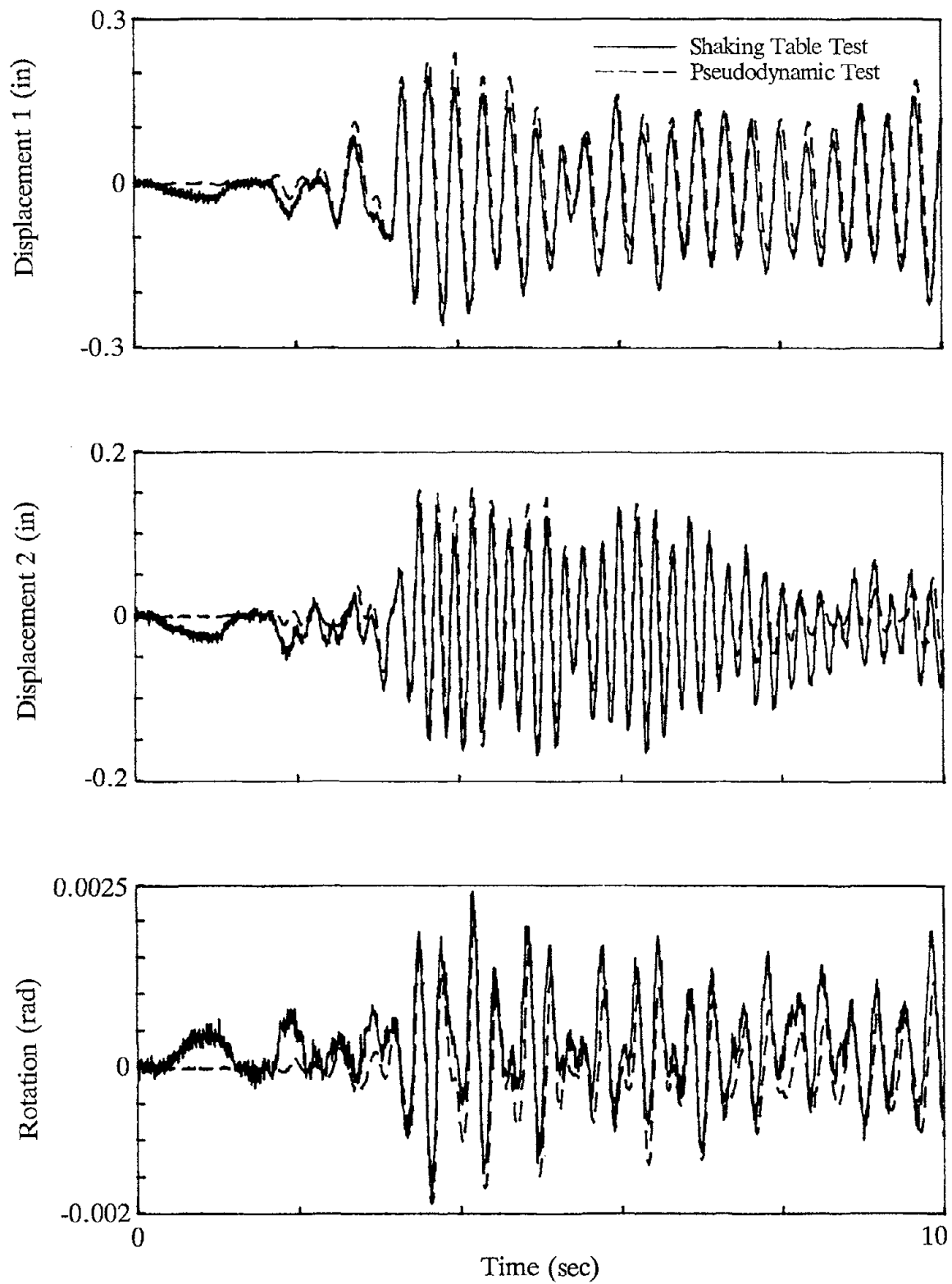


Figure 4.10 - Test 1 Displacement Response (Part 1)

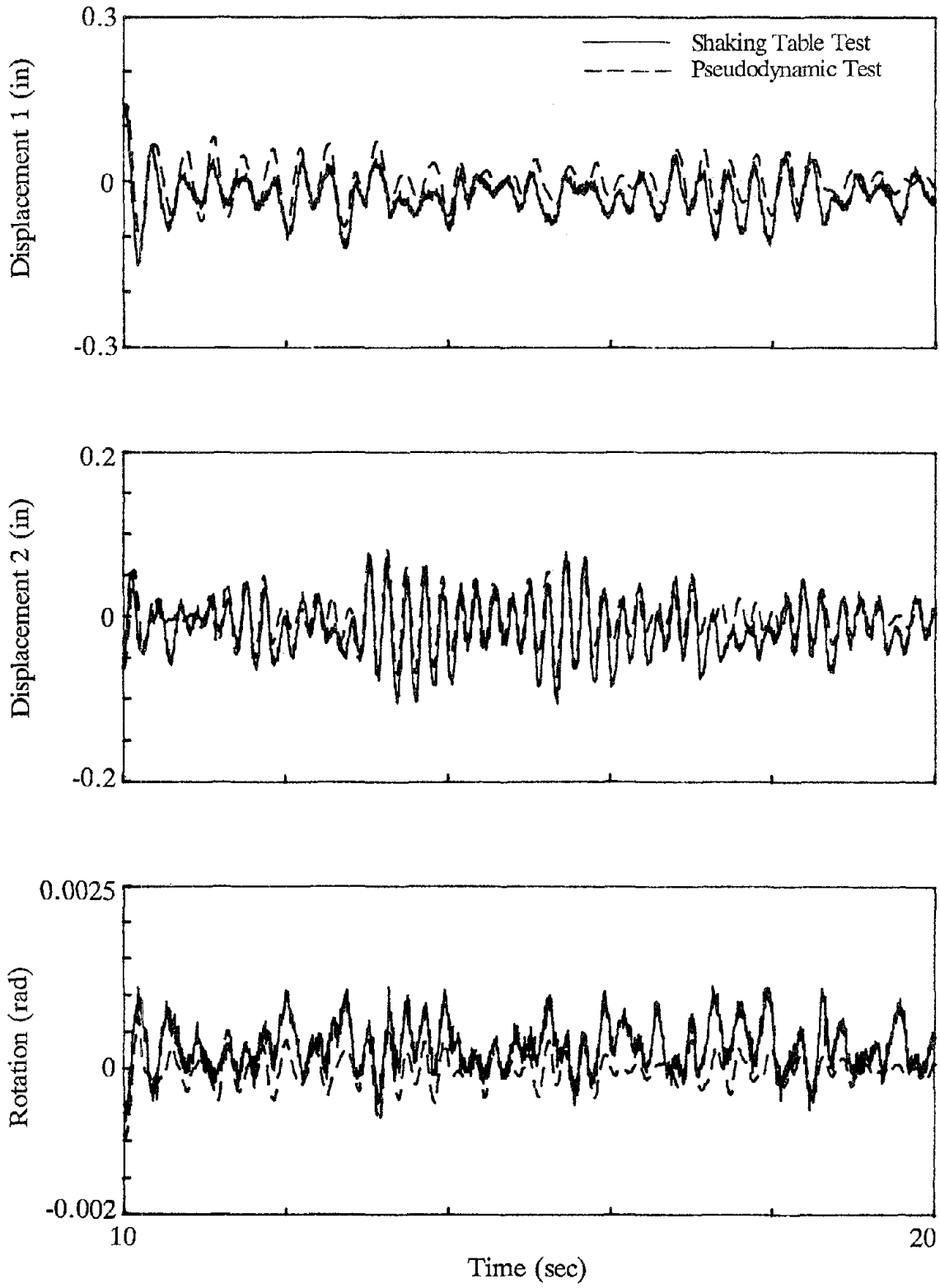


Figure 4.11 - Test 1 Displacement Response (Part 2)

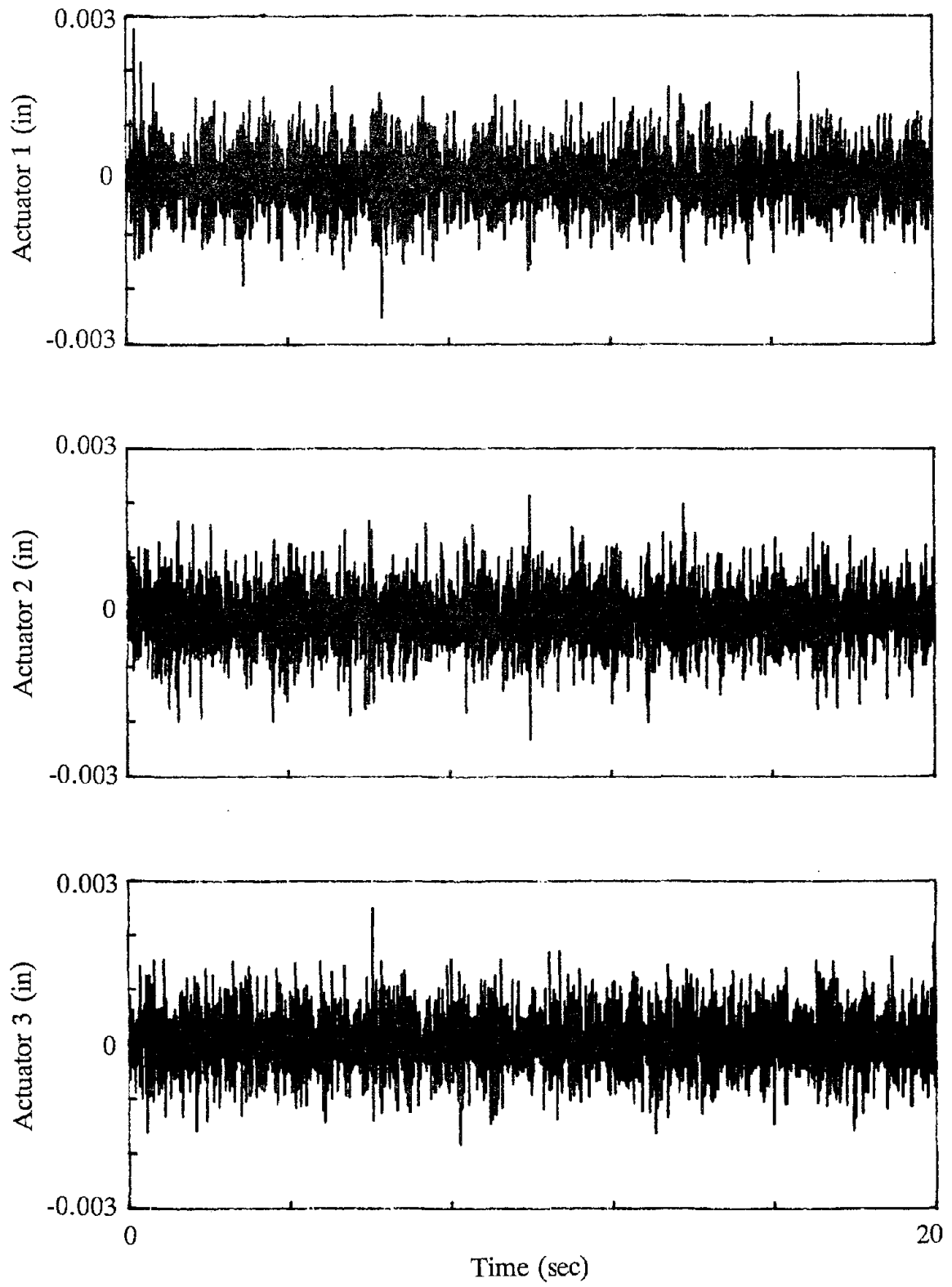


Figure 4.12 - Test 1 Displacement Error Histories

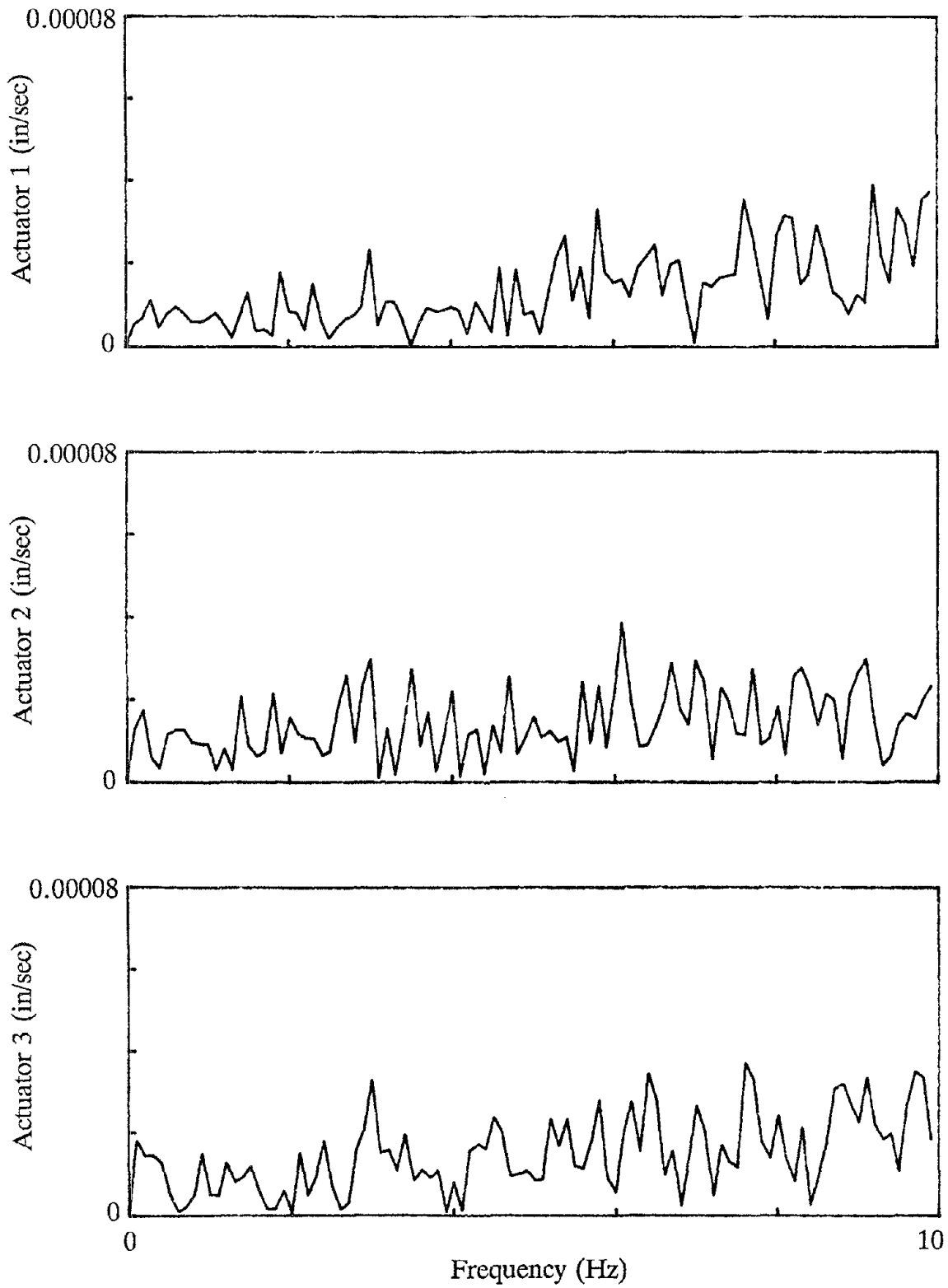


Figure 4.13 - Test 1 Displacement Error Fourier Amplitude Spectra

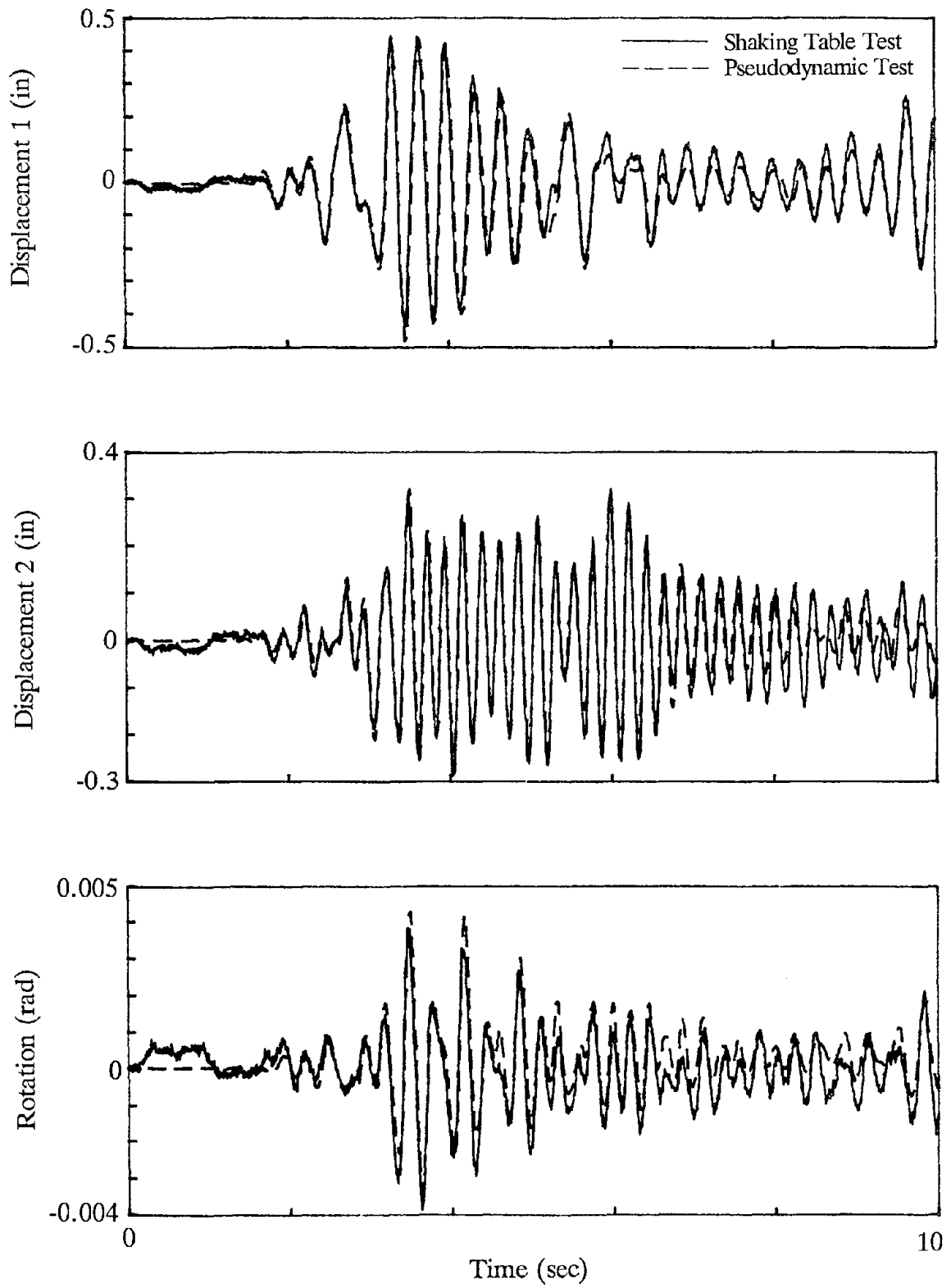


Figure 4.14 - Test 2 Displacement Response (Part 1)

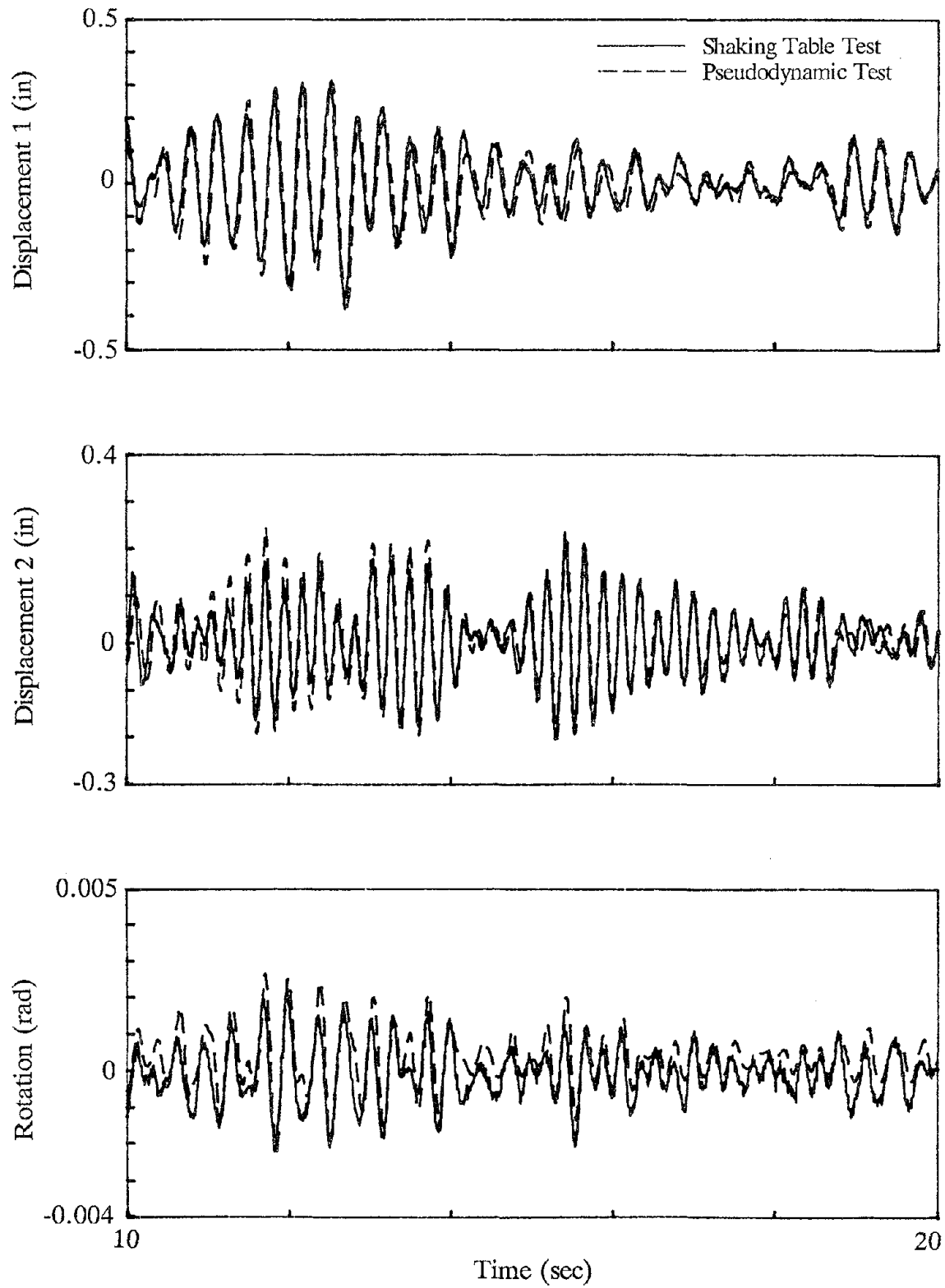


Figure 4.15 - Test 2 Displacement Response (Part 2)

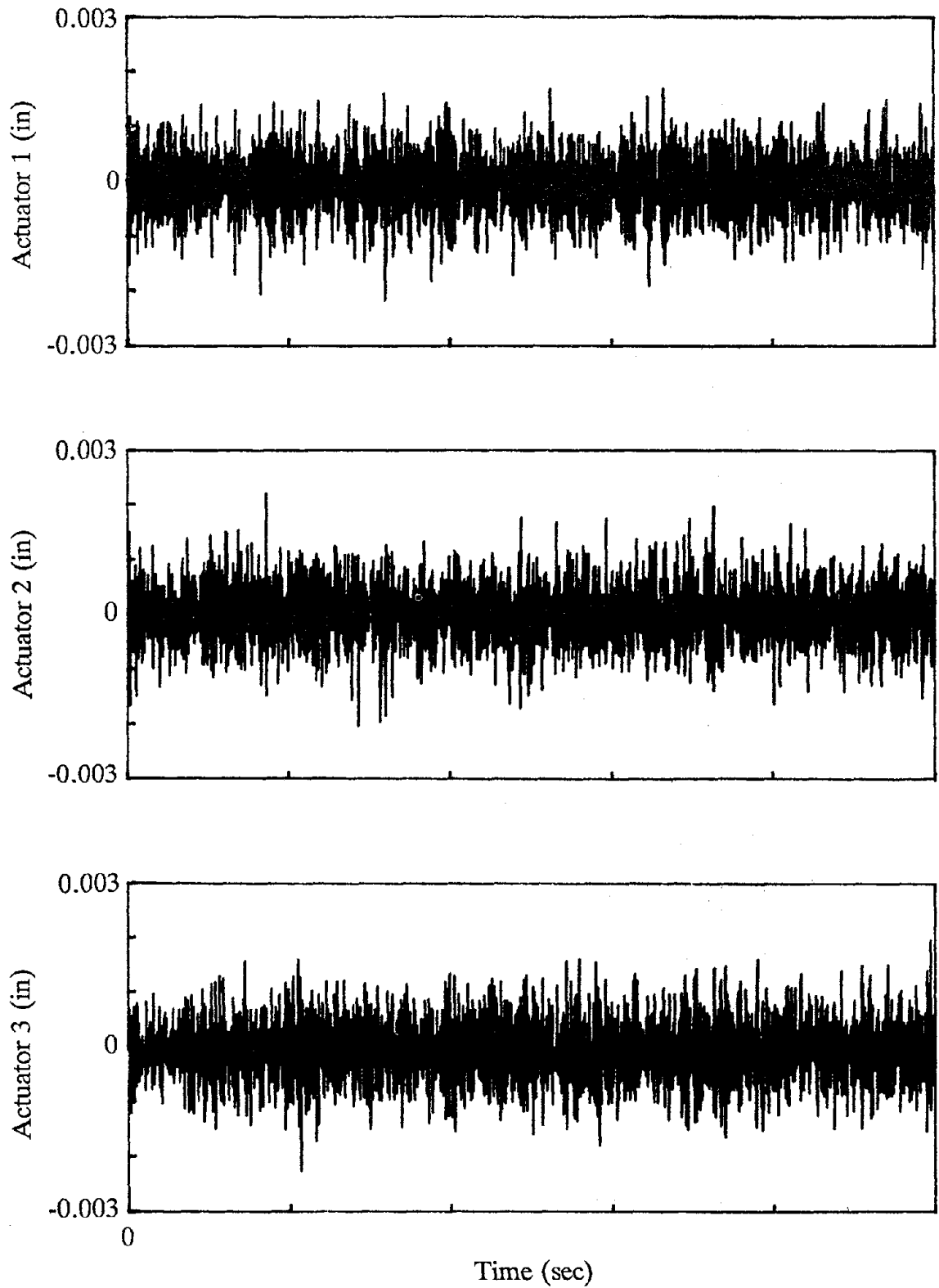


Figure 4.16 - Test 2 Displacement Error Histories

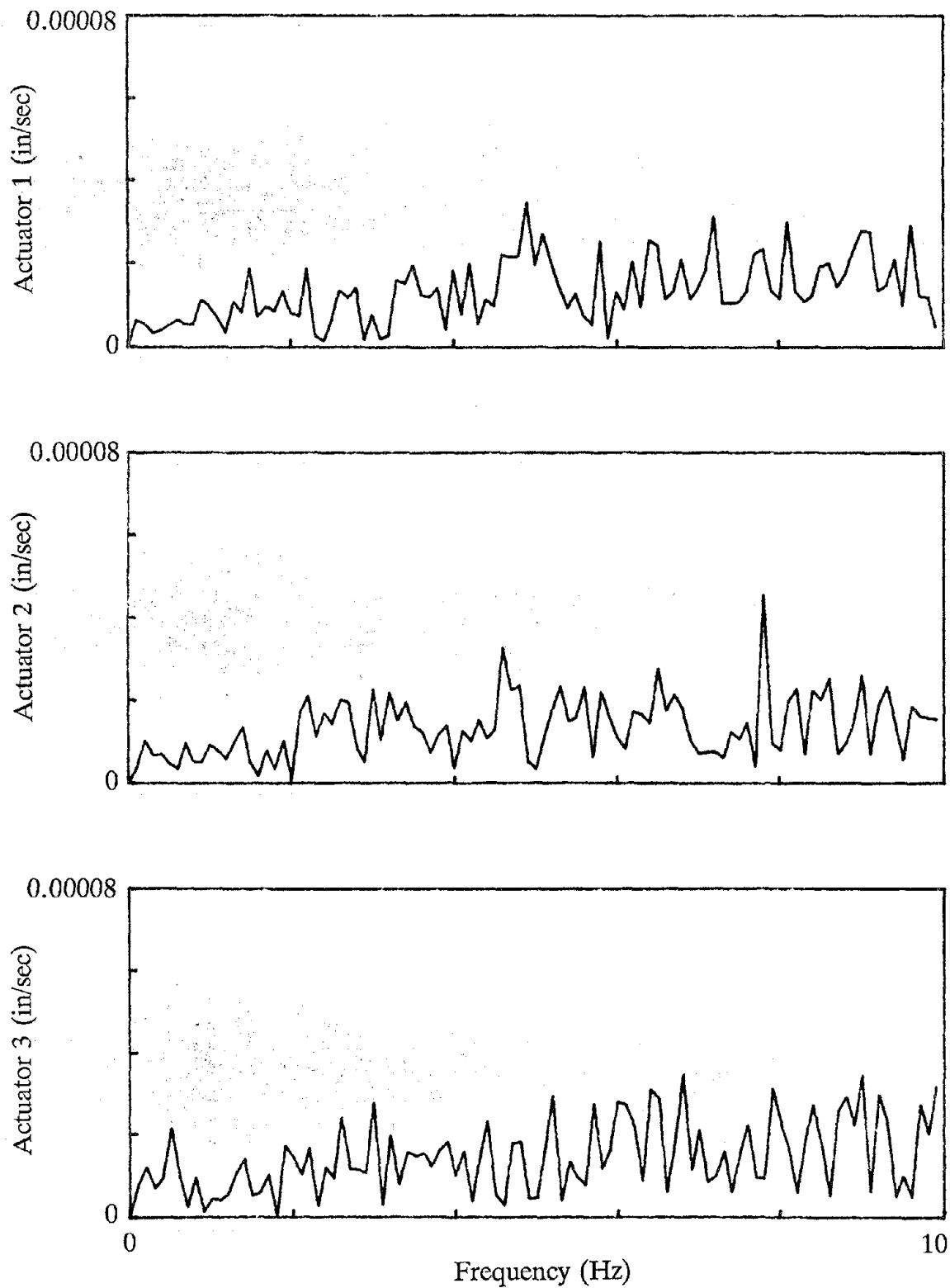


Figure 4.17 - Test 2 Displacement Error Fourier Amplitude Spectra

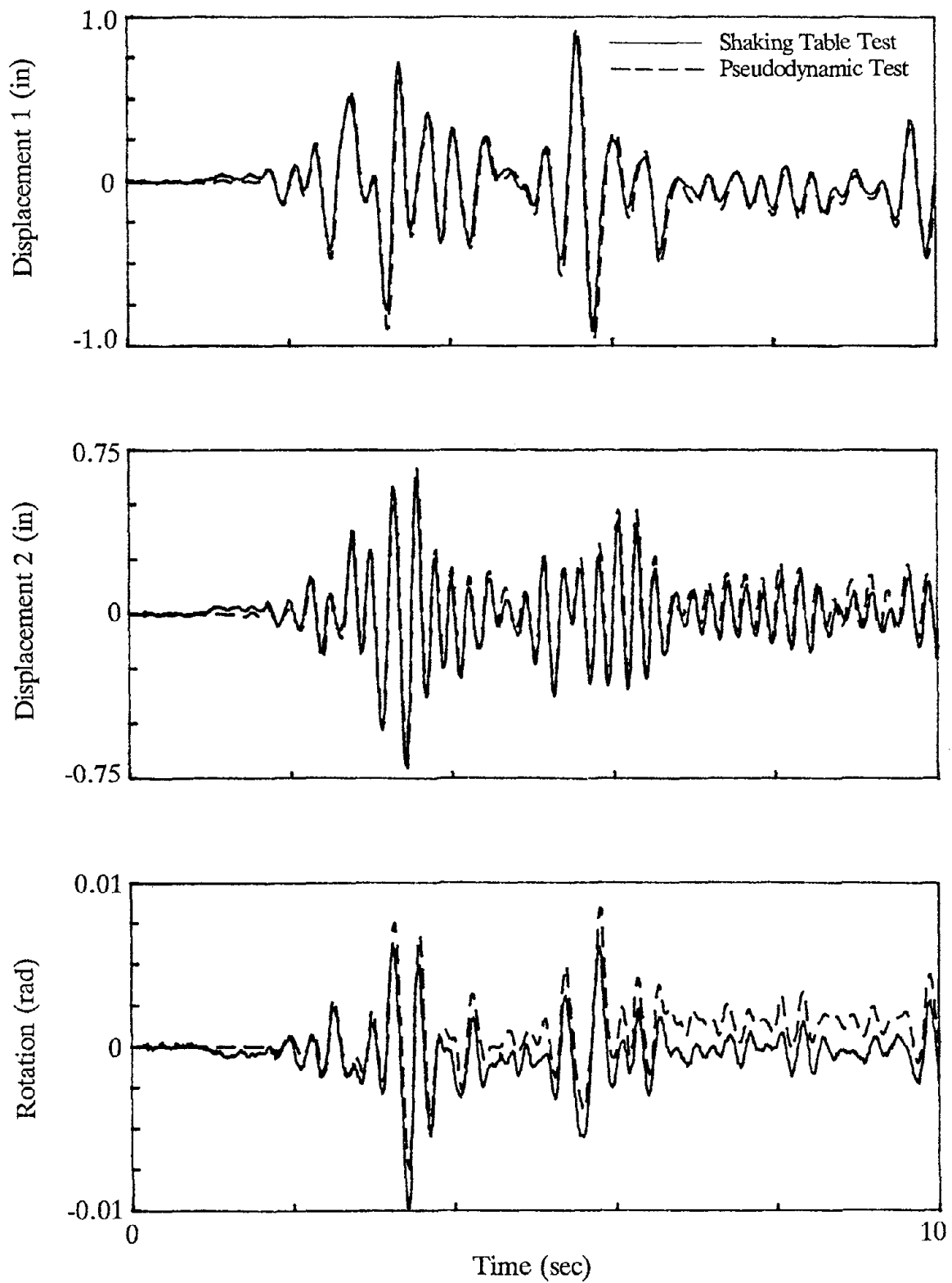


Figure 4.18 - Test 3 Displacement Response (Part 1)

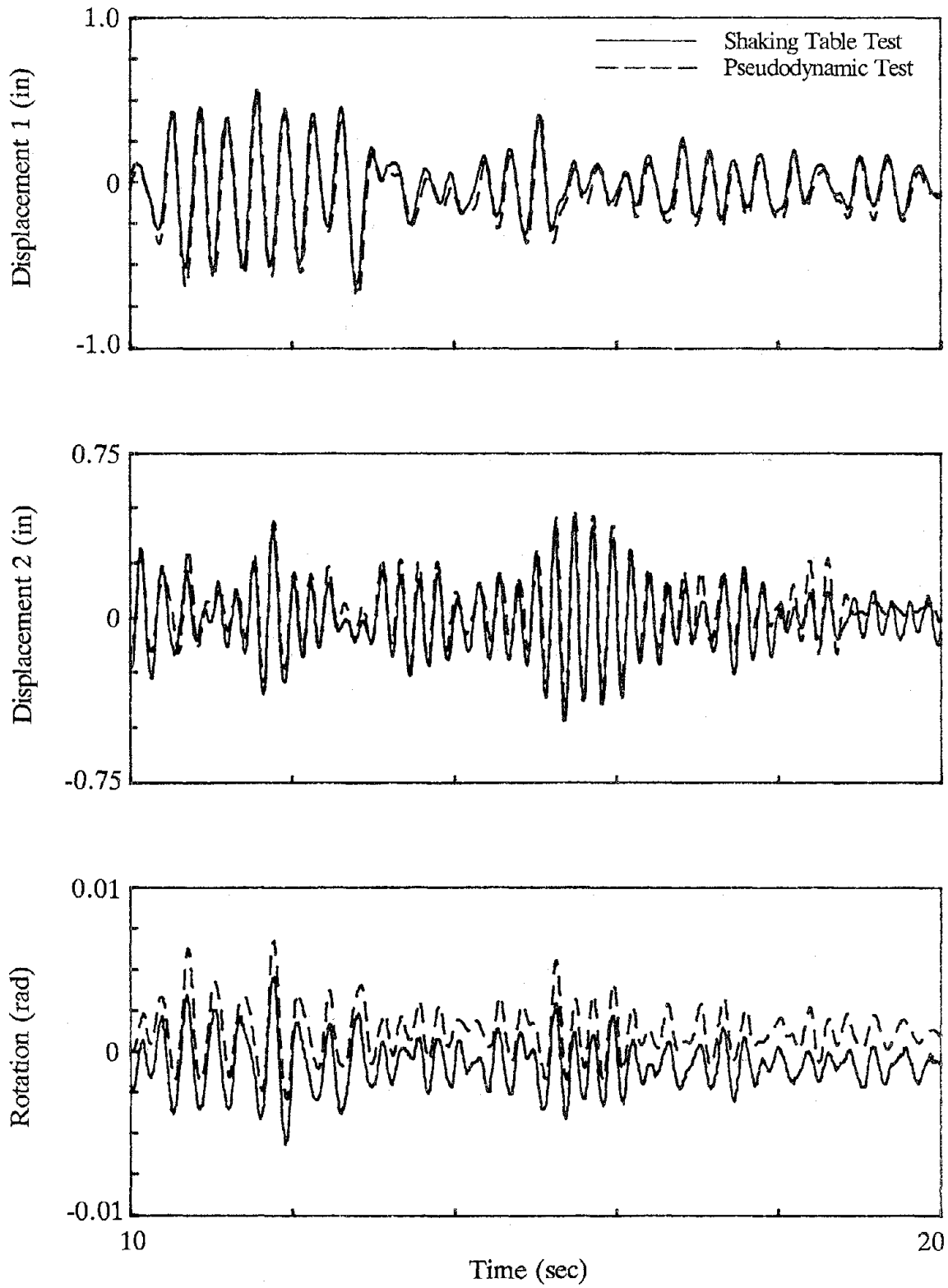


Figure 4.19 - Test 3 Displacement Response (Part 2)

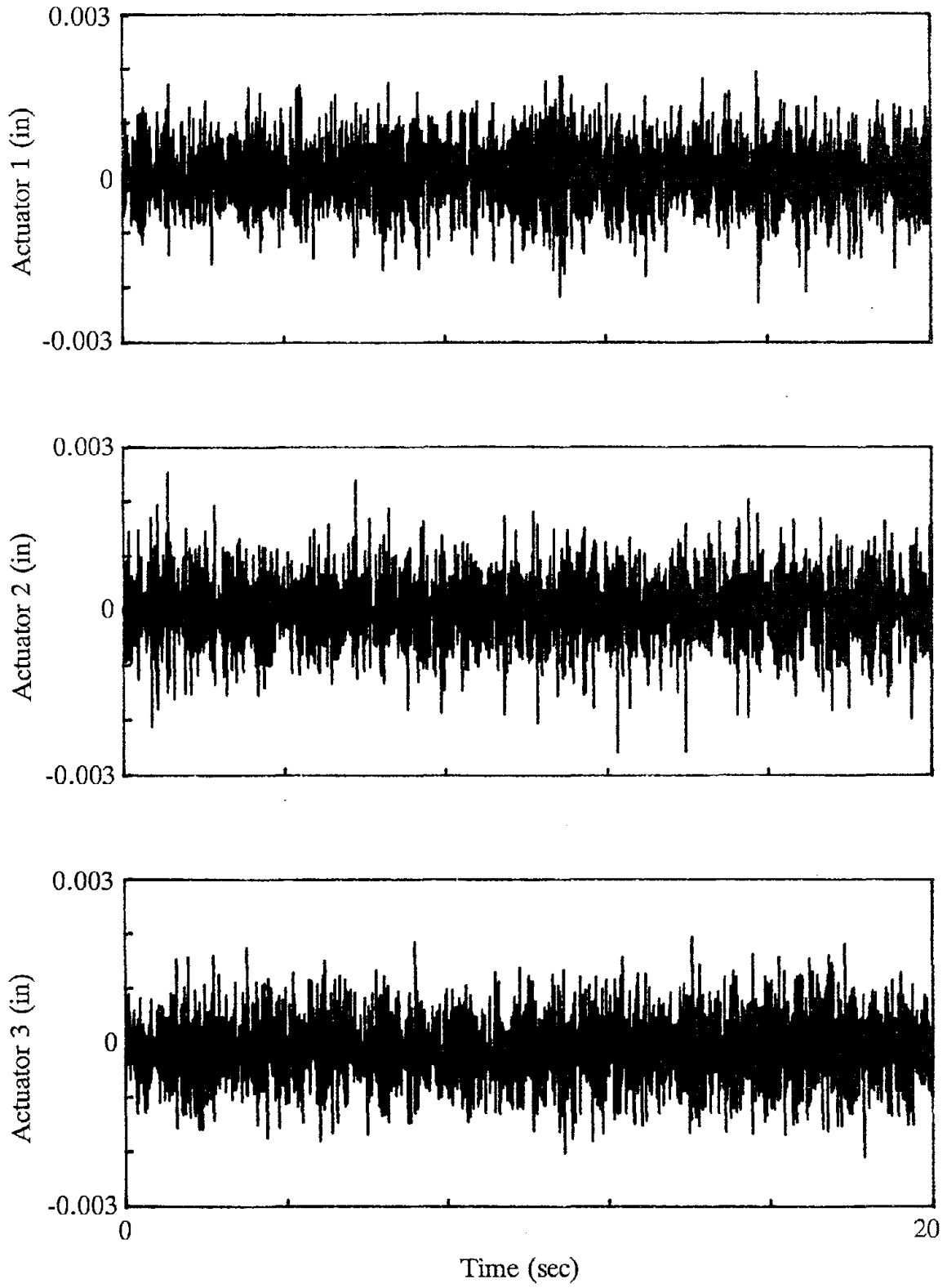


Figure 4.20 - Test 3 Displacement Error Histories

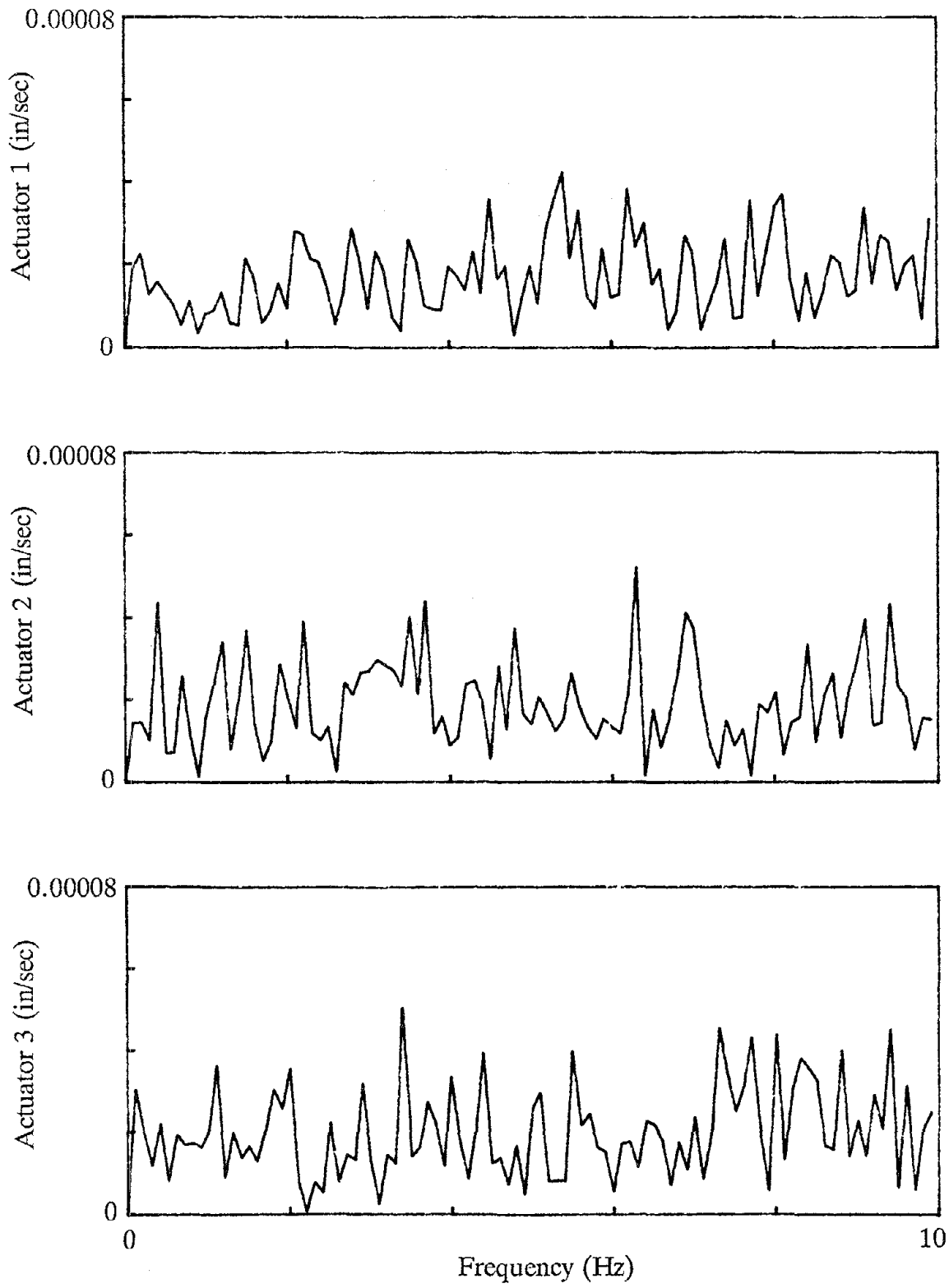


Figure 4.21 - Test 3 Displacement Error Fourier Amplitude Spectra

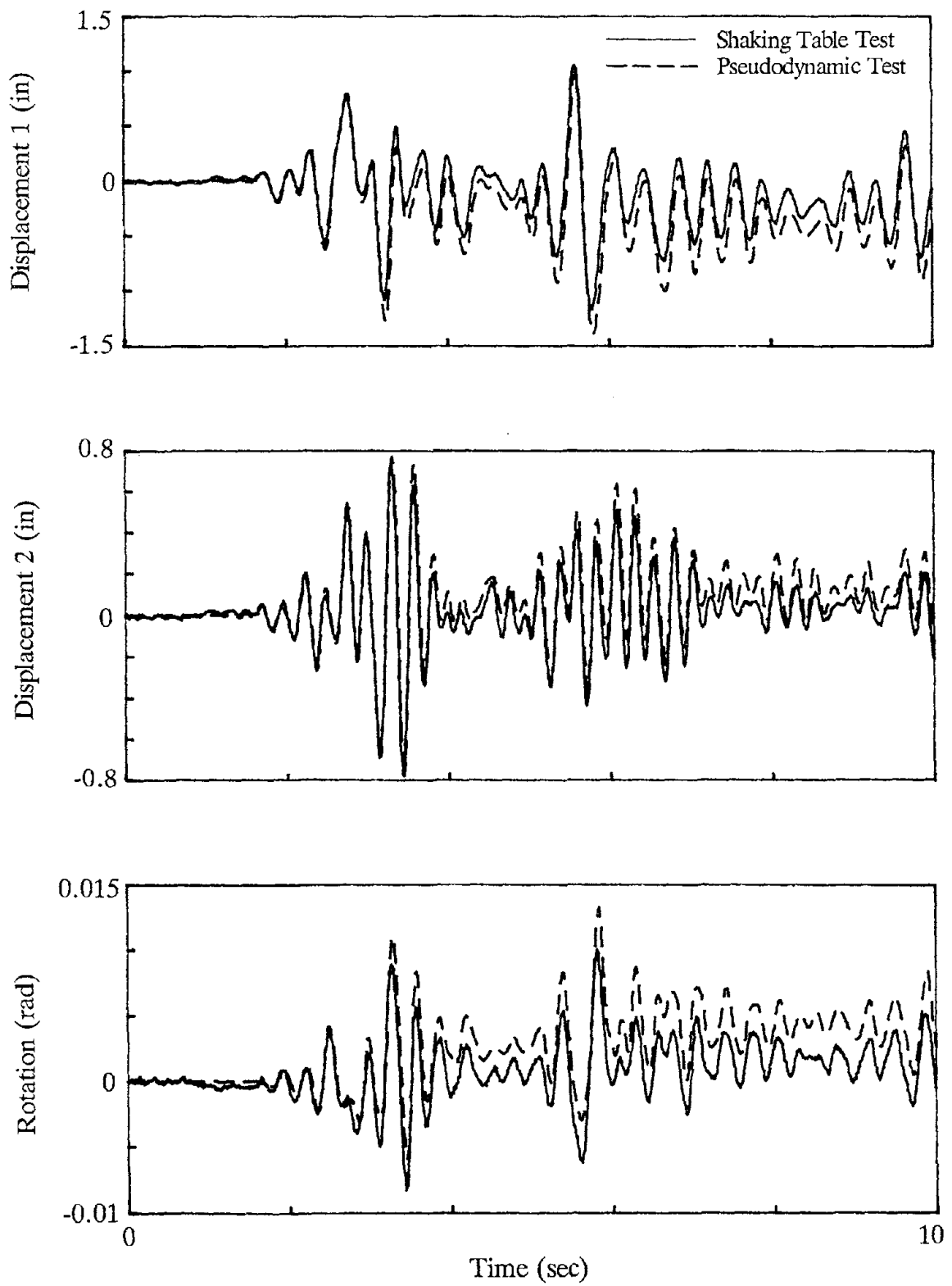


Figure 4.22 - Test 4 Displacement Response (Part 1)

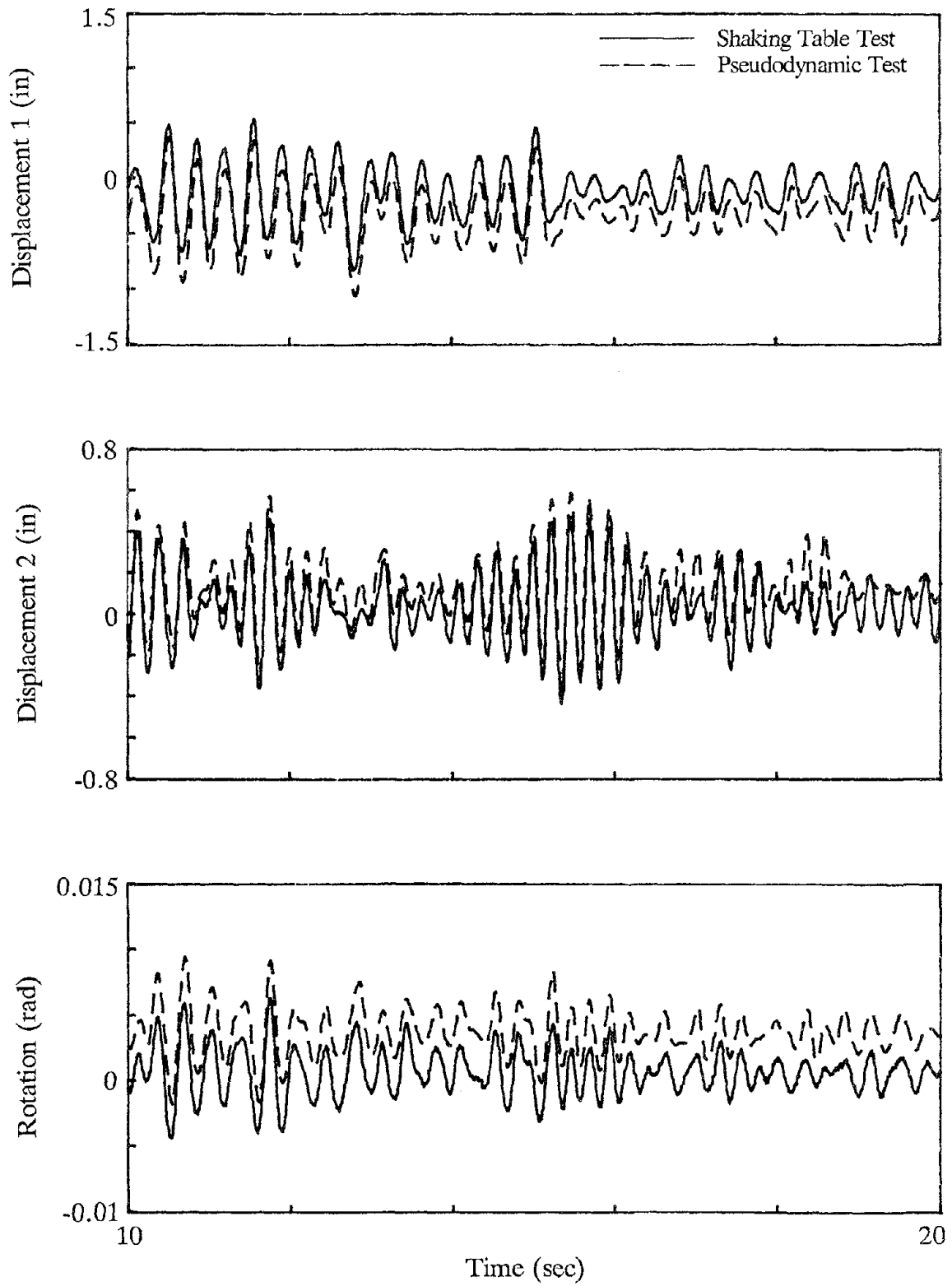


Figure 4.23 - Test 4 Displacement Response (Part 2)

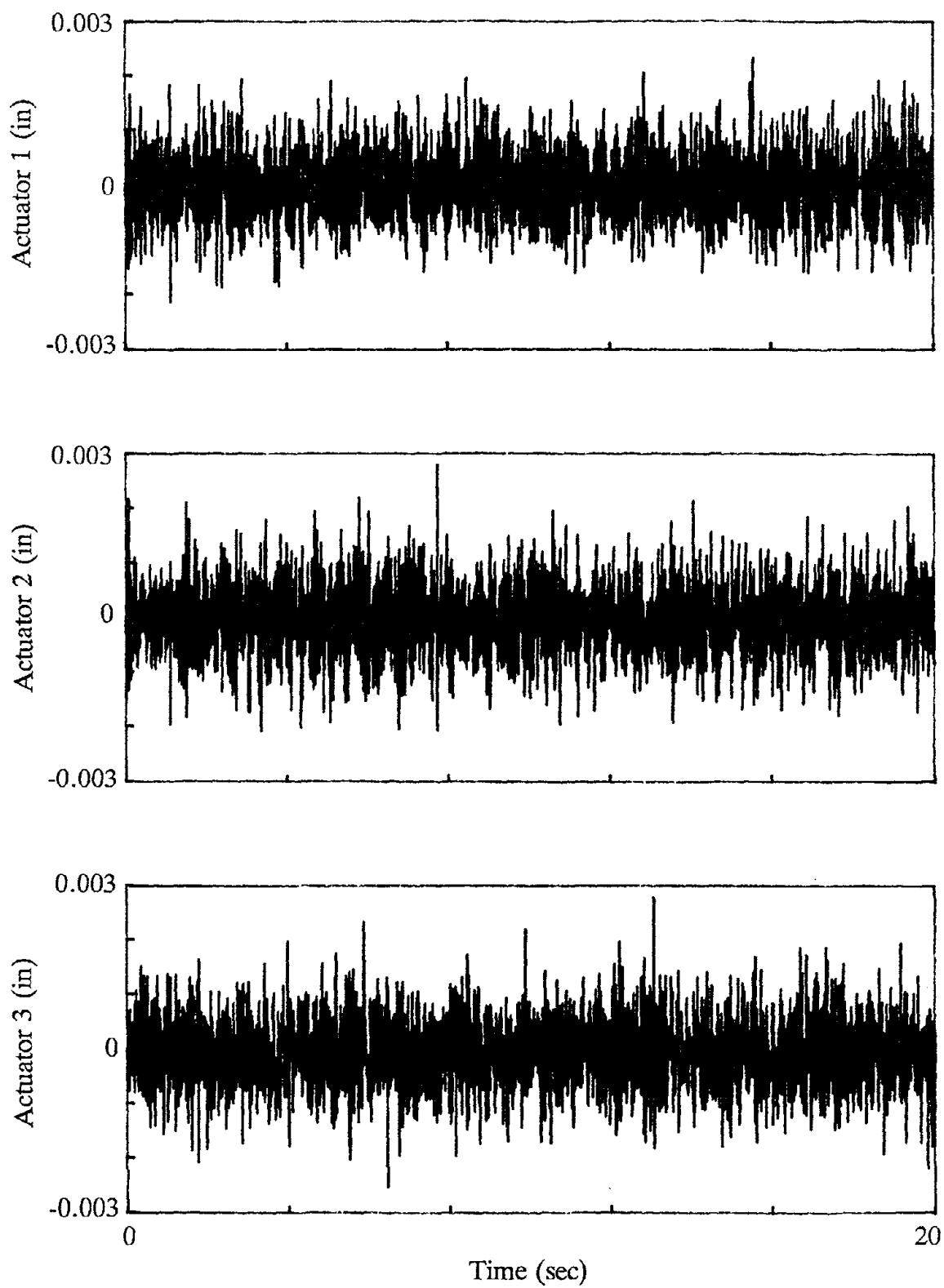


Figure 4.24 - Test 4 Displacement Error Histories

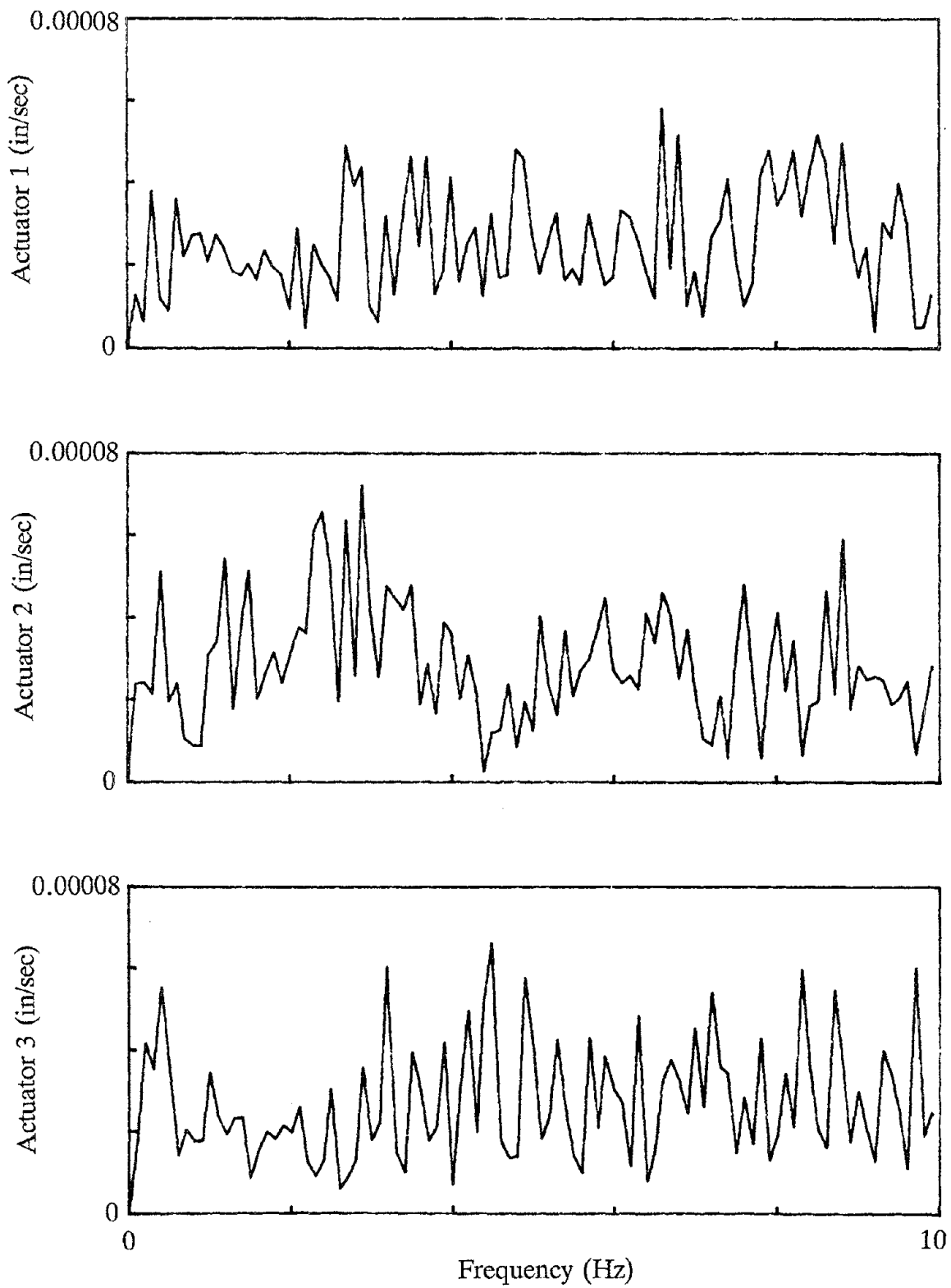


Figure 4.25 - Test 4 Displacement Error Fourier Amplitude Spectra

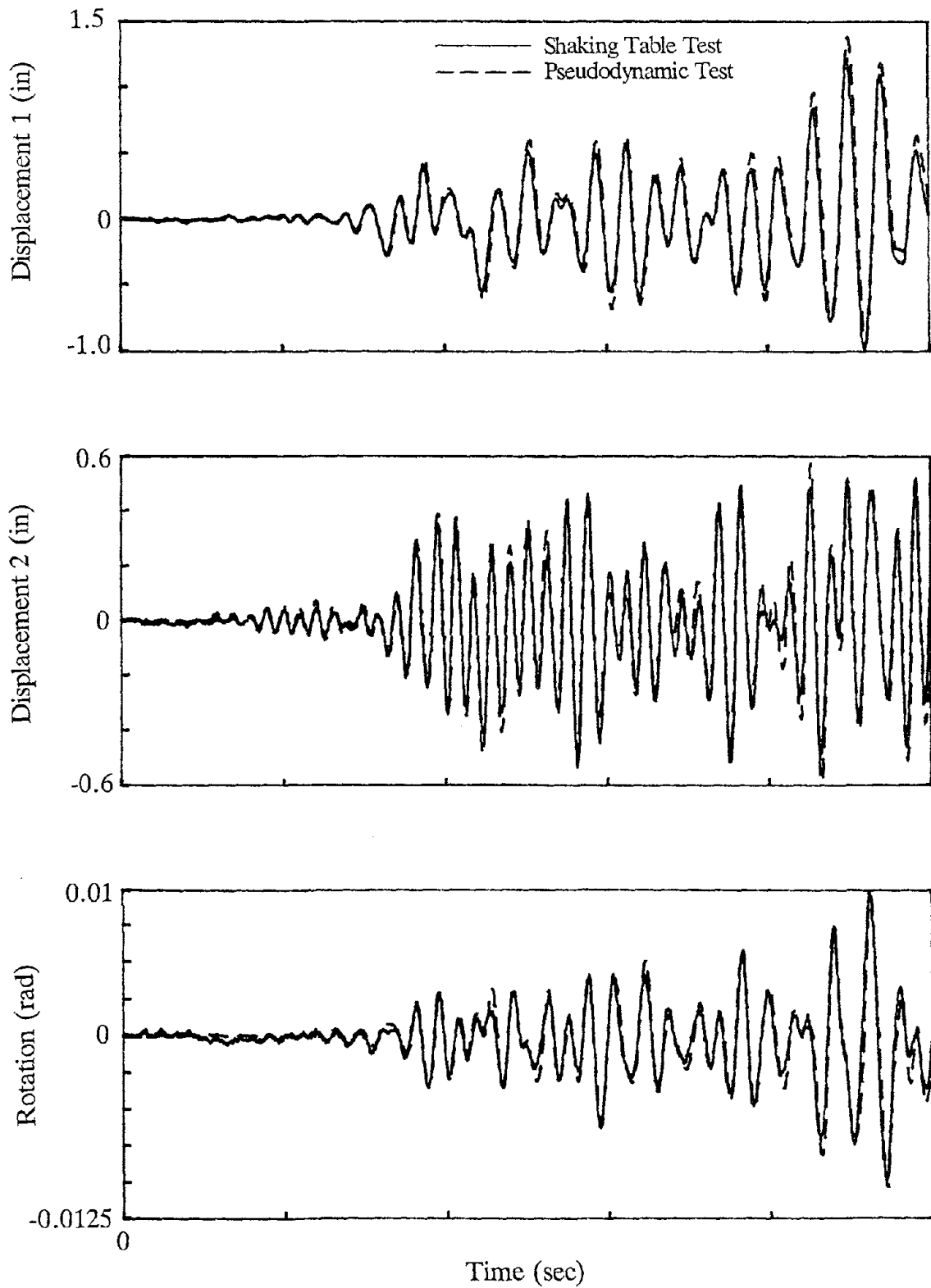


Figure 4.26 - Test 5 Displacement Response (Part 1)

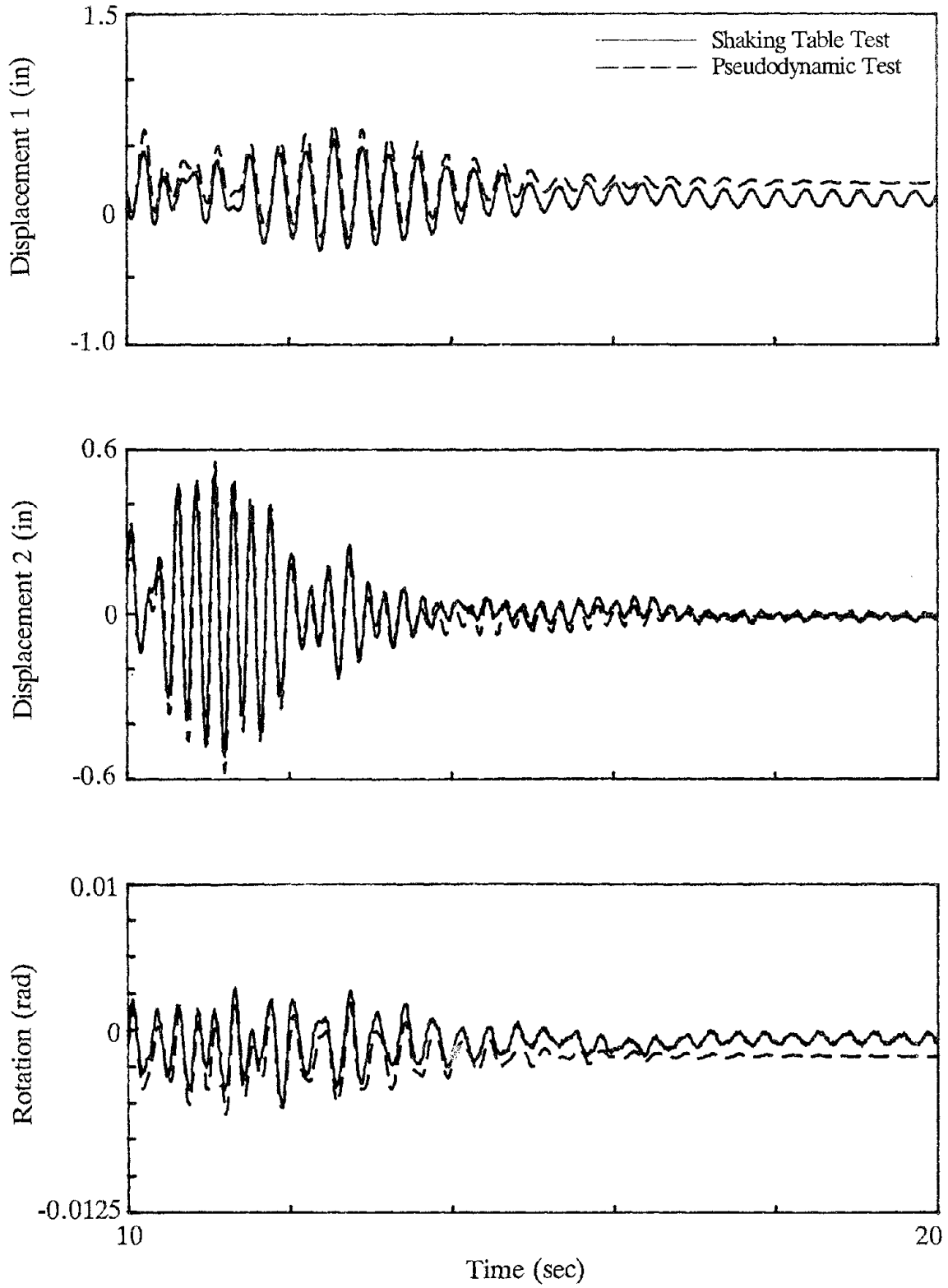


Figure 4.27 - Test 5 Displacement Response (Part 2)

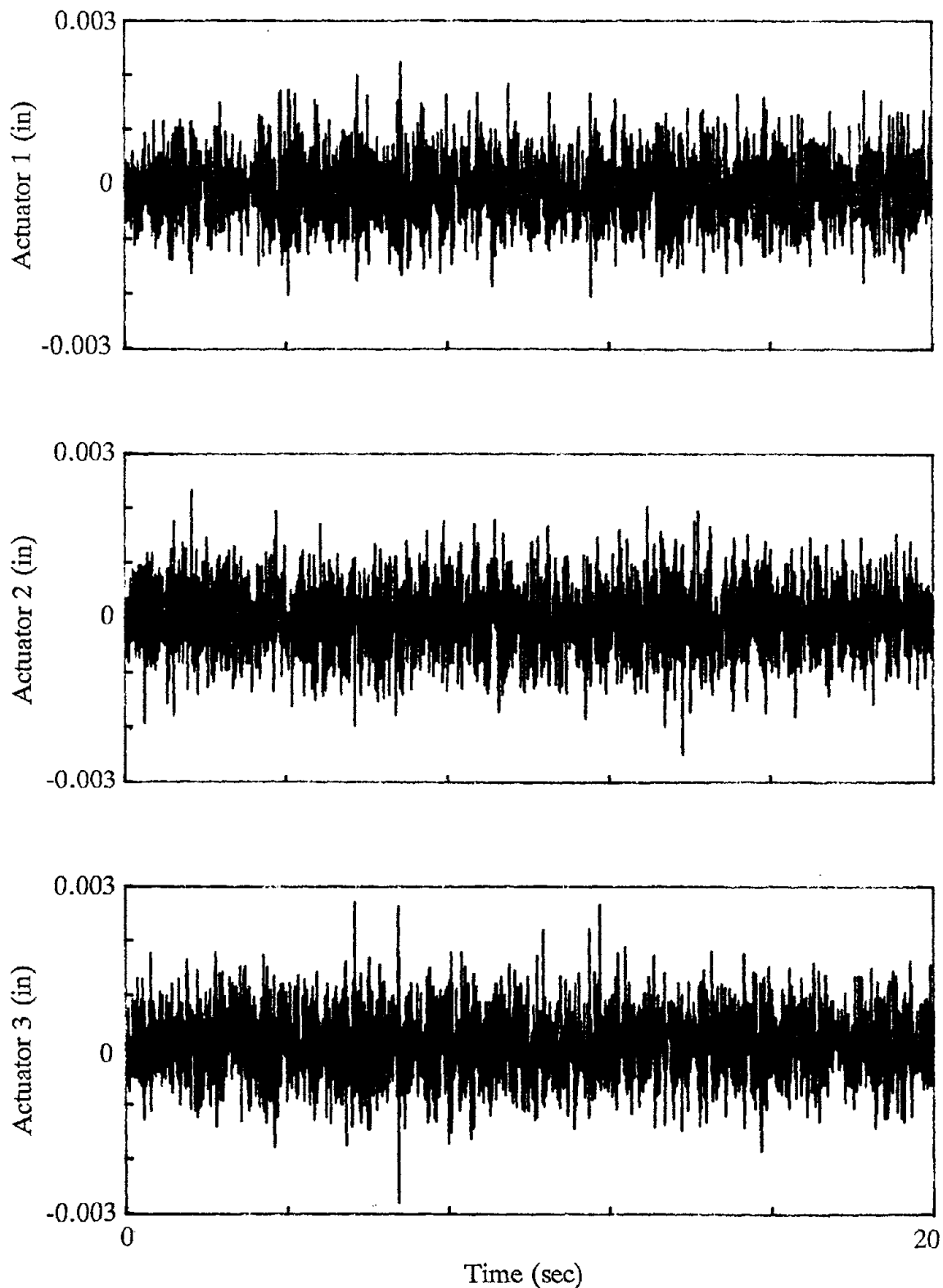


Figure 4.28 - Test 5 Displacement Error Histories

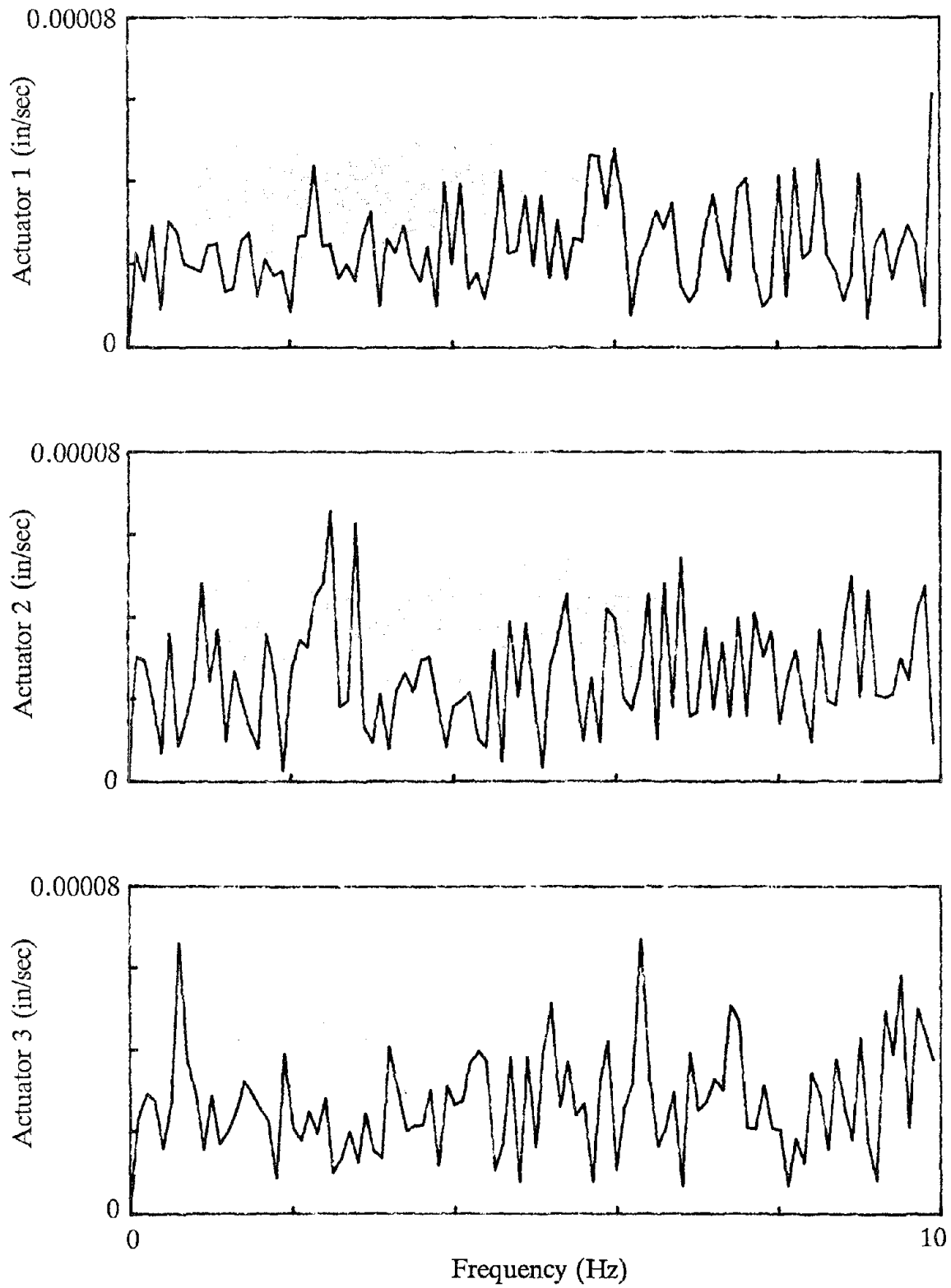


Figure 4.29 - Test 5 Displacement Error Fourier Amplitude Spectra

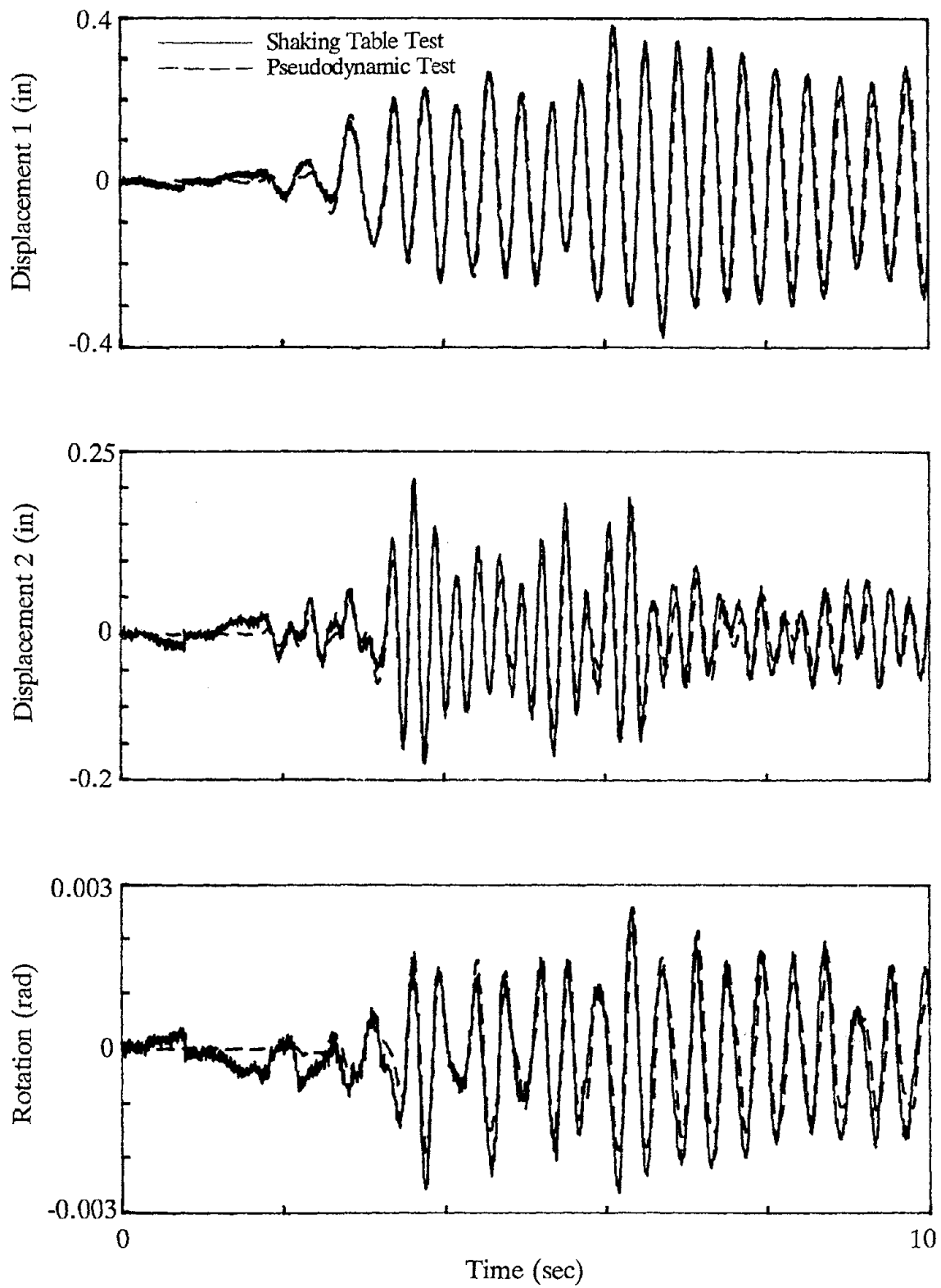


Figure 4.30 - Test 6 Displacement Response (Part 1)

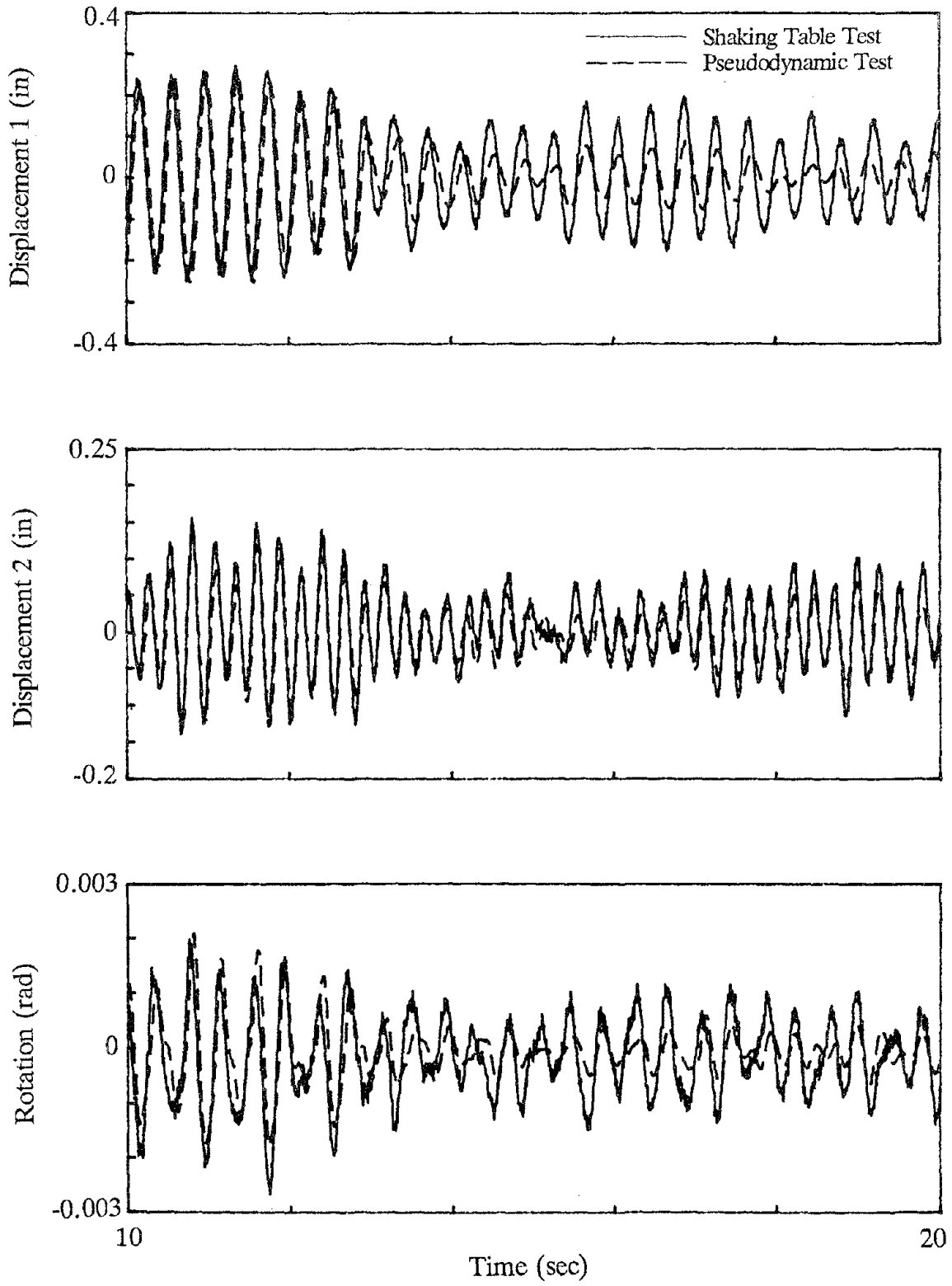


Figure 4.31 - Test 6 Displacement Response (Part 2)

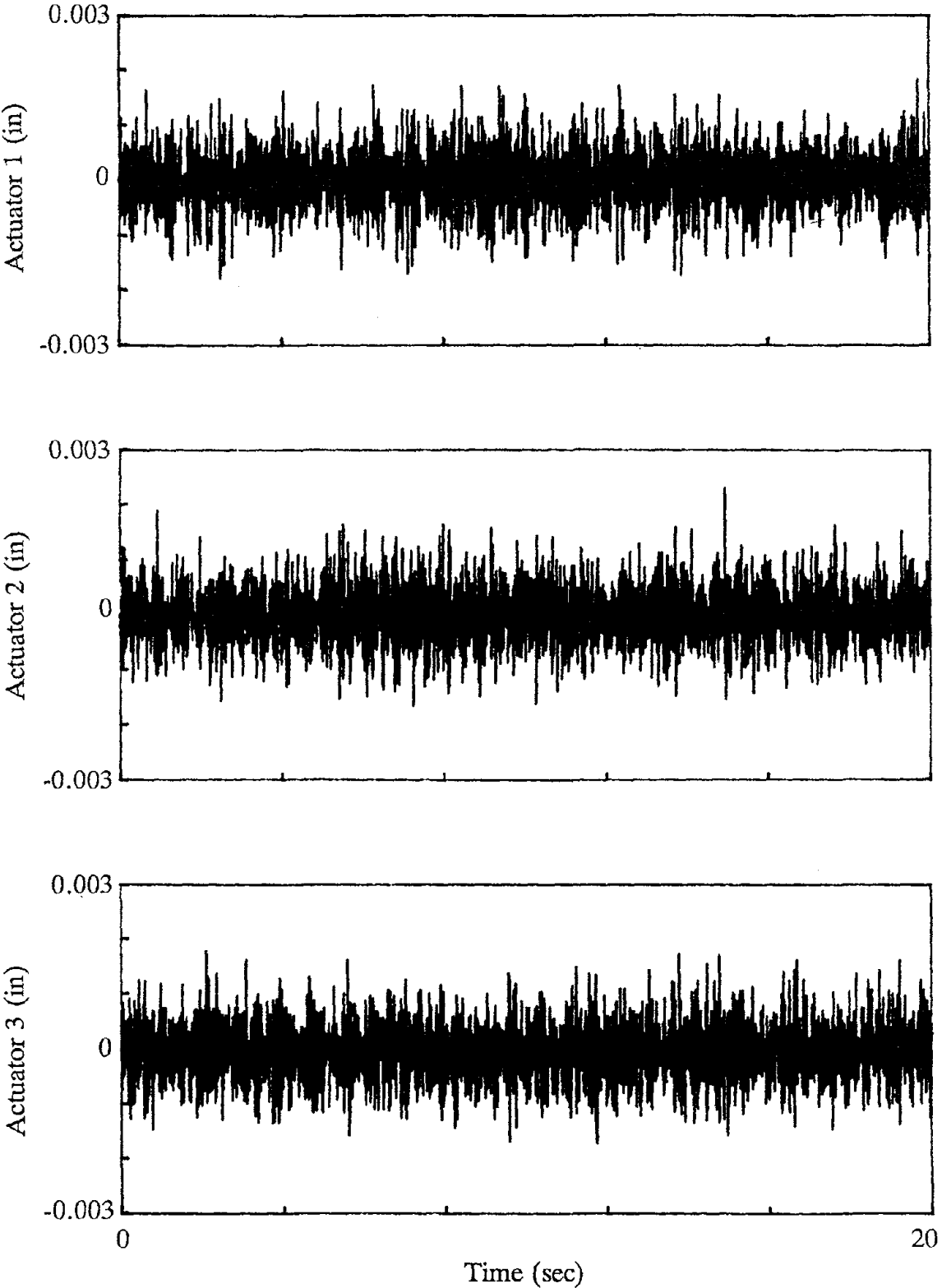


Figure 4.32 - Test 6 Displacement Error Histories

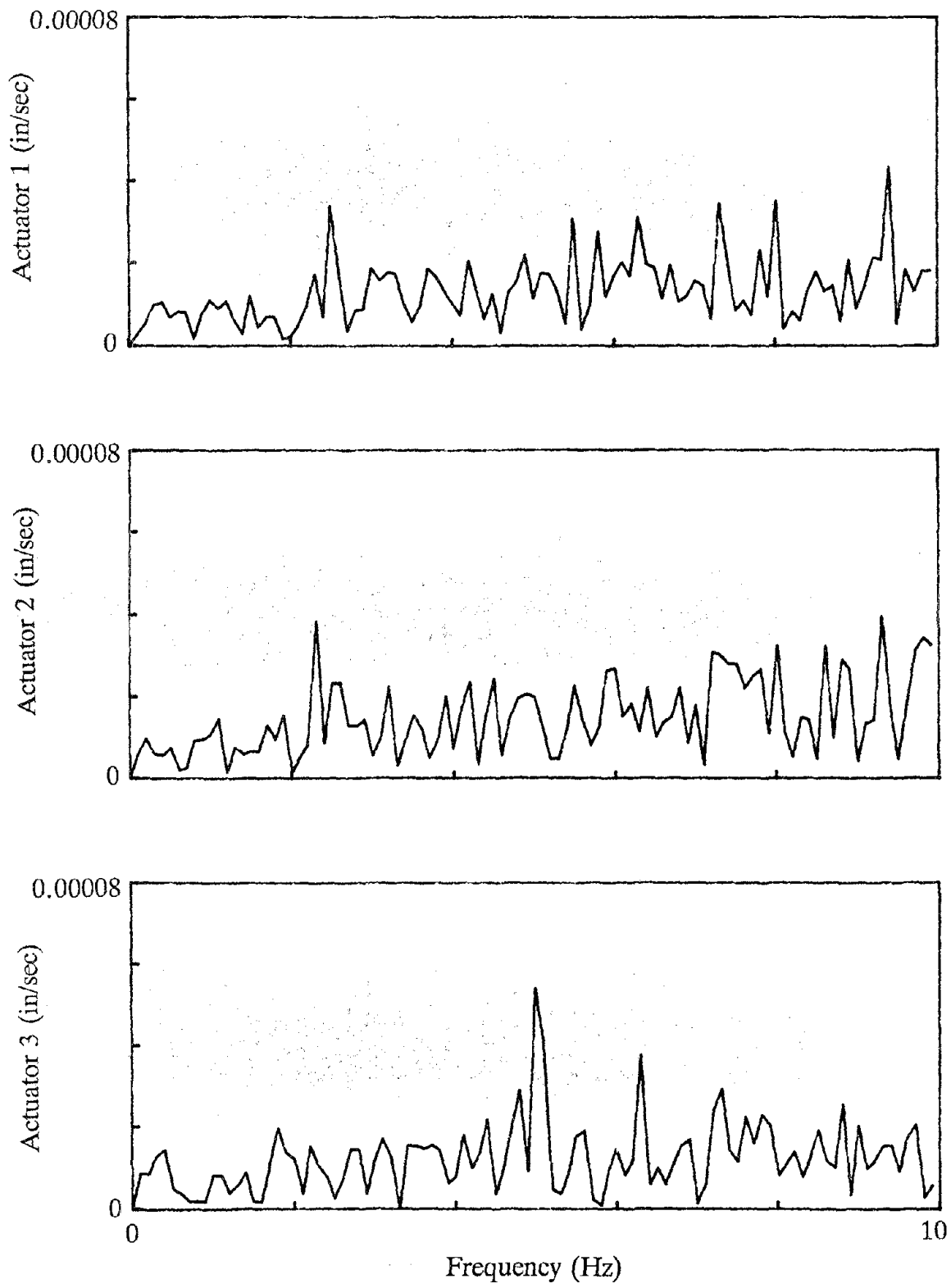


Figure 4.33 - Test 6 Displacement Error Fourier Amplitude Spectra

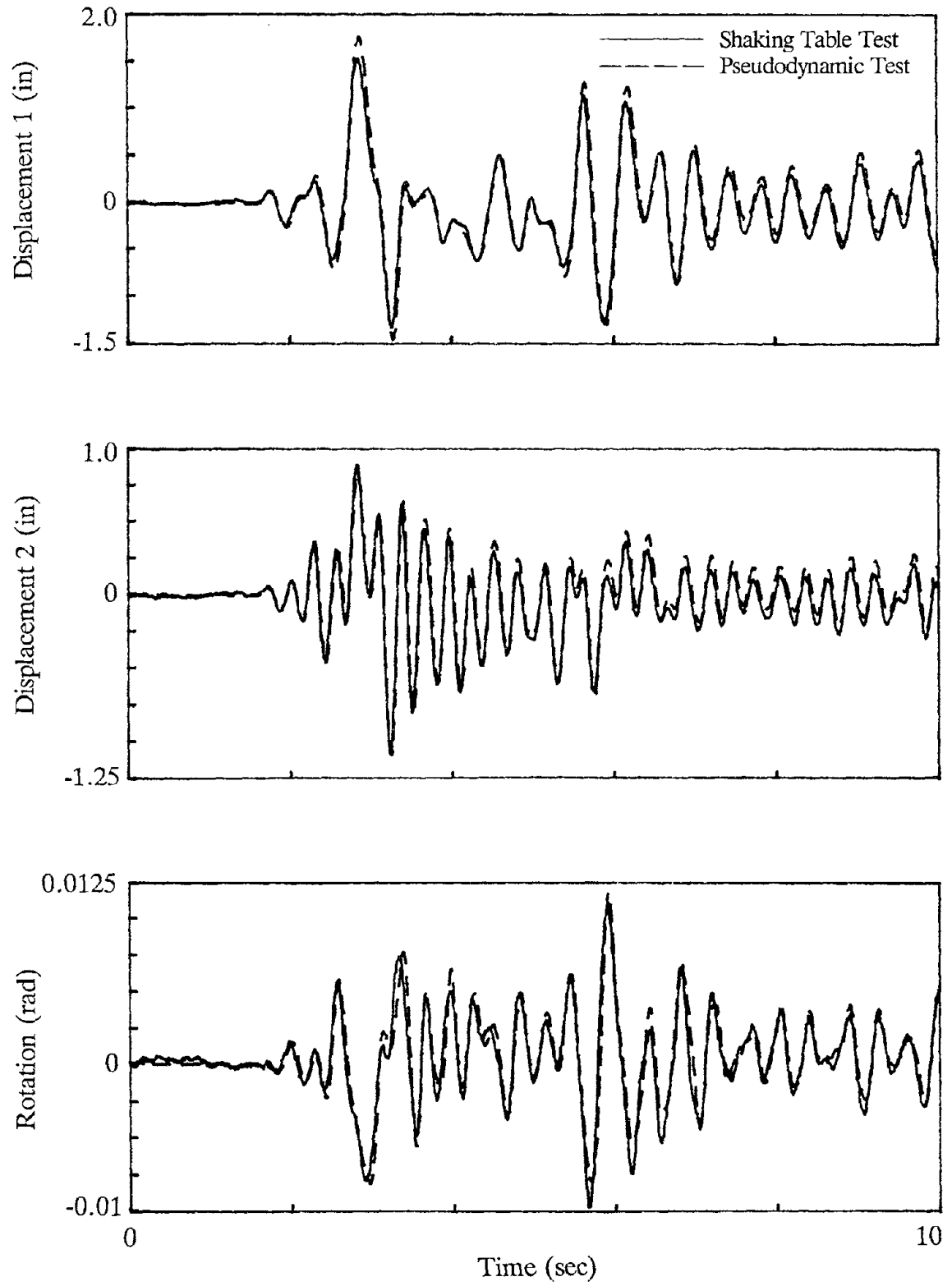


Figure 4.34 - Test 7 Displacement Response (Part 1)

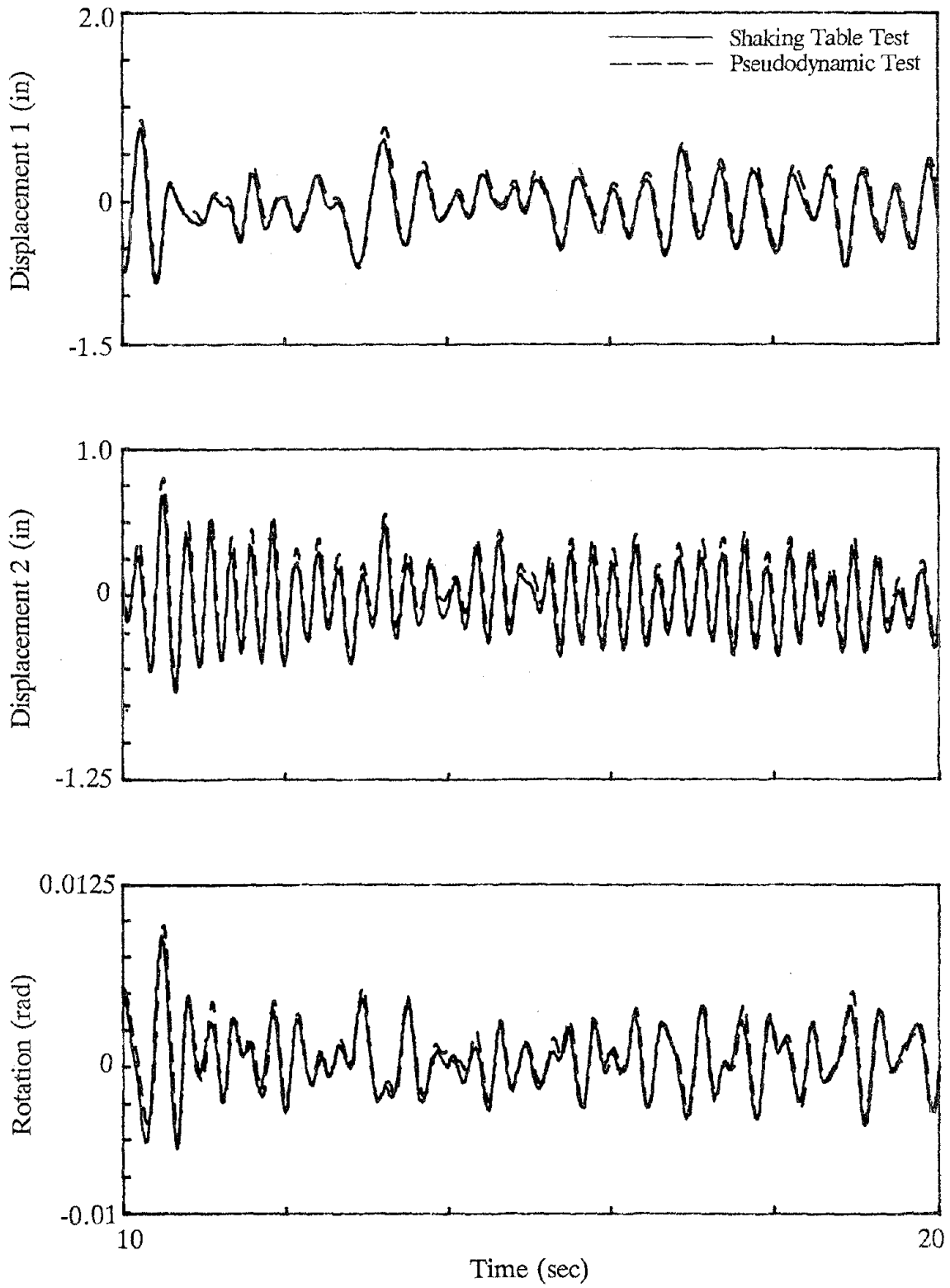


Figure 4.35 - Test 7 Displacement Response (Part 2)

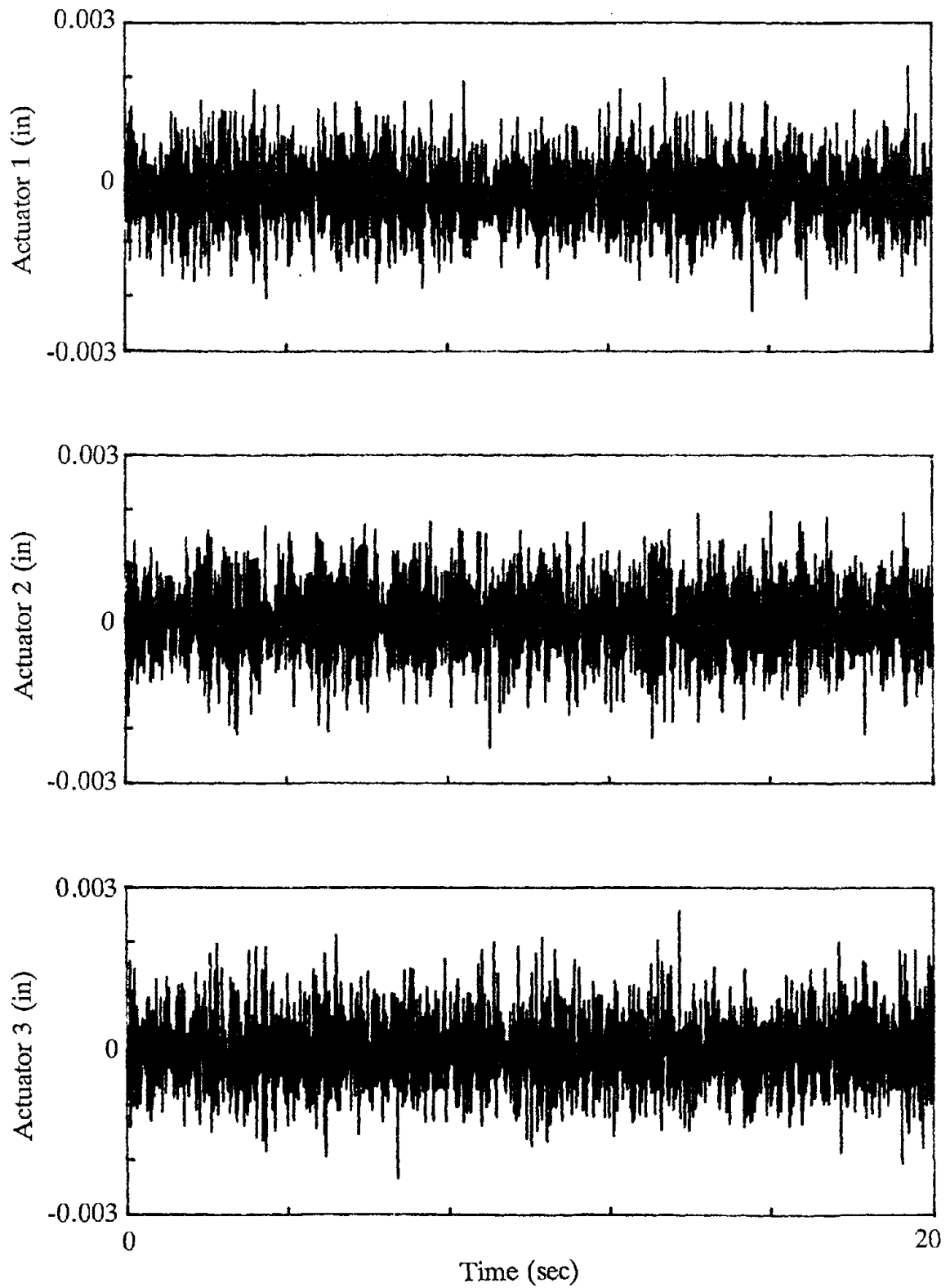


Figure 4.36 - Test 7 Displacement Error Histories

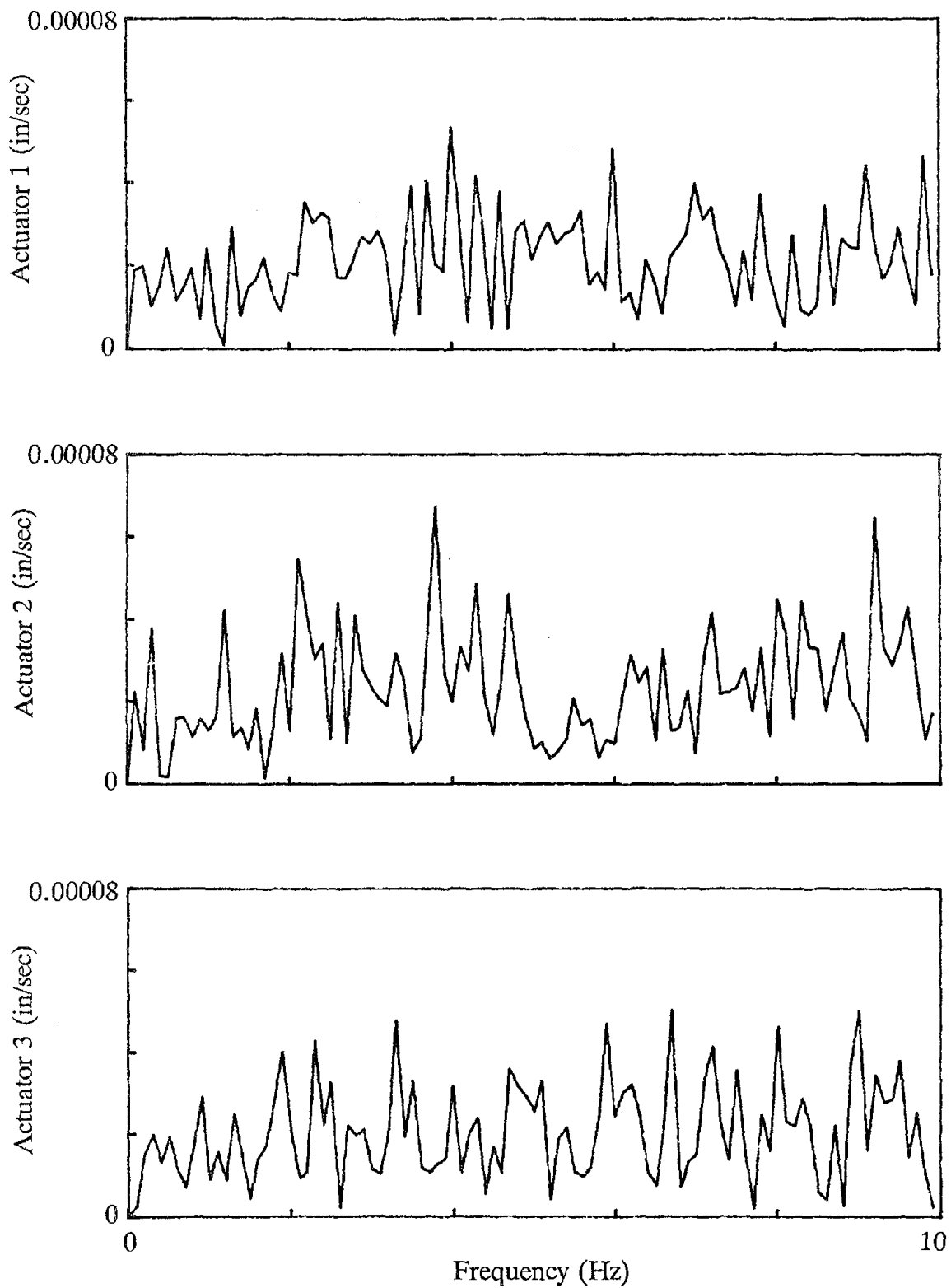


Figure 4.37 - Test 7 Displacement Error Fourier Amplitude Spectra

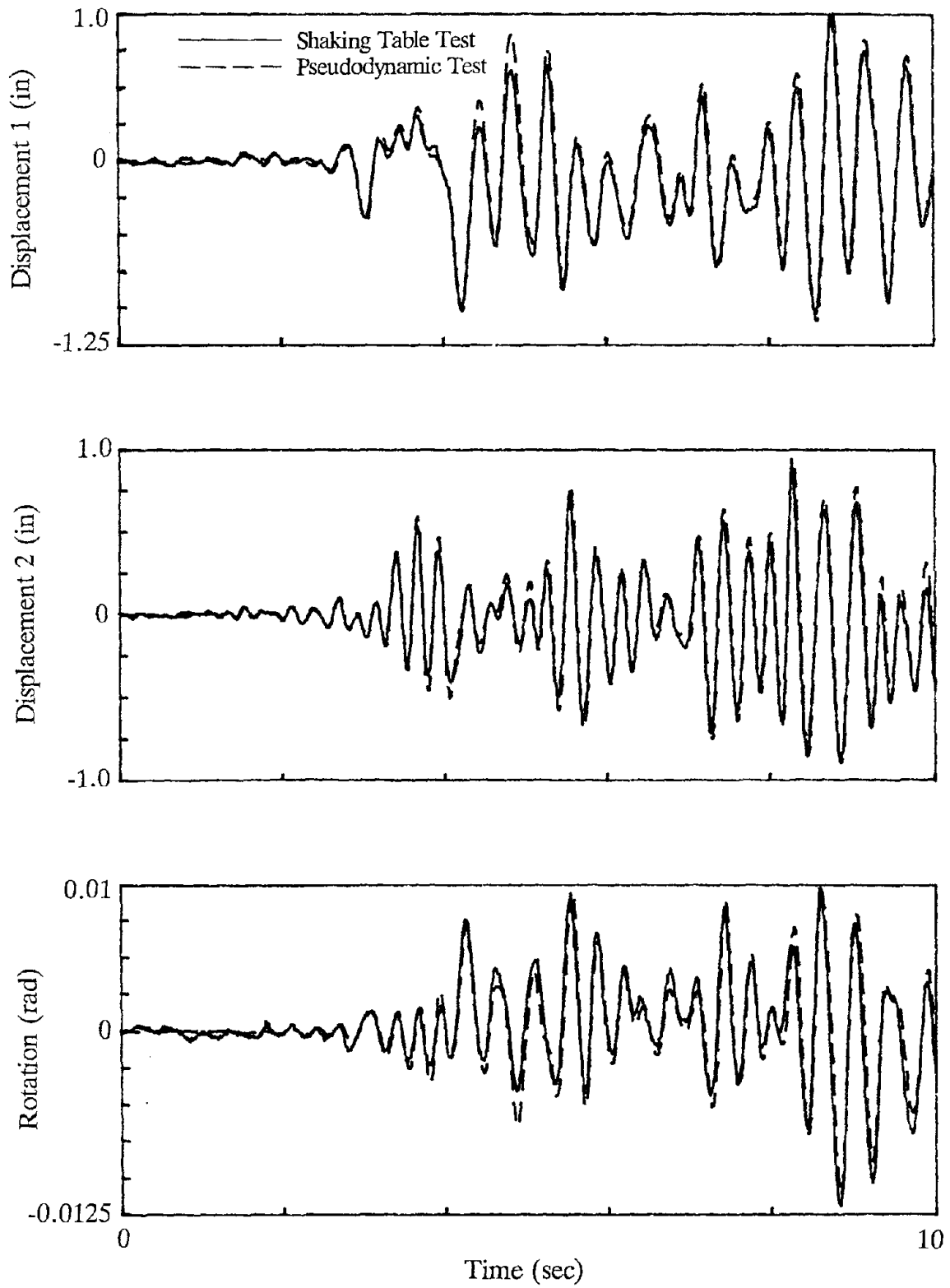


Figure 4.38 - Test 8 Displacement Response (Part 1)

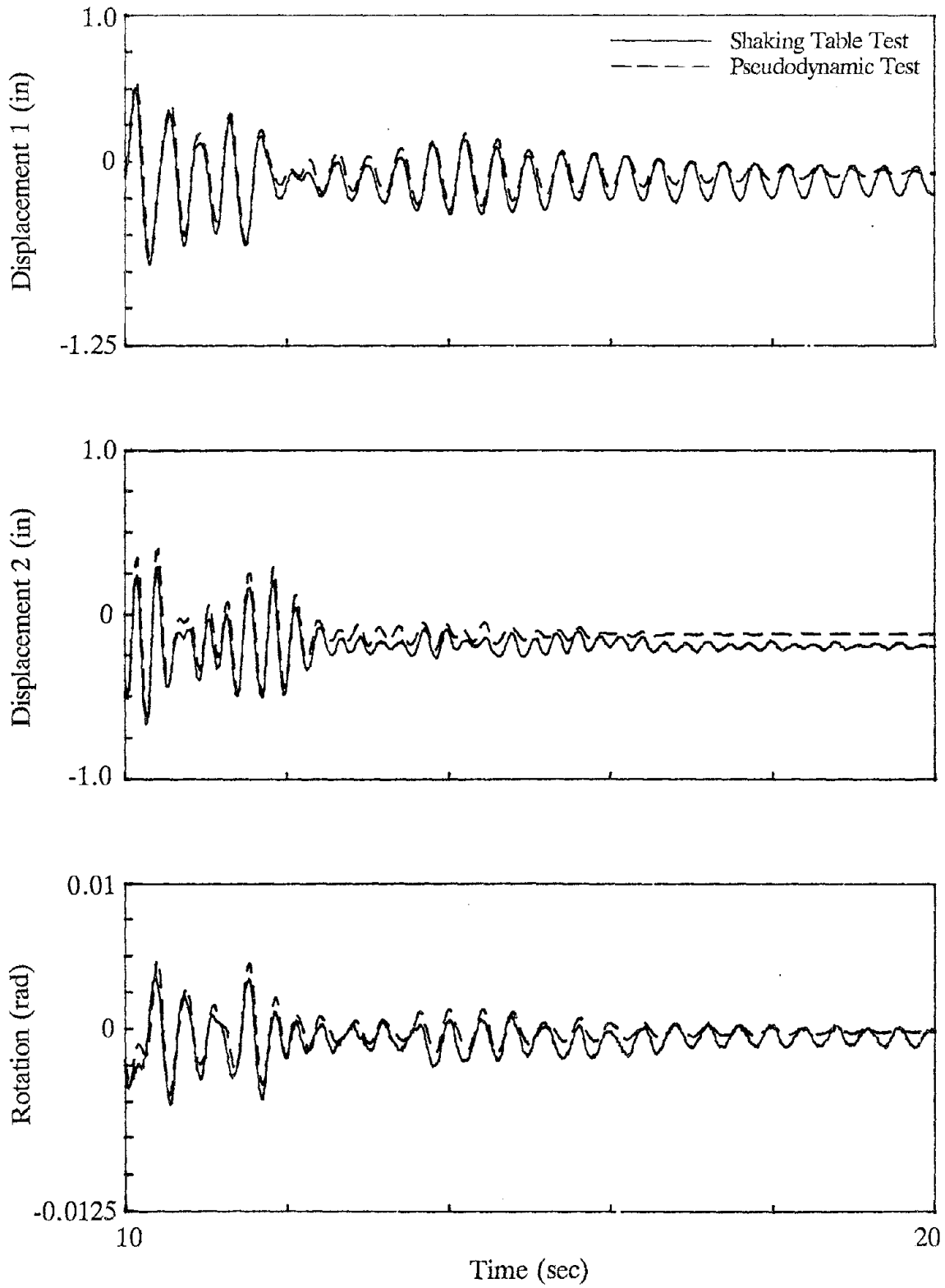


Figure 4.39 - Test 8 Displacement Response (Part 2)

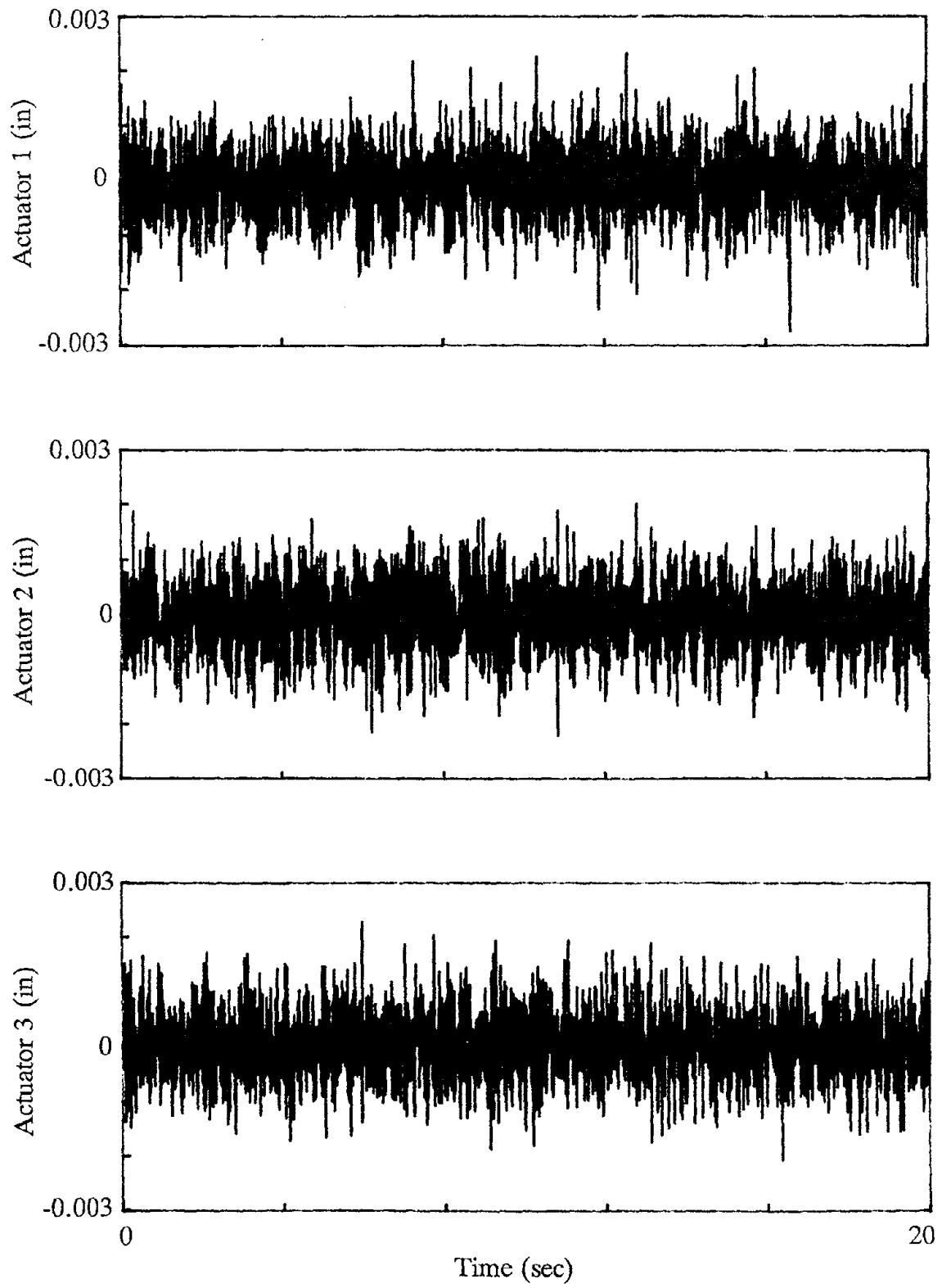


Figure 4.40 - Test 8 Displacement Error Histories

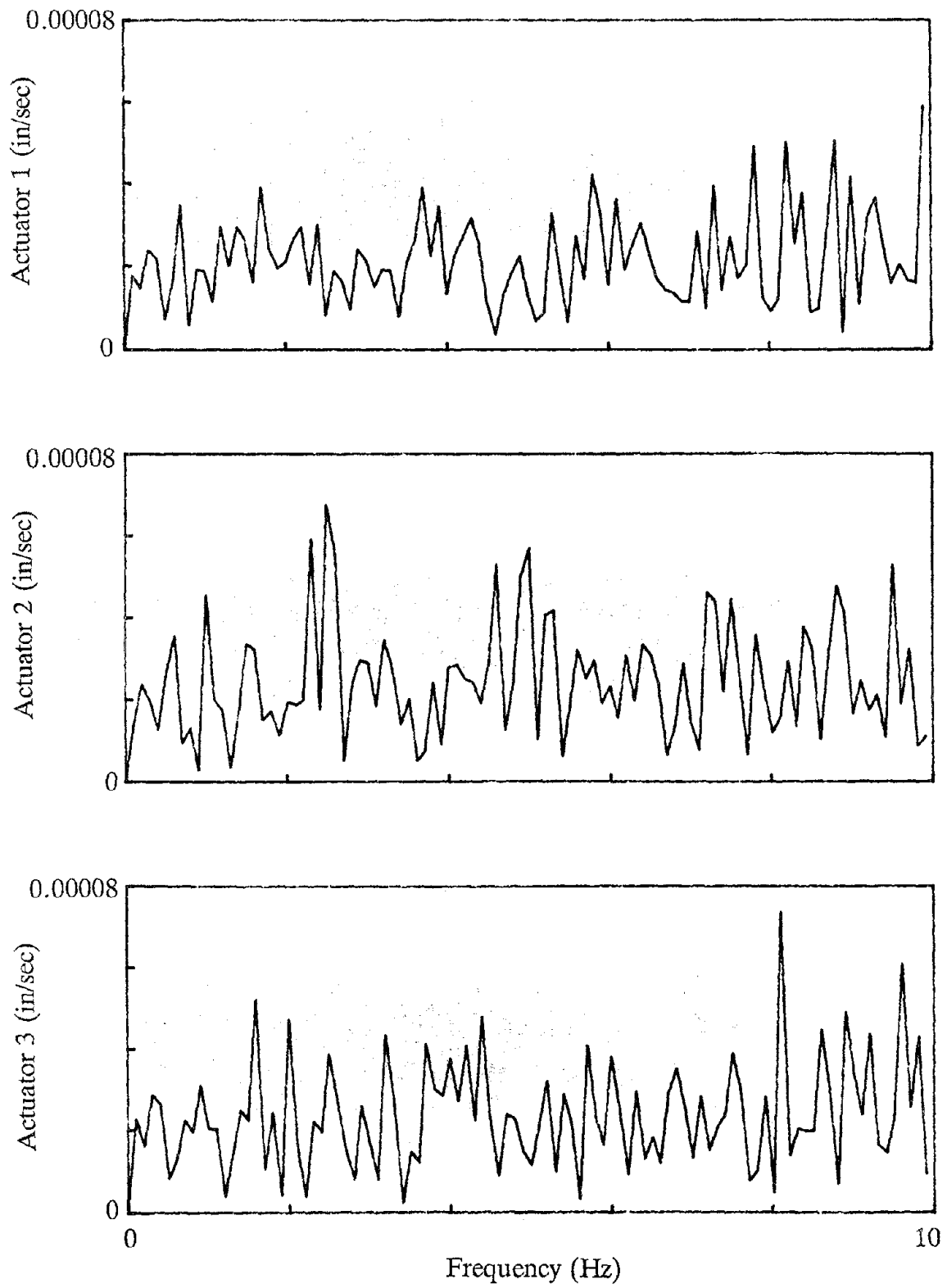


Figure 4.41 - Test 8 Displacement Error Fourier Amplitude Spectra

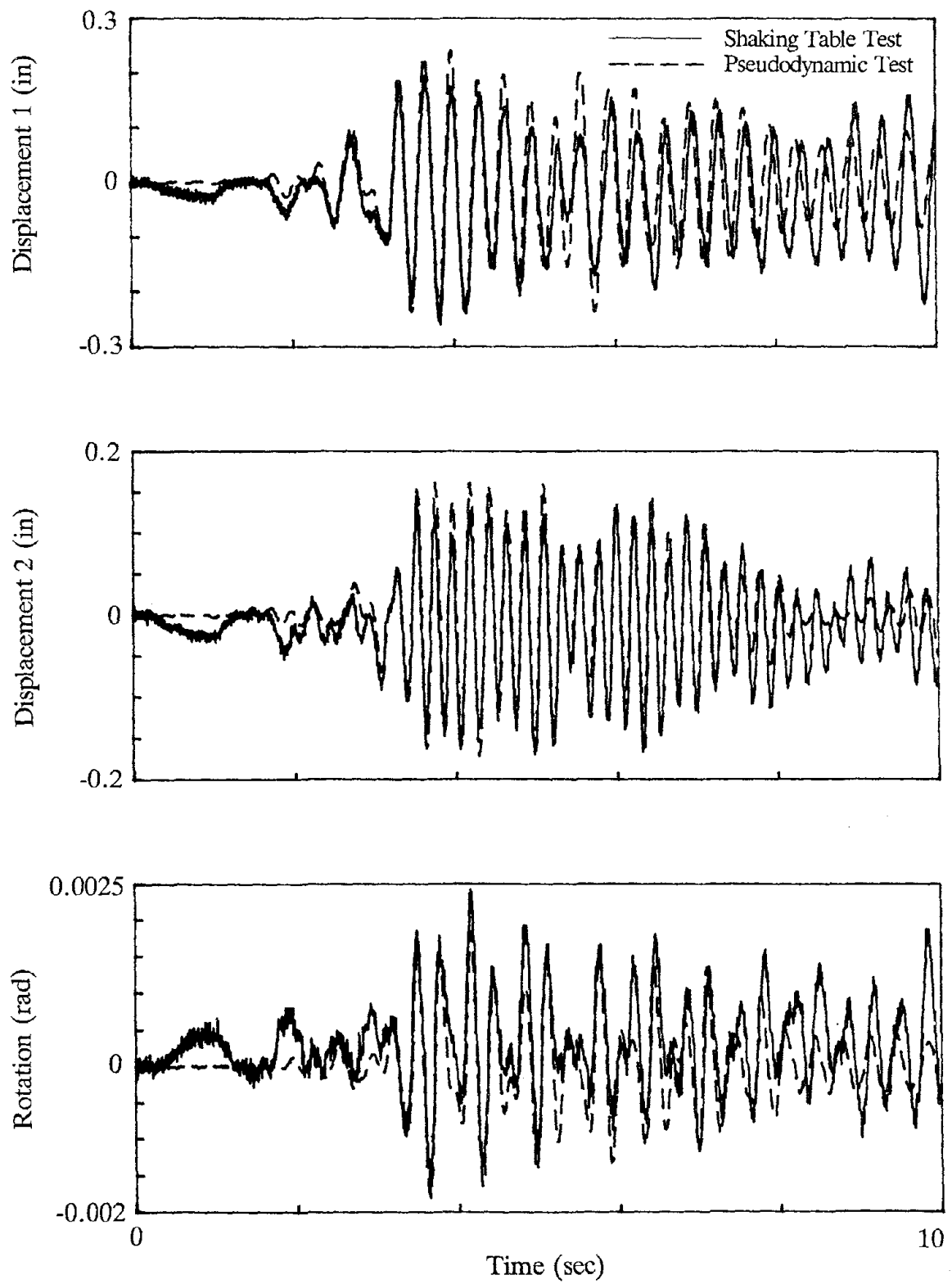


Figure 4.42 - Test 1 Displacement Response with Experimental Errors

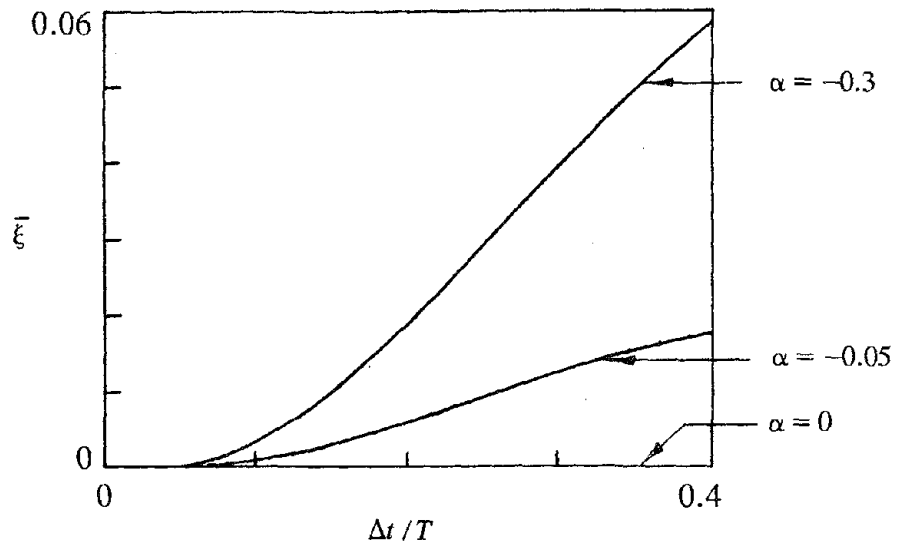


Figure 6.1 - Damping Characteristics of Hilber, Taylor and Hughes Method (after Hilber, Taylor and Hughes [24])

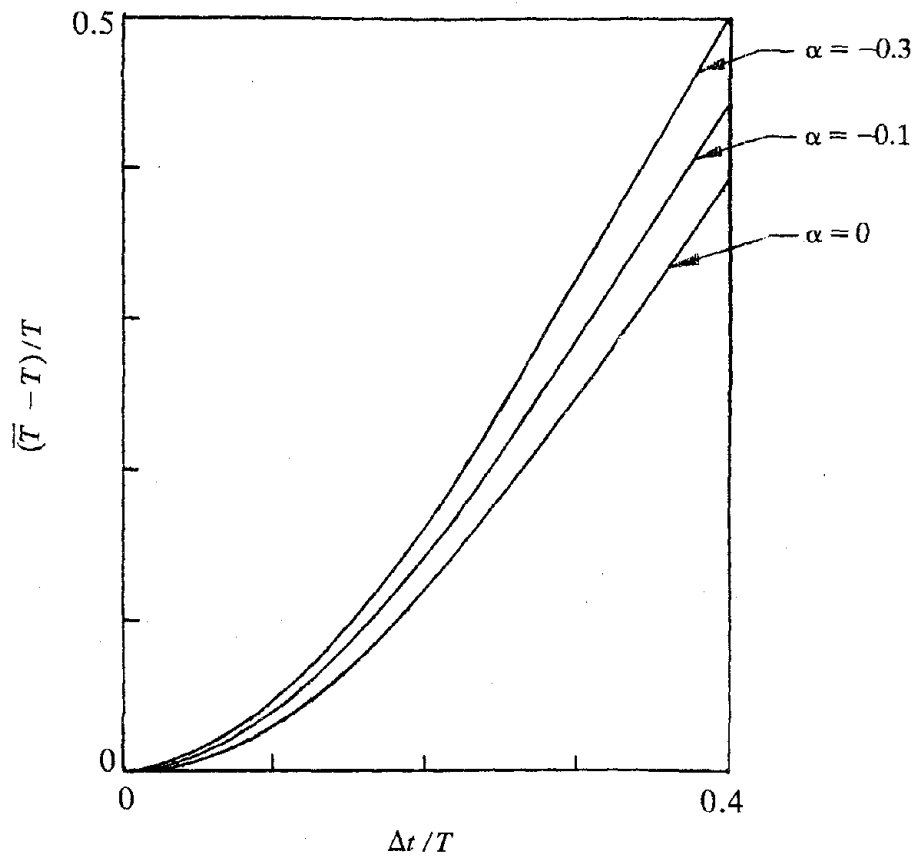
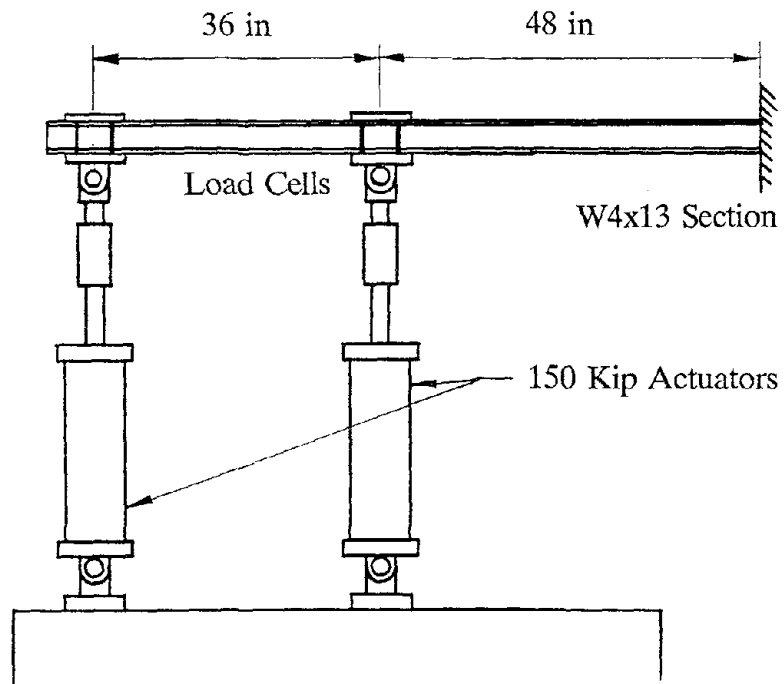
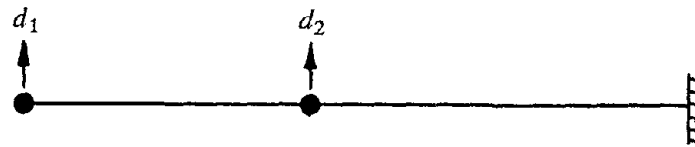


Figure 6.2 - Period Elongation Characteristics of Hilber, Taylor and Hughes Method (after Hilber, Taylor and Hughes [24])



(a) Physical Setup



(b) Analytical Model

Figure 6.3 - Two Degree of Freedom Setup for Implicit Verification Test

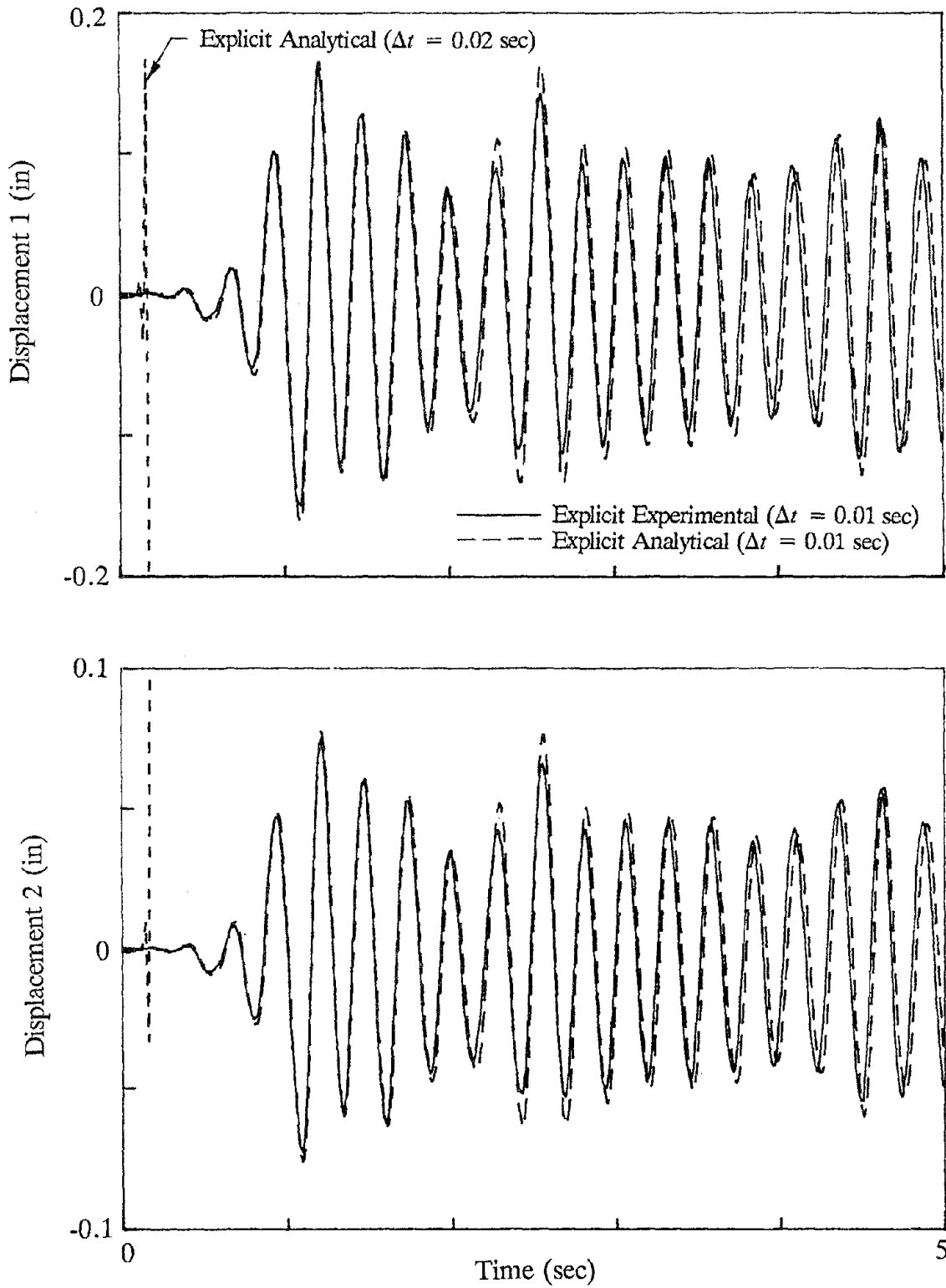


Figure 6.4 - Displacement Response

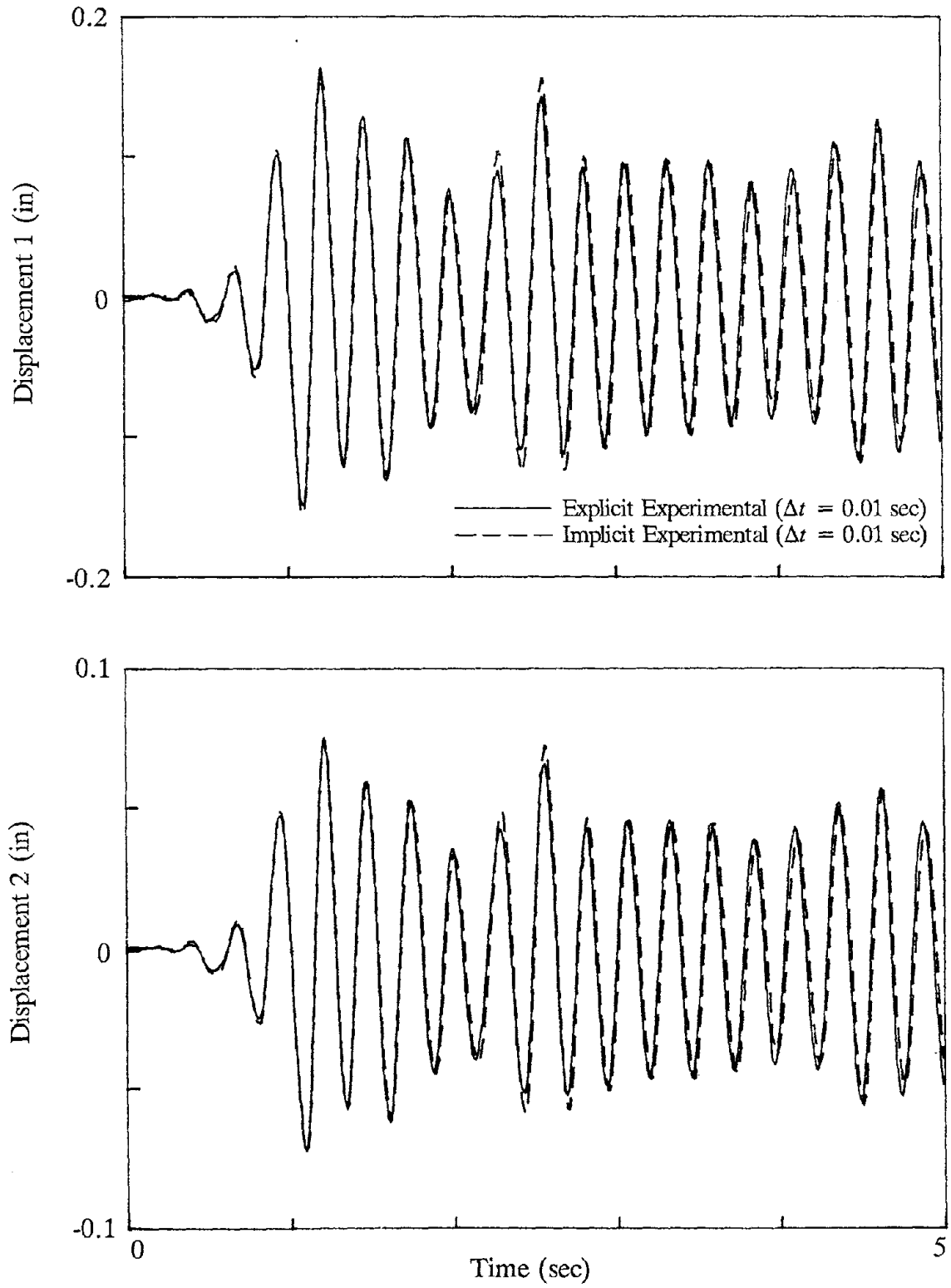


Figure 6.5 - Displacement Response

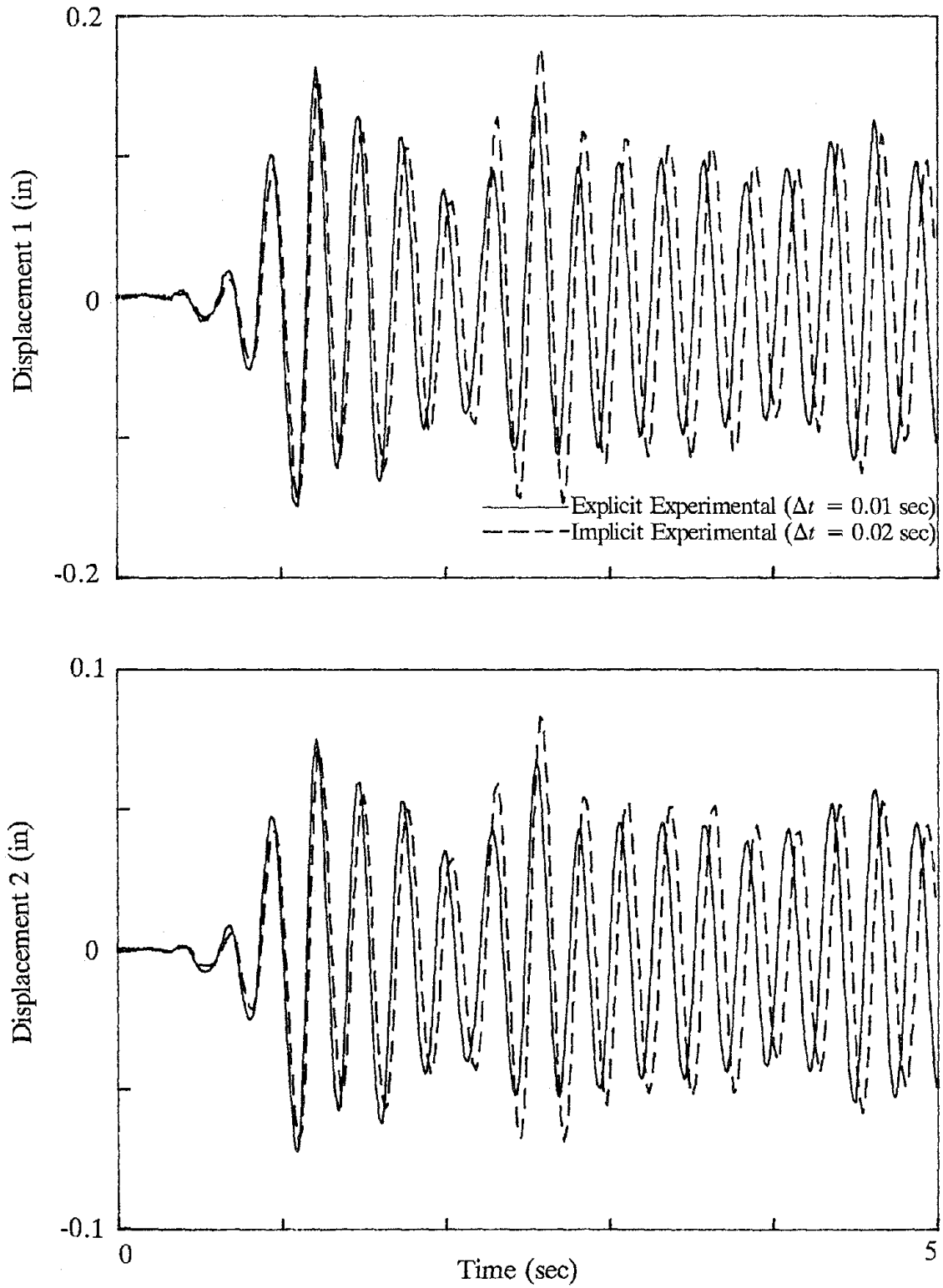


Figure 6.6 - Displacement Response

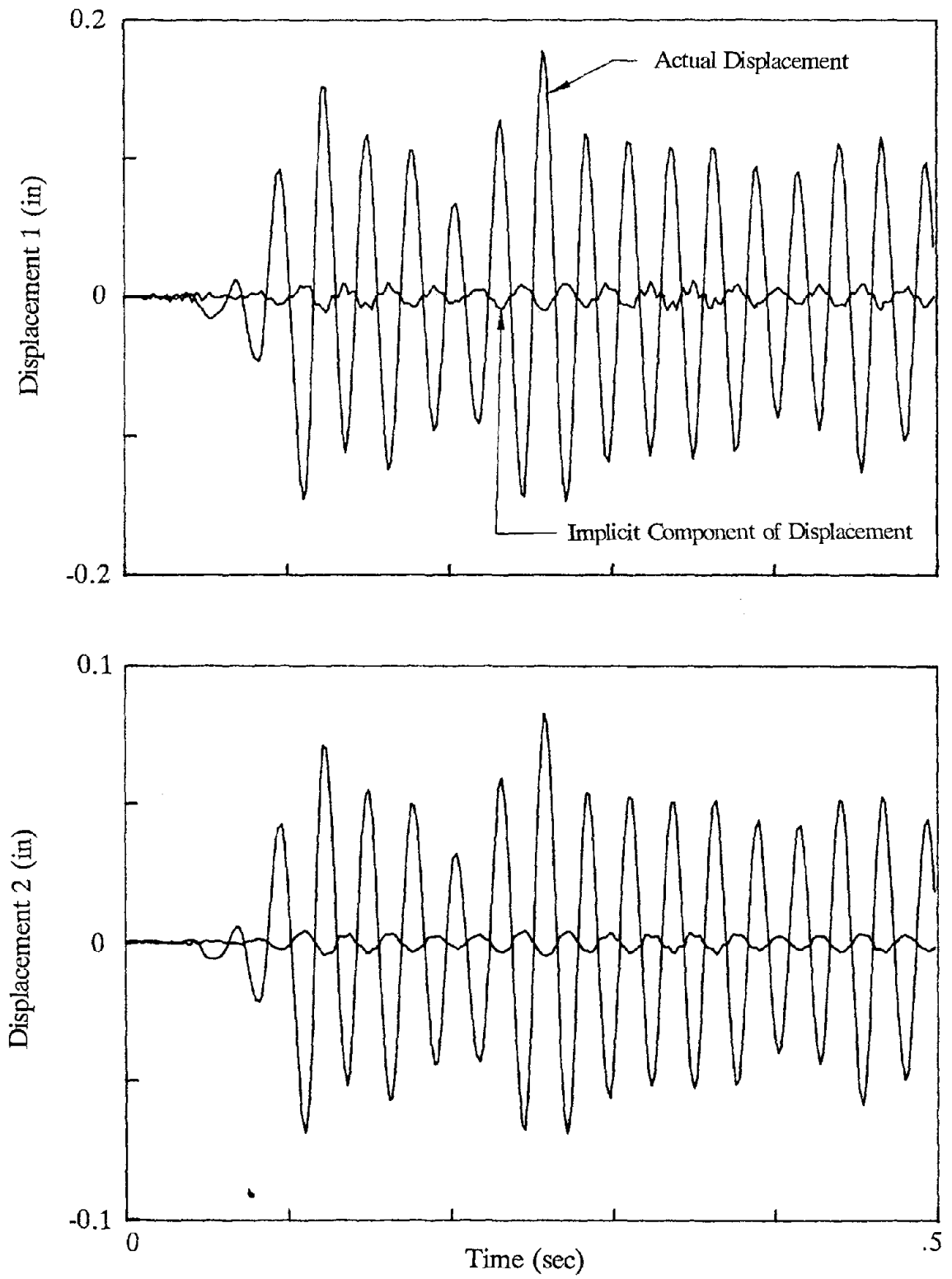


Figure 6.7 - Implicit Contribution to Displacement

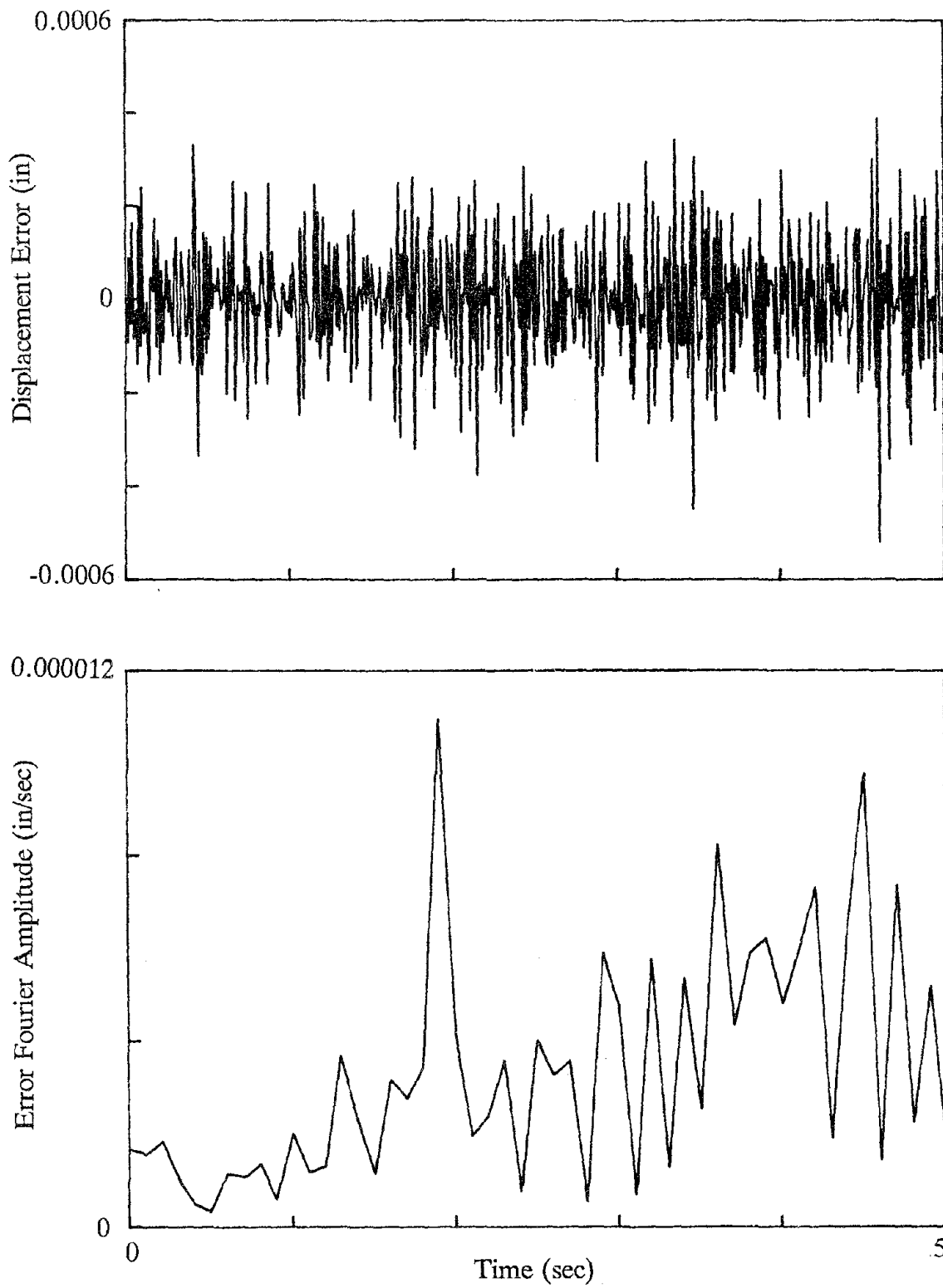


Figure 6.8 - Errors During Explicit Test

## EARTHQUAKE ENGINEERING RESEARCH CENTER REPORT SERIES

EERC reports are available from the National Information Service for Earthquake Engineering(NISEE) and from the National Technical Information Service(NTIS). Numbers in parentheses are Accession Numbers assigned by the National Technical Information Service; these are followed by a price code. Contact NTIS, 5285 Port Royal Road, Springfield Virginia, 22161 for more information. Reports without Accession Numbers were not available from NTIS at the time of printing. For a current complete list of EERC reports (from EERC 67-1) and availability information, please contact University of California, EERC, NISEE, 1301 South 46th Street, Richmond, California 94804.

- UCB/EERC-80/01 "Earthquake Response of Concrete Gravity Dams Including Hydrodynamic and Foundation Interaction Effects," by Chopra, A.K., Chakrabarti, P. and Gupta, S., January 1980. (AD-A087297)A10.
- UCB/EERC-80/02 "Rocking Response of Rigid Blocks to Earthquakes," by Yim, C.S., Chopra, A.K. and Penzien, J., January 1980. (PB80 166 002)A04.
- UCB/EERC-80/03 "Optimum Inelastic Design of Seismic-Resistant Reinforced Concrete Frame Structures," by Zagajski, S.W. and Bertero, V.V., January 1980. (PB80 164 635)A06.
- UCB/EERC-80/04 "Effects of Amount and Arrangement of Wall-Panel Reinforcement on Hysteretic Behavior of Reinforced Concrete Walls," by Iliya, R. and Bertero, V.V., February 1980. (PB81 122 525)A09.
- UCB/EERC-80/05 "Shaking Table Research on Concrete Dam Models," by Niwa, A. and Clough, R.W., September 1980. (PB81 122 368)A06.
- UCB/EERC-80/06 "The Design of Steel Energy-Absorbing Restrainers and their Incorporation into Nuclear Power Plants for Enhanced Safety (Vol 1a): Piping with Energy Absorbing Restrainers: Parameter Study on Small Systems," by Powell, G.H., Oughourlian, C. and Simons, J., June 1980.
- UCB/EERC-80/07 "Inelastic Torsional Response of Structures Subjected to Earthquake Ground Motions," by Yamazaki, Y., April 1980. (PB81 122 327)A08.
- UCB/EERC-80/08 "Study of X-Braced Steel Frame Structures under Earthquake Simulation," by Ghanaat, Y., April 1980. (PB81 122 335)A11.
- UCB/EERC-80/09 "Hybrid Modelling of Soil-Structure Interaction," by Gupta, S., Lin, T.W. and Penzien, J., May 1980. (PB81 122 319)A07.
- UCB/EERC-80/10 "General Applicability of a Nonlinear Model of a One Story Steel Frame," by Sveinsson, B.I. and McNiven, H.D., May 1980. (PB81 124 877)A06.
- UCB/EERC-80/11 "A Green-Function Method for Wave Interaction with a Submerged Body," by Kioka, W., April 1980. (PB81 122 269)A07.
- UCB/EERC-80/12 "Hydrodynamic Pressure and Added Mass for Axisymmetric Bodies," by Nilrat, F., May 1980. (PB81 122 343)A08.
- UCB/EERC-80/13 "Treatment of Non-Linear Drag Forces Acting on Offshore Platforms," by Dao, B.V. and Penzien, J., May 1980. (PB81 153 413)A07.
- UCB/EERC-80/14 "2D Plane/Axisymmetric Solid Element (Type 3-Elastic or Elastic-Perfectly Plastic)for the ANSR-II Program," by Mondkar, D.P. and Powell, G.H., July 1980. (PB81 122 350)A03.
- UCB/EERC-80/15 "A Response Spectrum Method for Random Vibrations," by Der Kiureghian, A., June 1981. (PB81 122 301)A03.
- UCB/EERC-80/16 "Cyclic Inelastic Buckling of Tubular Steel Braces," by Zayas, V.A., Popov, E.P. and Martin, S.A., June 1981. (PB81 124 885)A10.
- UCB/EERC-80/17 "Dynamic Response of Simple Arch Dams Including Hydrodynamic Interaction," by Porter, C.S. and Chopra, A.K., July 1981. (PB81 124 000)A13.
- UCB/EERC-80/18 "Experimental Testing of a Friction Damped Aseismic Base Isolation System with Fail-Safe Characteristics," by Kelly, J.M., Beucke, K.E. and Skinner, M.S., July 1980. (PB81 148 595)A04.
- UCB/EERC-80/19 "The Design of Steel Energy-Absorbing Restrainers and their Incorporation into Nuclear Power Plants for Enhanced Safety (Vol.1B): Stochastic Seismic Analyses of Nuclear Power Plant Structures and Piping Systems Subjected to Multiple Supported Excitations," by Lee, M.C. and Penzien, J., June 1980. (PB82 201 872)A08.
- UCB/EERC-80/20 "The Design of Steel Energy-Absorbing Restrainers and their Incorporation into Nuclear Power Plants for Enhanced Safety (Vol 1C): Numerical Method for Dynamic Substructure Analysis," by Dickens, J.M. and Wilson, E.L., June 1980.
- UCB/EERC-80/21 "The Design of Steel Energy-Absorbing Restrainers and their Incorporation into Nuclear Power Plants for Enhanced Safety (Vol 2): Development and Testing of Restraints for Nuclear Piping Systems," by Kelly, J.M. and Skinner, M.S., June 1980.
- UCB/EERC-80/22 "3D Solid Element (Type 4-Elastic or Elastic-Perfectly-Plastic) for the ANSR-II Program," by Mondkar, D.P. and Powell, G.H., July 1980. (PB81 123 242)A03.
- UCB/EERC-80/23 "Gap-Friction Element (Type 5) for the Ansr-II Program," by Mondkar, D.P. and Powell, G.H., July 1980. (PB81 122 285)A03.
- UCB/EERC-80/24 "U-Bar Restraint Element (Type 11) for the ANSR-II Program," by Oughourlian, C. and Powell, G.H., July 1980. (PB81 122 293)A03.
- UCB/EERC-80/25 "Testing of a Natural Rubber Base Isolation System by an Explosively Simulated Earthquake," by Kelly, J.M., August 1980. (PB81 201 360)A04.
- UCB/EERC-80/26 "Input Identification from Structural Vibrational Response," by Hu, Y., August 1980. (PB81 152 308)A05.
- UCB/EERC-80/27 "Cyclic Inelastic Behavior of Steel Offshore Structures," by Zayas, V.A., Mahin, S.A. and Popov, E.P., August 1980. (PB81 196 180)A15.
- UCB/EERC-80/28 "Shaking Table Testing of a Reinforced Concrete Frame with Biaxial Response," by Oliva, M.G., October 1980. (PB81 154 304)A10.
- UCB/EERC-80/29 "Dynamic Properties of a Twelve-Story Prefabricated Panel Building," by Bouwkamp, J.G., Kollegger, J.P. and Stephen, R.M., October 1980. (PB82 138 777)A07.
- UCB/EERC-80/30 "Dynamic Properties of an Eight-Story Prefabricated Panel Building," by Bouwkamp, J.G., Kollegger, J.P. and Stephen, R.M., October 1980. (PB81 200 313)A05.
- UCB/EERC-80/31 "Predictive Dynamic Response of Panel Type Structures under Earthquakes," by Kollegger, J.P. and Bouwkamp, J.G., October 1980. (PB81 152 316)A04.
- UCB/EERC-80/32 "The Design of Steel Energy-Absorbing Restrainers and their Incorporation into Nuclear Power Plants for Enhanced Safety (Vol 3): Testing of Commercial Steels in Low-Cycle Torsional Fatigue," by Spanner, P., Parker, E.R., Jongewaard, E. and Dory, M., 1980.

- UCB/EERC-80/33 "The Design of Steel Energy-Absorbing Restrainers and their Incorporation into Nuclear Power Plants for Enhanced Safety (Vol 4): Shaking Table Tests of Piping Systems with Energy-Absorbing Restrainers," by Stiemer, S.F. and Godden, W.G., September 1980. (PB82 201 880)A05.
- UCB/EERC-80/34 "The Design of Steel Energy-Absorbing Restrainers and their Incorporation into Nuclear Power Plants for Enhanced Safety (Vol 5): Summary Report," by Spencer, P., 1980.
- UCB/EERC-80/35 "Experimental Testing of an Energy-Absorbing Base Isolation System," by Kelly, J.M., Skinner, M.S. and Beucke, K.E., October 1980. (PB81 154 072)A04.
- UCB/EERC-80/36 "Simulating and Analyzing Artificial Non-Stationary Earth Ground Motions," by Nau, R.F., Oliver, R.M. and Pister, K.S., October 1980. (PB81 153 397)A04.
- UCB/EERC-80/37 "Earthquake Engineering at Berkeley - 1980," by , September 1980, (PB81 205 674)A09.
- UCB/EERC-80/38 "Inelastic Seismic Analysis of Large Panel Buildings," by Schricker, V. and Powell, G.H., September 1980. (PB81 154 338)A13.
- UCB/EERC-80/39 "Dynamic Response of Embankment, Concrete-Gavity and Arch Dams Including Hydrodynamic Interaction," by Hall, J.F. and Chopra, A.K., October 1980. (PB81 152 324)A11.
- UCB/EERC-80/40 "Inelastic Buckling of Steel Struts under Cyclic Load Reversal," by Black, R.G., Wenger, W.A. and Popov, E.P., October 1980. (PB81 154 312)A08.
- UCB/EERC-80/41 "Influence of Site Characteristics on Buildings Damage during the October 3,1974 Lima Earthquake," by Repetto, P., Arango, I. and Seed, H.B., September 1980. (PB81 161 739)A05.
- UCB/EERC-80/42 "Evaluation of a Shaking Table Test Program on Response Behavior of a Two Story Reinforced Concrete Frame," by Blondet, J.M., Clough, R.W. and Mahin, S.A., December 1980. (PB82 196 544)A11.
- UCB/EERC-80/43 "Modelling of Soil-Structure Interaction by Finite and Infinite Elements," by Medina, F., December 1980. (PB81 229 270)A04.
- UCB/EERC-81/01 "Control of Seismic Response of Piping Systems and Other Structures by Base Isolation," by Kelly, J.M., January 1981, (PB81 200 735)A05.
- UCB/EERC-81/02 "OPTNSR- An Interactive Software System for Optimal Design of Statically and Dynamically Loaded Structures with Nonlinear Response," by Bhatti, M.A., Ciampi, V. and Pister, K.S., January 1981, (PB81 218 851)A09.
- UCB/EERC-81/03 "Analysis of Local Variations in Free Field Seismic Ground Motions," by Chen, J.-C., Lysmer, J. and Seed, H.B., January 1981. (AD-A099508)A13.
- UCB/EERC-81/04 "Inelastic Structural Modeling of Braced Offshore Platforms for Seismic Loading," by Zayas, V.A., Shing, P.-S.B., Mahin, S.A. and Popov, E.P., January 1981, (PB82 138 777)A07.
- UCB/EERC-81/05 "Dynamic Response of Light Equipment in Structures," by Der Kiureghian, A., Sackman, J.L. and Nour-Omid, B., April 1981, (PB81 218 497)A04.
- UCB/EERC-81/06 "Preliminary Experimental Investigation of a Broad Base Liquid Storage Tank," by Bouwkamp, J.G., Kollegger, J.P. and Stephen, R.M., May 1981. (PB82 140 385)A03.
- UCB/EERC-81/07 "The Seismic Resistant Design of Reinforced Concrete Coupled Structural Walls," by Aktan, A.E. and Bertero, V.V., June 1981, (PB82 113 358)A11.
- UCB/EERC-81/08 "Unassigned," by Unassigned, 1981.
- UCB/EERC-81/09 "Experimental Behavior of a Spatial Piping System with Steel Energy Absorbers Subjected to a Simulated Differential Seismic Input," by Stiemer, S.F., Godden, W.G. and Kelly, J.M., July 1981. (PB82 201 898)A04.
- UCB/EERC-81/10 "Evaluation of Seismic Design Provisions for Masonry in the United States," by Sveinsson, B.L., Mayes, R.L. and McNiven, H.D., August 1981. (PB82 166 075)A08.
- UCB/EERC-81/11 "Two-Dimensional Hybrid Modelling of Soil-Structure Interaction," by Tzong, T.-J., Gupta, S. and Penzien, J., August 1981, (PB82 142 118)A04.
- UCB/EERC-81/12 "Studies on Effects of Infills in Seismic Resistant R/C Construction," by Brokken, S. and Bertero, V.V., October 1981, (PB82 166 190)A09.
- UCB/EERC-81/13 "Linear Models to Predict the Nonlinear Seismic Behavior of a One-Story Steel Frame," by Valdimarsson, H., Shah, A.H. and McNiven, H.D., September 1981, (PB82 138 793)A07.
- UCB/EERC-81/14 "TLUSH: A Computer Program for the Three-Dimensional Dynamic Analysis of Earth Dams," by Kagawa, T., Mejia, L.H., Seed, H.B. and Lysmer, J., September 1981, (PB82 139 940)A06.
- UCB/EERC-81/15 "Three Dimensional Dynamic Response Analysis of Earth Dams," by Mejia, L.H. and Seed, H.B., September 1981. (PB82 137 274)A12.
- UCB/EERC-81/16 "Experimental Study of Lead and Elastomeric Dampers for Base Isolation Systems," by Kelly, J.M. and Hodder, S.B., October 1981. (PB82 166 182)A05.
- UCB/EERC-81/17 "The Influence of Base Isolation on the Seismic Response of Light Secondary Equipment," by Kelly, J.M., April 1981. (PB82 255 266)A04.
- UCB/EERC-81/18 "Studies on Evaluation of Shaking Table Response Analysis Procedures," by Blondet, J. M., November 1981, (PB82 197 278)A10.
- UCB/EERC-81/19 "DELIGHT.STRUCT: A Computer-Aided Design Environment for Structural Engineering," by Balling, R.J., Pister, K.S. and Polak, E., December 1981. (PB82 218 496)A07.
- UCB/EERC-81/20 "Optimal Design of Seismic-Resistant Planar Steel Frames," by Balling, R.J., Ciampi, V. and Pister, K.S., December 1981. (PB82 220 179)A07.
- UCB/EERC-82/01 "Dynamic Behavior of Ground for Seismic Analysis of Lifeline Systems," by Sato, T. and Der Kiureghian, A., January 1982, (PB82 218 926)A05.
- UCB/EERC-82/02 "Shaking Table Tests of a Tubular Steel Frame Model," by Ghanaat, Y. and Clough, R.W., January 1982, (PB82 220 161)A07.

- UCB/EERC-82/03 "Behavior of a Piping System under Seismic Excitation: Experimental Investigations of a Spatial Piping System supported by Mechanical Shock Arrestors," by Schneider, S., Lee, H.-M. and Godden, W. G., May 1982. (PB83 172 544)A09.
- UCB/EERC-82/04 "New Approaches for the Dynamic Analysis of Large Structural Systems," by Wilson, E.L., June 1982. (PB83 148 080)A05.
- UCB/EERC-82/05 "Model Study of Effects of Damage on the Vibration Properties of Steel Offshore Platforms," by Shahrivar, F. and Bouwkamp, J.G., June 1982. (PB83 148 742)A10.
- UCB/EERC-82/06 "States of the Art and Practice in the Optimum Seismic Design and Analytical Response Prediction of R/C Frame Wall Structures," by Aktan, A.E. and Bertero, V.V., July 1982. (PB83 147 736)A05.
- UCB/EERC-82/07 "Further Study of the Earthquake Response of a Broad Cylindrical Liquid-Storage Tank Model," by Manos, G.C. and Clough, R.W., July 1982. (PB83 147 744)A11.
- UCB/EERC-82/08 "An Evaluation of the Design and Analytical Seismic Response of a Seven Story Reinforced Concrete Frame," by Charney, F.A. and Bertero, V.V., July 1982. (PB83 157 628)A09.
- UCB/EERC-82/09 "Fluid-Structure Interactions: Added Mass Computations for Incompressible Fluid," by Kuo, J.S.-H., August 1982. (PB83 156 281)A07.
- UCB/EERC-82/10 "Joint-Opening Nonlinear Mechanism: Interface Smeared Crack Model," by Kuo, J.S.-H., August 1982. (PB83 149 195)A05.
- UCB/EERC-82/11 "Dynamic Response Analysis of Tchi Dam," by Clough, R.W., Stephen, R.M. and Kuo, J.S.-H., August 1982. (PB83 147 496)A06.
- UCB/EERC-82/12 "Prediction of the Seismic Response of R/C Frame-Coupled Wall Structures," by Aktan, A.E., Bertero, V.V. and Piazza, M., August 1982. (PB83 149 203)A09.
- UCB/EERC-82/13 "Preliminary Report on the Smart 1 Strong Motion Array in Taiwan," by Bólt, B.A., Loh, C.H., Penzien, J. and Tsai, Y.B., August 1982. (PB83 159 400)A10.
- UCB/EERC-82/14 "Shaking-Table Studies of an Eccentrically X-Braced Steel Structure," by Yang, M.S., September 1982. (PB83 260 778)A12.
- UCB/EERC-82/15 "The Performance of Stairways in Earthquakes," by Roha, C., Axley, J.W. and Bertero, V.V., September 1982. (PB83 157 693)A08.
- UCB/EERC-82/16 "The Behavior of Submerged Multiple Bodies in Earthquakes," by Liao, W.-G., September 1982. (PB83 158 709)A07.
- UCB/EERC-82/17 "Effects of Concrete Types and Loading Conditions on Local Bond-Slip Relationships," by Cowell, A.D., Popov, E.P. and Bertero, V.V., September 1982. (PB83 153 577)A04.
- UCB/EERC-82/18 "Mechanical Behavior of Shear Wall Vertical Boundary Members: An Experimental Investigation," by Wagner, M.T. and Bertero, V.V., October 1982. (PB83 159 764)A05.
- UCB/EERC-82/19 "Experimental Studies of Multi-support Seismic Loading on Piping Systems," by Kelly, J.M. and Cowell, A.D., November 1982.
- UCB/EERC-82/20 "Generalized Plastic Hinge Concepts for 3D Beam-Column Elements," by Chen, P. F.-S. and Powell, G.H., November 1982. (PB83 247 981)A13.
- UCB/EERC-82/21 "ANSR-II: General Computer Program for Nonlinear Structural Analysis," by Oughourlian, C.V. and Powell, G.H., November 1982. (PB83 251 330)A12.
- UCB/EERC-82/22 "Solution Strategies for Statically Loaded Nonlinear Structures," by Simons, J.W. and Powell, G.H., November 1982. (PB83 197 970)A06.
- UCB/EERC-82/23 "Analytical Model of Deformed Bar Anchorages under Generalized Excitations," by Ciampi, V., Eligehausen, R., Bertero, V.V. and Popov, E.P., November 1982. (PB83 169 532)A06.
- UCB/EERC-82/24 "A Mathematical Model for the Response of Masonry Walls to Dynamic Excitations," by Sucuoglu, H., Mengi, Y. and McNiven, H.D., November 1982. (PB83 169 011)A07.
- UCB/EERC-82/25 "Earthquake Response Considerations of Broad Liquid Storage Tanks," by Cambra, F.J., November 1982. (PB83 251 215)A09.
- UCB/EERC-82/26 "Computational Models for Cyclic Plasticity, Rate Dependence and Creep," by Mosaddad, B. and Powell, G.H., November 1982. (PB83 245 829)A08.
- UCB/EERC-82/27 "Inelastic Analysis of Piping and Tubular Structures," by Mahasuverachai, M. and Powell, G.H., November 1982. (PB83 249 987)A07.
- UCB/EERC-83/01 "The Economic Feasibility of Seismic Rehabilitation of Buildings by Base Isolation," by Kelly, J.M., January 1983. (PB83 197 988)A05.
- UCB/EERC-83/02 "Seismic Moment Connections for Moment-Resisting Steel Frames," by Popov, E.P., January 1983. (PB83 195 412)A04.
- UCB/EERC-83/03 "Design of Links and Beam-to-Column Connections for Eccentrically Braced Steel Frames," by Popov, E.P. and Malley, J.O., January 1983. (PB83 194 811)A04.
- UCB/EERC-83/04 "Numerical Techniques for the Evaluation of Soil-Structure Interaction Effects in the Time Domain," by Bayo, E. and Wilson, E.L., February 1983. (PB83 245 605)A09.
- UCB/EERC-83/05 "A Transducer for Measuring the Internal Forces in the Columns of a Frame-Wall Reinforced Concrete Structure," by Sause, R. and Bertero, V.V., May 1983. (PB84 119 494)A06.
- UCB/EERC-83/06 "Dynamic Interactions Between Floating Ice and Offshore Structures," by Croteau, P., May 1983. (PB84 119 486)A16.
- UCB/EERC-83/07 "Dynamic Analysis of Multiply Tuned and Arbitrarily Supported Secondary Systems," by Igusa, T. and Der Kiureghian, A., July 1983. (PB84 118 272)A11.
- UCB/EERC-83/08 "A Laboratory Study of Submerged Multi-body Systems in Earthquakes," by Ansari, G.R., June 1983. (PB83 261 842)A17.
- UCB/EERC-83/09 "Effects of Transient Foundation Uplift on Earthquake Response of Structures," by Yim, C.-S. and Chopra, A.K., June 1983. (PB83 261 396)A07.
- UCB/EERC-83/10 "Optimal Design of Friction-Braced Frames under Seismic Loading," by Austin, M.A. and Pister, K.S., June 1983. (PB84 119 288)A06.
- UCB/EERC-83/11 "Shaking Table Study of Single-Story Masonry Houses: Dynamic Performance under Three Component Seismic Input and Recommendations," by Manos, G.C., Clough, R.W. and Mayes, R.L., July 1983. (UCB/EERC-83/11)A08.
- UCB/EERC-83/12 "Experimental Error Propagation in Pseudodynamic Testing," by Shiing, P.B. and Mahin, S.A., June 1983. (PB84 119 270)A09.
- UCB/EERC-83/13 "Experimental and Analytical Predictions of the Mechanical Characteristics of a 1/5-scale Model of a 7-story R/C Frame-Wall Building Structure," by Aktan, A.E., Bertero, V.V., Chowdhury, A.A. and Nagashima, T., June 1983. (PB84 119 213)A07.

- UCB/EERC-83/14 "Shaking Table Tests of Large-Panel Precast Concrete Building System Assemblages," by Oliva, M.G. and Clough, R.W., June 1983. (PB86 110 210/AS)A11.
- UCB/EERC-83/15 "Seismic Behavior of Active Beam Links in Eccentrically Braced Frames," by Hjelmstad, K.D. and Popov, E.P., July 1983. (PB84 119 676)A09.
- UCB/EERC-83/16 "System Identification of Structures with Joint Rotation," by Dimsdale, J.S., July 1983. (PB84 192 210)A06.
- UCB/EERC-83/17 "Construction of Inelastic Response Spectra for Single-Degree-of-Freedom Systems," by Mahin, S. and Lin, J., June 1983. (PB84 208 834)A05.
- UCB/EERC-83/18 "Interactive Computer Analysis Methods for Predicting the Inelastic Cyclic Behaviour of Structural Sections," by Kaba, S. and Mahin, S., July 1983. (PB84 192 012)A06.
- UCB/EERC-83/19 "Effects of Bond Deterioration on Hysteretic Behavior of Reinforced Concrete Joints," by Filippou, F.C., Popov, E.P. and Bertero, V.V., August 1983. (PB84 192 020)A10.
- UCB/EERC-83/20 "Analytical and Experimental Correlation of Large-Panel Precast Building System Performance," by Oliva, M.G., Clough, R.W., Velkov, M. and Gavrilovic, P., November 1983.
- UCB/EERC-83/21 "Mechanical Characteristics of Materials Used in a 1/5 Scale Model of a 7-Story Reinforced Concrete Test Structure," by Bertero, V.V., Aktan, A.E., Harris, H.G. and Chowdhury, A.A., October 1983. (PB84 193 697)A05.
- UCB/EERC-83/22 "Hybrid Modelling of Soil-Structure Interaction in Layered Media," by Tzong, T.-J. and Penzien, J., October 1983. (PB84 192 178)A08.
- UCB/EERC-83/23 "Local Bond Stress-Slip Relationships of Deformed Bars under Generalized Excitations," by Eligehausen, R., Popov, E.P. and Bertero, V.V., October 1983. (PB84 192 848)A09.
- UCB/EERC-83/24 "Design Considerations for Shear Links in Eccentrically Braced Frames," by Malley, J.O. and Popov, E.P., November 1983. (PB84 192 186)A07.
- UCB/EERC-84/01 "Pseudodynamic Test Method for Seismic Performance Evaluation: Theory and Implementation," by Shing, P.-S.B. and Mahin, S.A., January 1984. (PB84 190 644)A08.
- UCB/EERC-84/02 "Dynamic Response Behavior of Kiang Hong Dian Dam," by Clough, R.W., Chang, K.-T., Chen, H.-Q. and Stephen, R.M., April 1984. (PB84 209 402)A08.
- UCB/EERC-84/03 "Refined Modelling of Reinforced Concrete Columns for Seismic Analysis," by Kaba, S.A. and Mahin, S.A., April 1984. (PB84 234 384)A06.
- UCB/EERC-84/04 "A New Floor Response Spectrum Method for Seismic Analysis of Multiply Supported Secondary Systems," by Asfura, A. and Der Kiureghian, A., June 1984. (PB84 239 417)A06.
- UCB/EERC-84/05 "Earthquake Simulation Tests and Associated Studies of a 1/5th-scale Model of a 7-Story R/C Frame-Wall Test Structure," by Bertero, V.V., Aktan, A.E., Charney, F.A. and Sause, R., June 1984. (PB84 239 409)A09.
- UCB/EERC-84/06 "R/C Structural Walls: Seismic Design for Shear," by Aktan, A.E. and Bertero, V.V., 1984.
- UCB/EERC-84/07 "Behavior of Interior and Exterior Flat-Plate Connections subjected to Inelastic Load Reversals," by Zee, H.L. and Moehle, J.P., August 1984. (PB86 117 629/AS)A07.
- UCB/EERC-84/08 "Experimental Study of the Seismic Behavior of a Two-Story Flat-Plate Structure," by Moehle, J.P. and Diebold, J.W., August 1984. (PB86 122 553/AS)A12.
- UCB/EERC-84/09 "Phenomenological Modeling of Steel Braces under Cyclic Loading," by Ikeda, K., Mahin, S.A. and Dermitzakis, S.N., May 1984. (PB86 132 198/AS)A08.
- UCB/EERC-84/10 "Earthquake Analysis and Response of Concrete Gravity Dams," by Fenves, G. and Chopra, A.K., August 1984. (PB85 193 902/AS)A11.
- UCB/EERC-84/11 "EAGD-84: A Computer Program for Earthquake Analysis of Concrete Gravity Dams," by Fenves, G. and Chopra, A.K., August 1984. (PB85 193 613/AS)A05.
- UCB/EERC-84/12 "A Refined Physical Theory Model for Predicting the Seismic Behavior of Braced Steel Frames," by Ikeda, K. and Mahin, S.A., July 1984. (PB85 191 450/AS)A09.
- UCB/EERC-84/13 "Earthquake Engineering Research at Berkeley - 1984," by , August 1984. (PB85 197 341/AS)A10.
- UCB/EERC-84/14 "Moduli and Damping Factors for Dynamic Analyses of Cohesionless Soils," by Seed, H.B., Wong, R.T., Idriss, I.M. and Tokimatsu, K., September 1984. (PB85 191 468/AS)A04.
- UCB/EERC-84/15 "The Influence of SPT Procedures in Soil Liquefaction Resistance Evaluations," by Seed, H.B., Tokimatsu, K., Harder, L.F. and Chung, R.M., October 1984. (PB85 191 732/AS)A04.
- UCB/EERC-84/16 "Simplified Procedures for the Evaluation of Settlements in Sands Due to Earthquake Shaking," by Tokimatsu, K. and Seed, H.B., October 1984. (PB85 197 887/AS)A03.
- UCB/EERC-84/17 "Evaluation of Energy Absorption Characteristics of Bridges under Seismic Conditions," by Imbsen, R.A. and Penzien, J., November 1984.
- UCB/EERC-84/18 "Structure-Foundation Interactions under Dynamic Loads," by Liu, W.D. and Penzien, J., November 1984. (PB87 124 889/AS)A11.
- UCB/EERC-84/19 "Seismic Modelling of Deep Foundations," by Chen, C.-H. and Penzien, J., November 1984. (PB87 124 798/AS)A07.
- UCB/EERC-84/20 "Dynamic Response Behavior of Quan Shui Dam," by Clough, R.W., Chang, K.-T., Chen, H.-Q., Stephen, R.M., Ghanaat, Y. and Qi, J.-H., November 1984. (PB86 115177/AS)A07.
- UCB/EERC-85/01 "Simplified Methods of Analysis for Earthquake Resistant Design of Buildings," by Cruz, E.F. and Chopra, A.K., February 1985. (PB86 112299/AS)A12.
- UCB/EERC-85/02 "Estimation of Seismic Wave Coherency and Rupture Velocity using the SMART 1 Strong-Motion Array Recordings," by Abrahamson, N.A., March 1985. (PB86 214 343)A07.

- UCB/EERC-85/03 "Dynamic Properties of a Thirty Story Condominium Tower Building," by Stephen, R.M., Wilson, E.L. and Stander, N., April 1985, (PB86 118965/AS)A06.
- UCB/EERC-85/04 "Development of Substructuring Techniques for On-Line Computer Controlled Seismic Performance Testing," by Dermitzakis, S. and Mahin, S., February 1985, (PB86 132941/AS)A08.
- UCB/EERC-85/05 "A Simple Model for Reinforcing Bar Anchorages under Cyclic Excitations," by Filippou, F.C., March 1985, (PB86 112 919/AS)A05.
- UCB/EERC-85/06 "Racking Behavior of Wood-framed Gypsum Panels under Dynamic Load," by Oliva, M.G., June 1985.
- UCB/EERC-85/07 "Earthquake Analysis and Response of Concrete Arch Dams," by Fok, K.-L. and Chopra, A.K., June 1985, (PB86 139672/AS)A10.
- UCB/EERC-85/08 "Effect of Inelastic Behavior on the Analysis and Design of Earthquake Resistant Structures," by Lin, J.P. and Mahin, S.A., June 1985, (PB86 135340/AS)A08.
- UCB/EERC-85/09 "Earthquake Simulator Testing of a Base-Isolated Bridge Deck," by Kelly, J.M., Buckle, I.G. and Tsai, H.-C., January 1986, (PB87 124 152/AS)A06.
- UCB/EERC-85/10 "Simplified Analysis for Earthquake Resistant Design of Concrete Gravity Dams," by Fenves, G. and Chopra, A.K., June 1986, (PB87 124 160/AS)A08.
- UCB/EERC-85/11 "Dynamic Interaction Effects in Arch Dams," by Clough, R.W., Chang, K.-T., Chen, H.-Q. and Ghanaat, Y., October 1985, (PB86 135027/AS)A05.
- UCB/EERC-85/12 "Dynamic Response of Long Valley Dam in the Mammoth Lake Earthquake Series of May 25-27, 1980," by Lai, S. and Seed, H.B., November 1985, (PB86 142304/AS)A05.
- UCB/EERC-85/13 "A Methodology for Computer-Aided Design of Earthquake-Resistant Steel Structures," by Austin, M.A., Pister, K.S. and Mahin, S.A., December 1985, (PB86 159480/AS)A10.
- UCB/EERC-85/14 "Response of Tension-Leg Platforms to Vertical Seismic Excitations," by Liou, G.-S., Penzien, J. and Yeung, R.W., December 1985, (PB87 124 871/AS)A08.
- UCB/EERC-85/15 "Cyclic Loading Tests of Masonry Single Piers: Volume 4 - Additional Tests with Height to Width Ratio of 1," by Sveinsson, B., McNiven, H.D. and Sucuoglu, H., December 1985.
- UCB/EERC-85/16 "An Experimental Program for Studying the Dynamic Response of a Steel Frame with a Variety of Infill Partitions," by Yanev, B. and McNiven, H.D., December 1985.
- UCB/EERC-86/01 "A Study of Seismically Resistant Eccentrically Braced Steel Frame Systems," by Kasai, K. and Popov, E.P., January 1986, (PB87 124 178/AS)A14.
- UCB/EERC-86/02 "Design Problems in Soil Liquefaction," by Seed, H.B., February 1986, (PB87 124 186/AS)A03.
- UCB/EERC-86/03 "Implications of Recent Earthquakes and Research on Earthquake-Resistant Design and Construction of Buildings," by Bertero, V.V., March 1986, (PB87 124 194/AS)A05.
- UCB/EERC-86/04 "The Use of Load Dependent Vectors for Dynamic and Earthquake Analyses," by Leger, P., Wilson, E.L. and Clough, R.W., March 1986, (PB87 124 202/AS)A12.
- UCB/EERC-86/05 "Two Beam-To-Column Web Connections," by Tsai, K.-C. and Popov, E.P., April 1986, (PB87 124 301/AS)A04.
- UCB/EERC-86/06 "Determination of Penetration Resistance for Coarse-Grained Soils using the Becker Hammer Drill," by Harder, L.F. and Seed, H.B., May 1986, (PB87 124 210/AS)A07.
- UCB/EERC-86/07 "A Mathematical Model for Predicting the Nonlinear Response of Unreinforced Masonry Walls to In-Plane Earthquake Excitations," by Mengi, Y. and McNiven, H.D., May 1986, (PB87 124 780/AS)A06.
- UCB/EERC-86/08 "The 19 September 1985 Mexico Earthquake: Building Behavior," by Bertero, V.V., July 1986.
- UCB/EERC-86/09 "EACD-3D: A Computer Program for Three-Dimensional Earthquake Analysis of Concrete Dams," by Fok, K.-L., Hall, J.F. and Chopra, A.K., July 1986, (PB87 124 228/AS)A08.
- UCB/EERC-86/10 "Earthquake Simulation Tests and Associated Studies of a 0.3-Scale Model of a Six-Story Concentrically Braced Steel Structure," by Uang, C.-M. and Bertero, V.V., December 1986, (PB87 163 564/AS)A17.
- UCB/EERC-86/11 "Mechanical Characteristics of Base Isolation Bearings for a Bridge Deck Model Test," by Kelly, J.M., Buckle, I.G. and Koh, C.-G., 1987.
- UCB/EERC-86/12 "Effects of Axial Load on Elastomeric Isolation Bearings," by Koh, C.-G. and Kelly, J.M., 1987.
- UCB/EERC-87/01 "The FPS Earthquake Resisting System: Experimental Report," by Zayas, V.A., Low, S.S. and Mahin, S.A., June 1987.
- UCB/EERC-87/02 "Earthquake Simulator Tests and Associated Studies of a 0.3-Scale Model of a Six-Story Eccentrically Braced Steel Structure," by Whittaker, A., Uang, C.-M. and Bertero, V.V., July 1987.
- UCB/EERC-87/03 "A Displacement Control and Uplift Restraint Device for Base-Isolated Structures," by Kelly, J.M., Griffith, M.C. and Aiken, I.G., April 1987.
- UCB/EERC-87/04 "Earthquake Simulator Testing of a Combined Sliding Bearing and Rubber Bearing Isolation System," by Kelly, J.M. and Chalhoub, M.S., 1987.
- UCB/EERC-87/05 "Three-Dimensional Inelastic Analysis of Reinforced Concrete Frame-Wall Structures," by Moazzami, S. and Bertero, V.V., May 1987.
- UCB/EERC-87/06 "Experiments on Eccentrically Braced Frames with Composite Floors," by Ricles, J. and Popov, E., June 1987.
- UCB/EERC-87/07 "Dynamic Analysis of Seismically Resistant Eccentrically Braced Frames," by Ricles, J. and Popov, E., June 1987.
- UCB/EERC-87/08 "Undrained Cyclic Triaxial Testing of Gravels-The Effect of Membrane Compliance," by Evans, M.D. and Seed, H.B., July 1987.
- UCB/EERC-87/09 "Hybrid Solution Techniques for Generalized Pseudo-Dynamic Testing," by Thewalt, C. and Mahin, S.A., July 1987.

